Design and Analysis of a Hybrid Renewable Power Systems for an Industrial Plant in Lahore Pakistan

Written by

©Luqman Ahsan

A Thesis Submitted to the School of Graduate Studies in partial fulfillment of the requirements for the degree of

Master of Engineering

Faculty of Engineering and Applied Science
Memorial University of Newfoundland

October 2022

St. John's Newfoundland and Labrador Canada

Abstract

The fossil fuel prices are increasing continuously and the electricity generation from these resources is expensive along with the carbon emissions. The developed countries are taking steps to shift towards clean and green energy resources but due to lack of budget, poor countries are still striving to get reliable and clean energy. Therefore, the design & analysis of a low-cost hybrid power system has been carried out in this thesis for a Pakistani industrial unit. The sizing ie capacities of power resources which gave minimum per unit cost along with the capital cost are calculated using the HOMER PRO. In HOMER, three cases have been discussed including off-grid and grid-tied, the most feasible case needs an 8283 kW PV array to fulfill the demand of the plant with a 76 % load factor. This most economical case grants 0.102 $ per unit of electricity which is the cheapest among all cases. To study the dynamic of the system, the modeling of the designed system has been carried out in MATLAB/Simulink with the help of Simscape blockset. The information is used in designing each parameter of MPPT, Inverter, and LCL filter. The system is tested, and its transient time came out to be 1.5 s and after that it becomes stable. The designed system is tested under load variations and results show that it can deliver or receive the power from the grid in a smooth manner depending upon the PV generation. In addition, an abrupt change in system cloud movement has been observed, the system can handle 300 W/m^2 irradiance change while maintaining its frequency and voltage within the permissible limits. For operations purposes, a low-cost monitoring SCADA system has been designed using EMONCMS which is an open-source web view platform. Designed SCADA also acts as a local server and stores the reading locally along with a user-friendly environment. Thesis shows, the designed hybrid power system is economically feasible, reliable, and safe which will help to reduce the carbon emissions along with low-cost electricity.

Acknowledgments

First and foremost, thanks to Allah Almighty who gave me strength and enabled me to sail through this fantastic journey of Master's in Electrical Engineering.

I want to express my sincere gratitude to my supervisor Dr. Mohammad Tariq Iqbal, whose immense knowledge and expertise in electrical power and renewable energy proved to be generous support and a great help throughout my Master's degree. He was very helpful, accommodating, and responsive whenever I turned to him for advice regarding my research. His support during COVID-19 times in terms of being flexible was the one that allowed me to carry out my research work without feeling overwhelmed.

I also would like to thank the School of Graduate Studies, my Engineering, and Applied Sciences department, and my funding agency NSERC (Natural Sciences and Engineering Research Council), for their financial support. This support enabled me to utilize all my efforts in research without worrying about meeting my ends.

Finally, I want to thank all my teachers at Memorial University of Newfoundland, class fellows, and my family. I want to thank my parents, who have always been role models and go-to person throughout my life so far; their motivation kept me floating even during these challenging times.

Table of Contents

List of Tables

List of Figures

List of Abbreviations and Symbols

PV	Photovoltaic
MATLAB	Matrix Laboratory
HOMER	Hybrid Optimization Model for Electric Renewables
VSI	Voltage Source Inverter
SPWM	Sinusoidal Pulse Width Modulation
SVPWM	Space Vector Pulse Width Modulation
NPC	Net Present Cost
MPPT	Maximum power point tracking
MPP	Maximum power point
SCADA	Supervisory Control and Data Acquisition

Chapter 1

Introduction

1.1 Background

Electricity is a fundamental need of humans. It is just like water for human survival but different resources are being used for generating electricity which impacts the environment in different forms. At this time, the world is going through the transition phase due to global warming and abrupt temperature change. But poor countries like Pakistan, have energy crises and still rely on fossil fuels for generating electricity.

Pakistan is a South Asian country with the world's 6th most populous country with 220 million people and having an energy demand of 30,000 MW [1]. According to the economic survey of Pakistan, the installed generation capacity is 41,557 MW [2] and most of them are coal, furnace oil, and gas power plant which puts an extra burden on a politically destabilized country that highly relies on imported oil and energy resources. That ultimately put pressure on the end user and industrial consumer which causes inflation and poverty in the country. To breach this chronic ornamentation of stagnation, Pakistan requires more power from alternative resources.

The indigenous resources of power including PV and wind are the cheapest resource because both air and sunshine are free, only capital and maintenance costs decide the per unit cost of energy. Figure 1.1 shows the per unit cost of energy from different resources [3]. It can be seen from figure 1.1, that the per unit cost of electricity from oil is 25 PKR (0.1388USD, April 17, 2022) which is unjustifiable for a country that is going through a development phase. Rather than this, the social cost is highest for the conventional power plants which are the main reason for high fuel adjustment

prices (FAP) in Pakistan. Social cost is the cost that public has to bear and head up when production or consumption cost are passed on to third parties, like future generations.

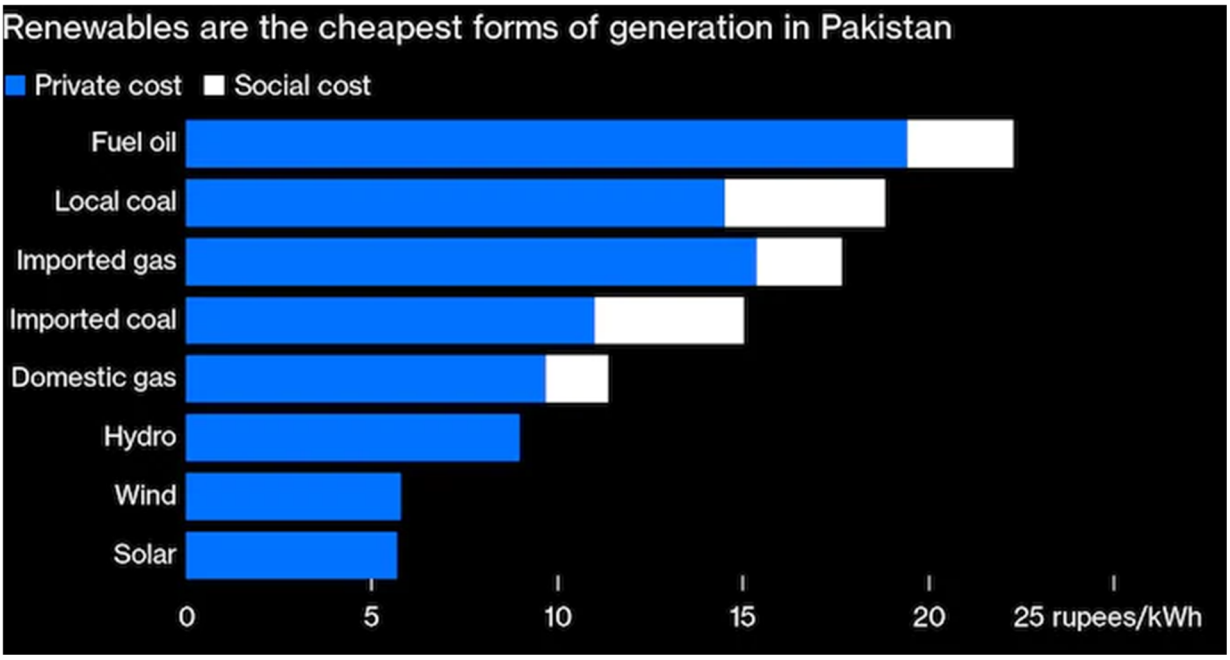

Figure 1.1: Per Unit Energy Cost Analysis in Pakistan

Other than these issues, these things produce uncertainty among investors and industrialists who hesitate to invest in such type of circumstances which might cause economic disaster. In such type of circumstances, it is inevitable to use the renewable energy potential for producing on-grid and off-grid energy.

Pakistan has massive potential for renewable energy. According to the world bank, using only 0.071 % of the total country area will be enough to meet the whole nation's demand and the overall renewable potential is 167.7 GW [4]. The wind is also abundant in Pakistan with an average speed of 7.87 m/s in Bahawalpur. The solar irradiance map is shown in figure 1.2. It can be seen that the country has widespread solar irradiance throughout the year which can be utilized effectively.

Under this dilemma, for economic development, there should be a paradigm change in power source of industries from oil to PV systems which ultimately reduced the manufacturing cost of products along with reducing carbon emissions.

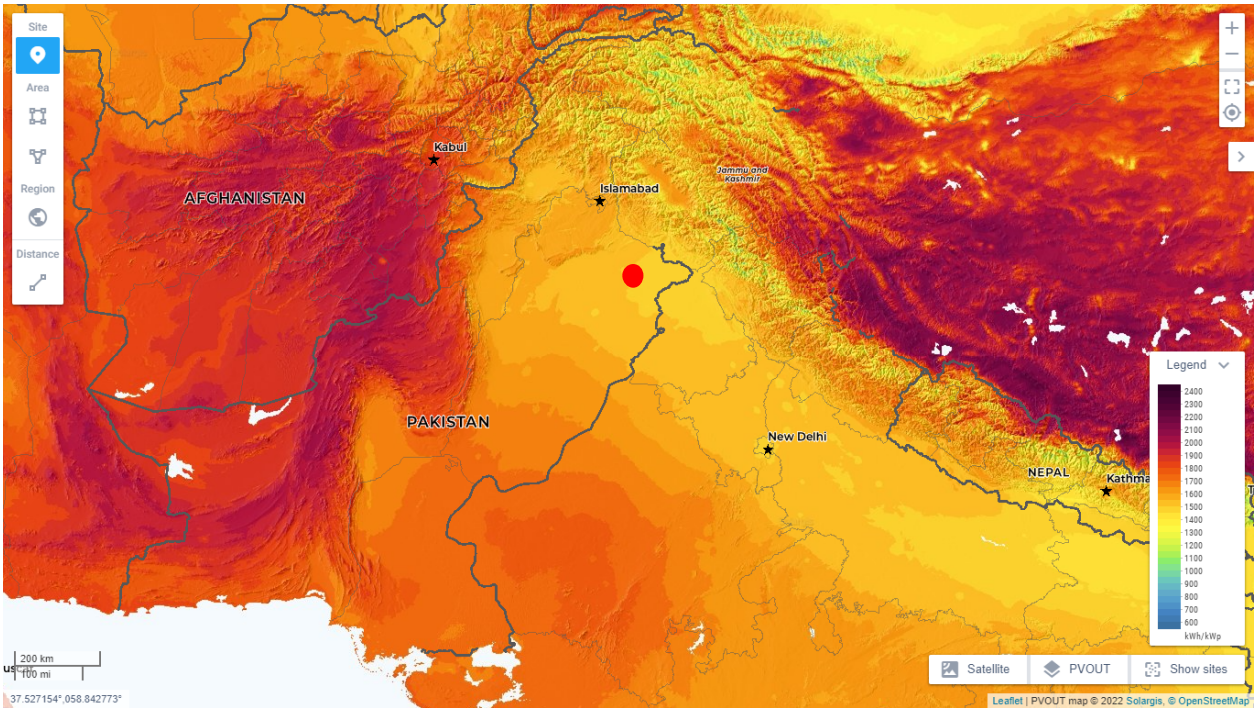

Figure 1.2: Irradiance Map of Pakistan [4]

1.2 Site Selection

The site selection plays a vital role in the feasibility of a PV power plant. Therefore, a site is selected in capital city Lahore industrial area. The selected insdustrial unit name " Shafi Texcel Limited" is a textile company and has 4 units ranging from Dying, Weaving, Processing, and Garments. Due to the different process as per product need, there is a lot of load variations for which a rugged PV system is designed. The site Global horizontal index and Direct normal index are given in figure 1.3. Figure 1.3 depicts that minimum irradiance occurs during January and it was 375.8 Wh/m^2 and the maximum occurs during April ie 569.1 Wh/m^2 [5]. Figure 1.4 shows the

angle variation of the sun with respect to the horizontal surface. The angle of the sun position concerning the north coordinate in clockwise direction is called the azimuth angle and it has a direct impact on the solar irradiance and energy output. Electrically, the site has an average load of 2485.6 kW and a peak load of 3257.7 kW with a load factor of 76 %.

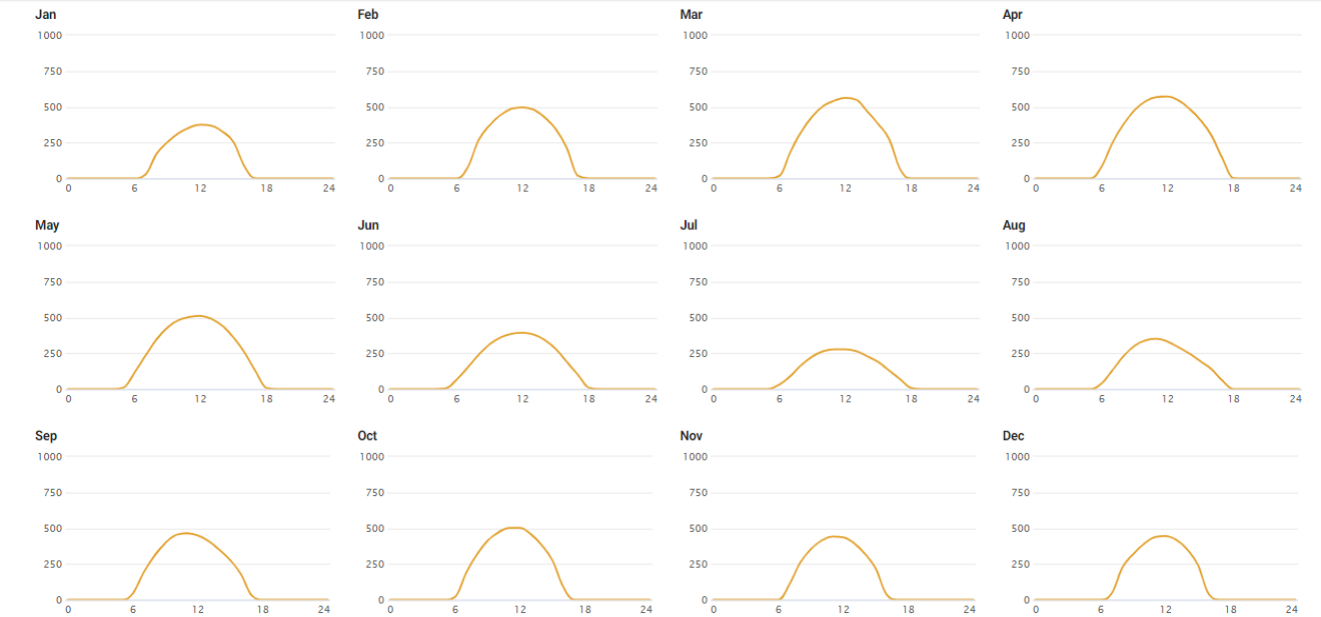

Figure 1.3: Monthly Irradiance of Selected Site

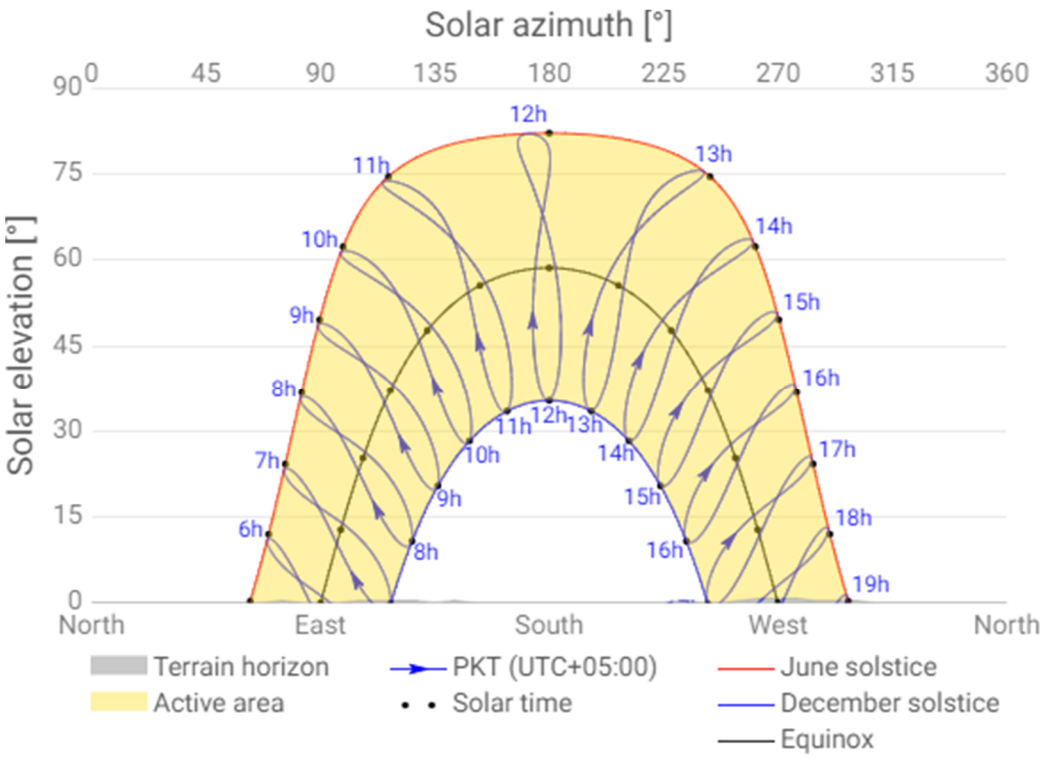

Figure 1.4: Site azimuthal angle variation throughout the year.

1.3 PV Modules

PV cell is the smallest unit of PV module. Every module is comprised of several in the range of 100 cells which defines the output voltage, current, and power of PV module. PV cell is a semiconductor material and can conduct electricity better than an insulator but not as well as conductor. When the light strikes the semiconductor, the light energy is transferred to the electrons which cause the movement of electrons called electric current. The amount of generated current depends upon the properties of striking light like wavelength and intensity of light. It can be seen from figure 1.5, that the wavelength of particular light can only cause the knocking of electrons and become a root of electric current.

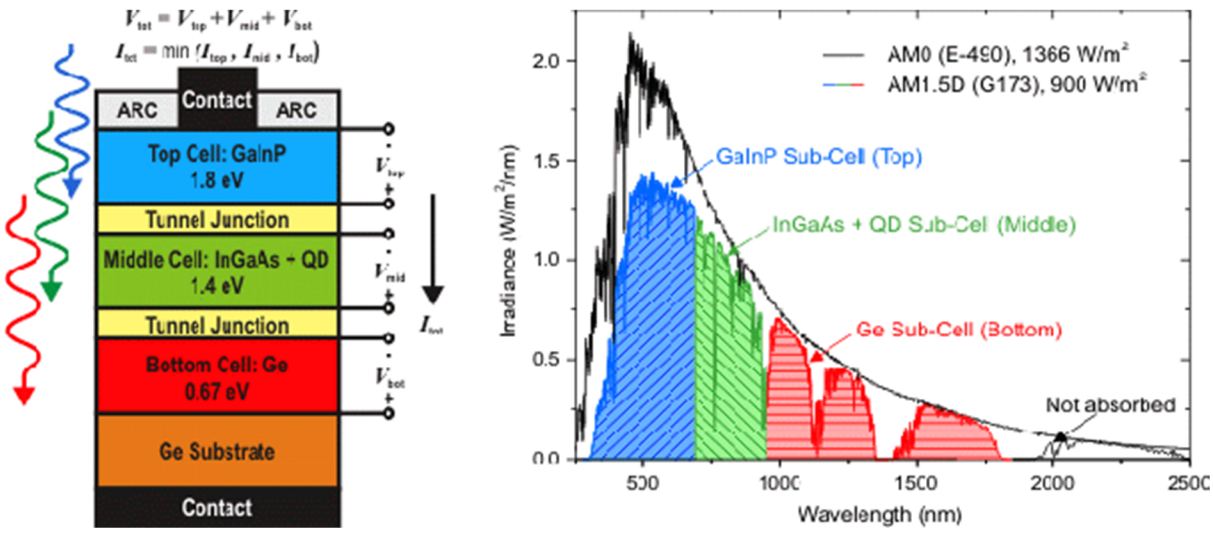

Figure 1.5: Energy band gap of PV cell [5]

The most commonly PV used at that time is divided into three types.

- Monocrystalline cell
- Polycrystalline cell
- Thin Film cell

1.3.1 Monocrystalline Cell

A monocrystalline cell is also called a single crystal silicon cell in which the whole crytal lattice of solid is continuous and prepared as an intrinsic semiconductor material. They have the highest efficiency and also need less per unit power area. However, their performance is highly affected by the temperature and also has highest price in the market. A typical monocrystalline cell is displayed in the figure 1.6.

Figure 1.6: Monoctystalline PV Panel

1.3.2 Polycrystalline Cell

A polycrystalline cell is also called a multi-crystalline solar cell which has a different crystal of silicon in a single cell. These are more eco-friendly and most of the silicon is used during the manufacturing process as compared to the monocrystalline cell. They operate within the temperature range of -40 °C to 80 °C [6] and have high power per unit area. A typical polycrystalline cell is shown in figure 1.7.

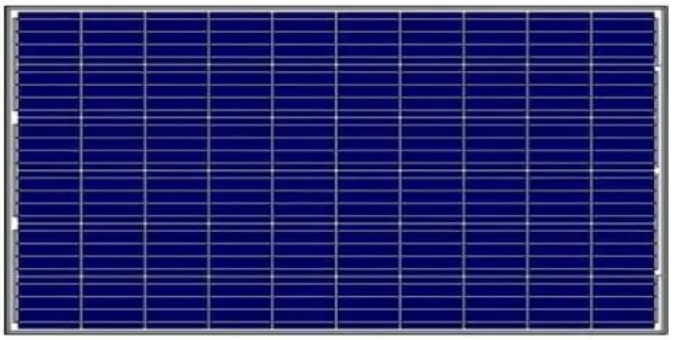

Figure 1.7: Polycrystalline PV panel

1.3.3 Thin-Film Cell

This is the second generation of solar cell which is manufactured by toppling multiple layers of PV material on a substrate. The most commonly used materials in the market are cadmium telluride (CdTe), copper indium gallium diselenide (CIGS), and amorphous thin-film silicon (a-Si, TF-Si).

The thickness varies from a few nanometers to micrometers. They have low efficiency and cost, so mainly are used for large-scale utility companies due to easiness in mass production.

Figure 1.8: Thin flim PV panel

1.4 PV Electronics

The power produced by the PV is highly dependent on the irradiance which keeps on changing continuously but it also hinges upon the load. Therefore, for getting the maximum efficiency and stable output, an electronics circuit is needed between the load and PV source. This circuitry has the following modules.

- DC-DC Converter (Controlled by MPPT Mechanism)
- DC-AC Converter (Controlled by SPWM, SVPWM)
- LCL Filter

1.4.1 DC-DC Converter

DC-DC converters are power processor that changes the output voltage level depending on the system design. Buck converter is used to lower the output voltage as compared to input voltage while on the other hand boost converter is used to up the output voltage as compared to the input voltage. The designed boost converter in the system is shown in figure 1.9.

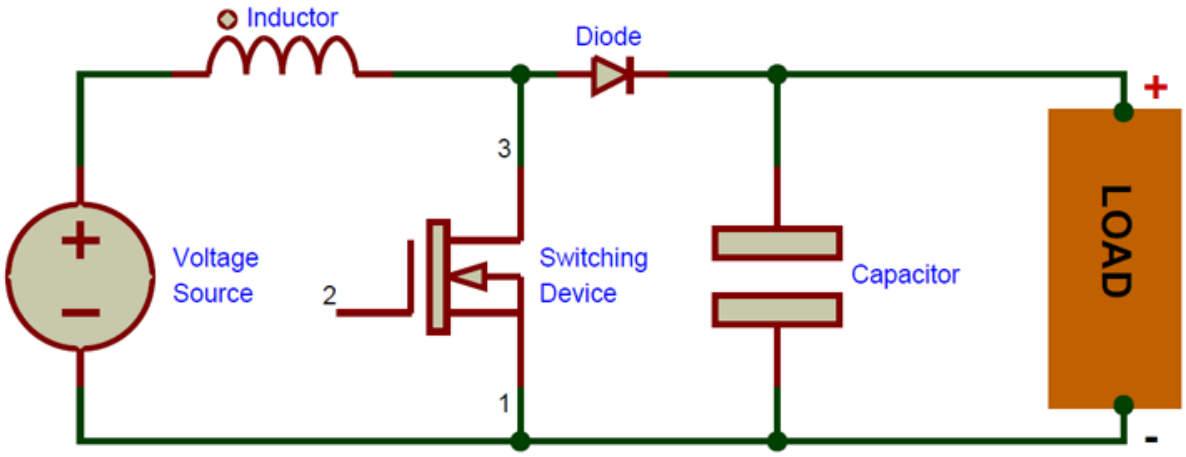

Figure 1.9: Boost converter [6]

1.4.1.1 Maximum Power Point Tracking technique (MPPT)

MPPT is a technique utilized to harvest the maximum power from any irregular power source. It is mostly renowned for PV systems but can also be implemented for wind farms and thermophotovoltaics. Photovoltaics cell has a non-linear complex between the operating environment and output power production. The fill factor is a parameter used for elaborating the non-linear behavior of a solar cell.

$$P = FF \times V_{oc} \times I_{sc}$$

Different techniques are used to extract the maximum power from the PV system. The most commonly used and computation friendly are given below.

- Perturb and observe (P & O)
- Incremental conductance (I & C)
- Incremental conductance with integral control
- Fuzzy logic based MPPT

Incremental conductance with an integral control technique is used in the designed system. The biggest disadvantage of P &O and IC method is the power oscillations at maximum point. At this time, there will be to and fro motion around that point, to overcome this issue, Incremental

conductance with integral control is used which reduced the error to zero due to the integration at the final stage.

1.4.2 DC-AC Converter

DC-AC converter is used to transform the dc power into ac because most of the load available in the industry are AC and also power grid as well.

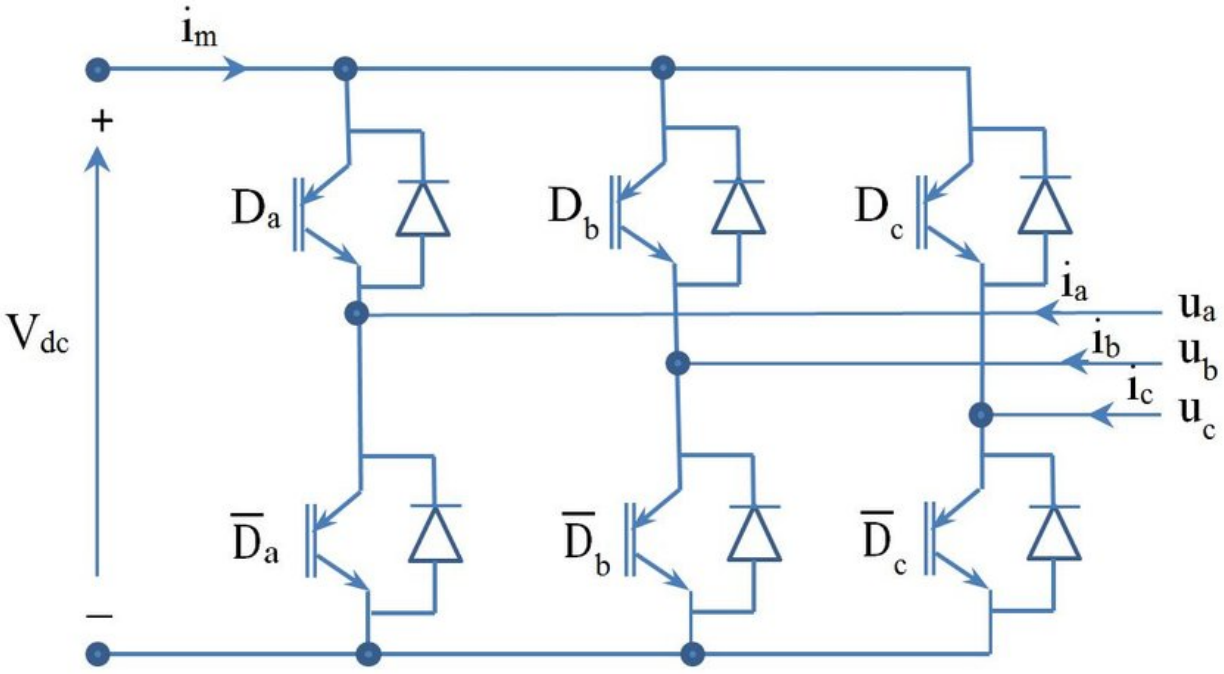

Figure 1.10: DC-AC converter [7]

During the DC-AC conversion process, different control techniques along with different hardware topologies are used. The designed system is using the neutral point clamping (NPC) topology along with the sine wave pulse width modulation technique shown in figure 1.10.

1.5 PV SCADA

Supervisory Control and Data Acquisition is commonly known by its acronym “SCADA”. The main objective of SCADA is to monitor the real-time system data on the remote sites and log this

data after a particular moment on a HOST software. There are different architectures and stages of SCADA through which it is evolved which are discussed below.

1.5.1 First Generation - Monolithic SCADA

At the time of SCADA invention, the networks didn't come into being. It is just a standalone system with no connection to any other equipment. It was furnished using the Wide area network (WAN) which communicates with the remote terminal units (RTUs). The architectural layout of a monolithic SCADA system is shown in figure 1.11 [7].

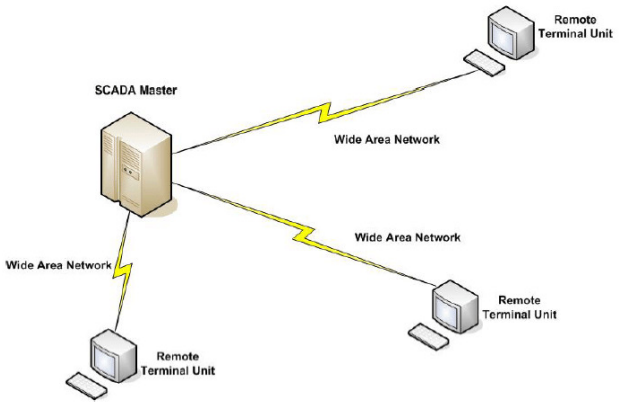

Figure 1.11: Monolithic SCADA

1.5.2 Second Generation - Distributed SCADA

The second generation of SCADA took the advantage of local area network and uses it as a communication channel with the other device which ultimately increased the range of communications. This generation is affordable and modern as compared to the forerunner generation. It also enhanced the computation power, reliability, and efficiency of system. The detailed layout of that generation is illustrated in figure 1.12 [8].

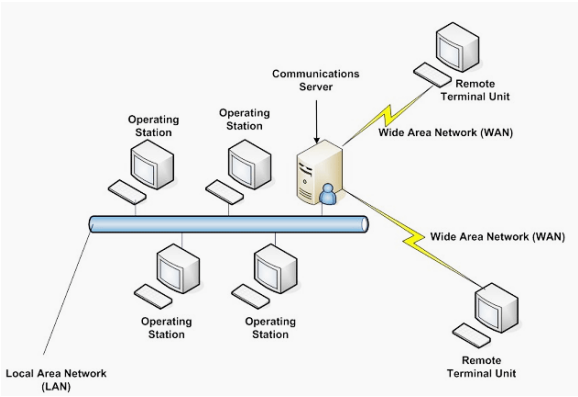

Figure 1.12: Distributed SCADA

1.5.3 Third Generation - Networked SCADA

This generation of SCADA system is similar to the 2nd generation, but it is a modified version of that one. Contrasting to the 2nd generation, networked SCADA can be connected with the internet and also other peripherals using the Internet Protocol [8].

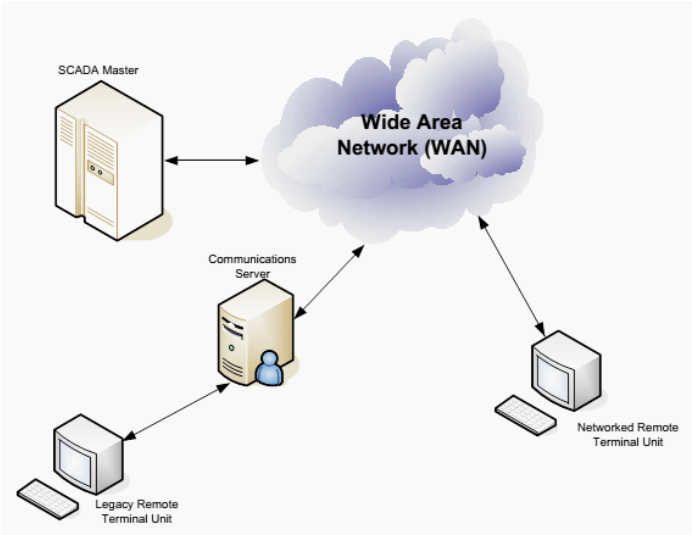

Figure 1.13: Networked SCADA

1.5.4 Fourth Generation - Internet of Things (IoT) based SCADA

Merging the conventional ie Networked SCADA with the cloud gives a most recent and advanced SCADA named as Internet of Things (IoT) SCADA which involves the use of complex data

modeling, artificial intelligence techniques, and algorithms that make it completely independent without any human intervention [9].

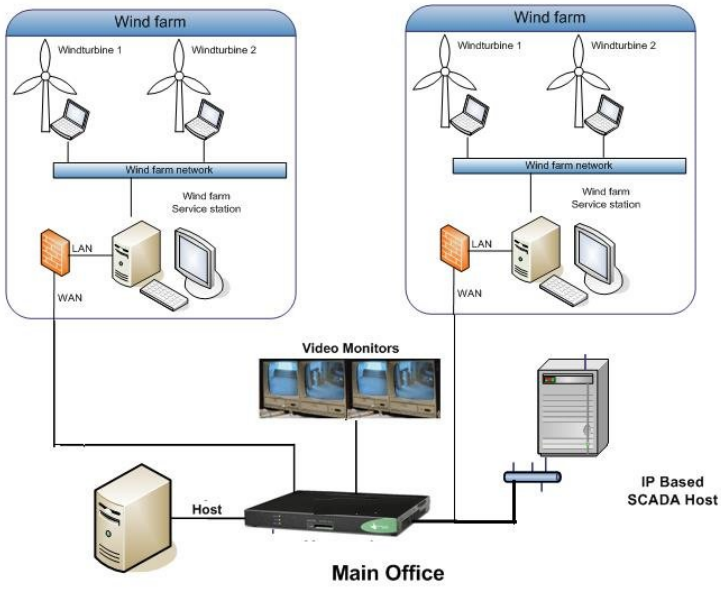

Figure 1.14: IoT SCADA

The SCADA was developed but it is mainly used for commercial purposes only and it is also manufacturer specific. It is called proprietary SCADA in which the customer has to purchase all components from the manufacturer. Companies also provide a turnkey solution but with the commercial SCADA, the reliability and security of a system are absolutely dependent on the manufacturer which stalks the user to only one option. To overcome this issue an Open source 4th generation SCADA has been developed using instruments from different manufacturers which ultimately decreases the cost of the system.

1.6 Problem Statements/Motivation

Electricity is the backbone of modern society. It is generated in remote areas and then after the transmission, it is distributed with the help of lines & feeders. It supports humanity to evolve through various stages of development. The thirst to achieve low-cost, pollution-free energy is still not over. Even in the modern 21st century, some countries are facing an energy crisis and demand &

generation shortfalls. While on the other hand, developed countries are trying to reduce carbon emissions because, in developed countries, most of the energy is produced by burning fossil fuels which are the main cause of global warming and carbon emissions. Therefore, the generation of clean, reliable, and low-cost energy is still a problem of world.

Secondly, the capital cost of clean/renewable resources is very high for generating the desired amount of power. PV and wind farms need a lot of land area for installation. Effective land management is also a major problem.

Scarcity of knowledge in the general public about the use of PV systems is also a major problem. Most of the fossil fuel-based plants are in the public area and provide employment to the local communities but they are not aware of the hazard and diseases they are getting. So, it is a need of time to make some feasibility study of PV and optimistically set some examples of PV system at a micro level.

The aim of this research part is to provide the low-cost monitoring equipment for renewable systems as compare to recent proprietary SCADA. Most of the utility companies purchase the turnkey solution from different suppliers which is out of range of small and medium organizations. Mainly, the purchase has to be dependent on a single supplier for this purpose. For that reason, open-source SCADA should be configured and programmed to monitor and control the PV system.

Therefore, this research aims to provide the optimal solution of a hybrid power system with a renewable energy mix which will reduce the per unit cost of electricity along with the carbon emission. In addition, to verify the behavior of system the dynamic modeling of the system has been done to look into the steady state and transient response of the system. For proper monitoring at lowest cost, SCADA system has been designed which shows the real-time parameters and also logs the data from hour to year.

1.7 Research Objectives

The problem statement and motivation mentioned in the previous section led to the establishment of following key objectives of this research. These are given below.

1. Analyze the potential of renewable energy in poor countries to reduce per unit cost of energy and the impact of climate change all over the world.
2. Design a hybrid power plant for an industrial unit that gives lowest possible per unit cost of energy along with the reliability and security of a system.
3. Create awareness among public and industrialists about the distributed power generation to earn revenue by selling the electricity to utility companies through net metering.
4. Study the dynamics of hybrid power plants during the load variations and abrupt irradiance change due to clouds.
5. Design a low-cost, open-source SCADA system for distributed PV generation to record the system behavior for future planning purposes.

Bibliography

[1] K. S. Khan et al., "Statistical Energy Information and Analysis of Pakistan Economic Corridor Based on Strengths, Availabilities, and Future Roadmap," *in IEEE Access,* vol. 8, pp. 169701-169739, 2020, doi: 10.1109/ACCESS.2020.3023647.

[2] M. F. Siddiqui, T. J. Soleja and A. Waseem, "A Calculation of the cost and energy savings resulting from the replacement of conventional lighting with led lighting for Karachi, Pakistan," *2017 Asian Conference on Energy, Power and Transportation Electrification (ACEPT)*, 2017, pp. 1-3, doi: 10.1109/ACEPT.2017.8168605.

[3] N. Jamal and O. Hohmeyer, "Solar resources' potential role in the development of renewable based electric power system by 2050: The case of Pakistan prospects of solar in Pakistan," *2014 International Conference on Energy Systems and Policies (ICESP)*, 2014, pp. 1-7, doi: 10.1109/ICESP.2014.7347005.

[4] N. Jamal and O. Hohmeyer, "Solar resources' potential role in the development of renewable based electric power system by 2050: The case of Pakistan prospects of solar in Pakistan," *2014 International Conference on Energy Systems and Policies (ICESP)*, 2014, pp. 1-7, doi: 10.1109/ICESP.2014.7347005.

[5] General Discussion, "Best solar panel for cloudy days" https://diysolarforum.com/threads/best-solar-panel-for-cloudy-days.4098/ (accessed Aug. 5, 2022).

[6] Boost Converter, "Medium" https://medium.com/@kekreaditya/boost-converter-a66846520eea (accessed Aug. 5, 2022).

[7] T. H. Pham, L. Lefevre, D. Genon-Catalot, and V. T. Pham, "An energy-based control model for autonomous lifts," *IECON 2014 - 40th Annual Conference of the IEEE Industrial Electronics Society. IEEE,* Oct. 2014. doi: 10.1109/iecon.2014.7049147.

[8] S. Kanwal, B. Khan and M. Q. Rauf, "Infrastructure of Sustainable Energy Development in Pakistan: A Review," *in Journal of Modern Power Systems and Clean Energy*, vol. 8, no. 2, pp. 206-218, March 2020, doi: 10.35833/MPCE.2019.000252.

[9] R. Islam and M. M. Abrar, "Comparative Analysis of a Bifacial and a Polycrystalline Solar Cell Device Performances by Optimizing Effective Parameters Using PC1D," *2020 International Conference on Smart Grid and Clean Energy Technologies (ICSGCE)*, 2020, pp. 16-20, doi: 10.1109/ICSGCE49177.2020.9275602.

[10] R. H. McClanahan, "The benefits of networked SCADA systems utilizing IP-enabled networks," *2002 Rural Electric Power Conference. Papers Presented at the 46th Annual Conference (Cat. No. 02CH37360)*, 2002, pp. C5-1, doi: 10.1109/REPCON.2002.1002297.

[11] V. Stanisavljević, "Near real-time data aggregation using foreign data wrappers from a network of sensors," *2019 18th International Symposium INFOTEH-JAHORINA (INFOTEH)*, 2019, pp. 1-5, doi: 10.1109/INFOTEH.2019.8717758.

[12] N. Du and H. Hu, "Robust control of Mono-T-Semiflow Processes with resources using Petri nets," *2016 IEEE 55th Conference on Decision and Control (CDC)*, 2016, pp. 4778-4784, doi: 10.1109/CDC.2016.7798998.

Co-authorship Statement

I am the main author of all the research papers compiled in composing this thesis, and my supervisor, Dr. M. Tariq Iqbal, is a co-author of all articles. As the lead author, did most of the research work, did the literature reviews, carried out the designs, hardware implementations, experimental setups, and analysis of the results in each of the manuscripts. I also formulate the original manuscripts and later edited each of them based on comments from the co-author and peer reviewers throughout the peer review process. Co-author Dr. M. Tariq Iqbal supervised all the research work, revised, and corrected each one of the manuscripts, acquired the funding, provided research material, contributed research ideas throughout the research, and updated each of the manuscripts.

Chapter 2

Design of an Optimal Hybrid Energy System for a Captive Power Plant in Pakistan

Preface

A version of this manuscript has been peer-reviewed, accepted, and presented in the conference proceedings of the ***2021 IEEE 12th Annual Information Technology, Electronics and Mobile Communication Conference (IEMCON).*** *The paper has also been published on IEEE Xplore Database as a part of the* ***IEEE IEMCON 2021 conference proceedings (doi: 10.1109/IEMCON53756.2021.9623260)****. I am the primary author, and I carried out most of the research work performed the literature reviews, carried out the system design, implementations, and analysis of the results. I also prepared the first draft of the manuscript and subsequently revised the final manuscript based on the feedback from the co-author and the peer review process. The Co-author, Dr. M. Tariq Iqbal, supervised the research, acquired and made available the research funding, provided the research guide, reviewed and corrected the manuscript, and contributed research ideas to the actualization of the manuscript.*

Abstract

This paper is about the design and feasibility of a grid-connected hybrid power system for an industrial unit. Due to the increase in greenhouse gases by burning fossil fuels, it is necessary to generate electricity from renewable resources. Solar energy is dependent on solar irradiance, which varies from site to site. A site (Shafi Texcel Limited) is selected, which is situated on Raiwind Manga Road Lahore, Pakistan. The average load demand is 2415 kW, for which a hybrid captive power plant has been designed. The sources of electricity are Grid, CATERPILLER Gas & Diesel GENSET, and the proposed solar system. For this system, optimization analysis has been carried out using HOMER and PVWatt software. Three different grid-connected cases are considered with 0% renewable energy (RE) constraints, 70% RE constraints, and with battery storage. The system parameters are different for each case and land requisition analysis has been done using PVWatt. The NPC, cost of energy, capital cost, replacement cost for each case has been discussed in detail. The result shows that the proposed system is suitable for a selected site and can provide significant saving. At the end, final results and possible future work has been discussed.

Keywords- Hybrid Power System; Solar Energy; Renewable Energy; HOMER Pro; PVWatt.

2.1 Introduction

Electricity is the fundamental need of every human. It is generated using different resources like hydro, coal, gas, furnace oil, etc. Recently, most generation is done using conventional resources which emit carbon dioxide in the environment and cause global warming. Countries like Pakistan are going through the phase of development and Industrialization; if they rely on conventional resources, it will be harmful to the environment and nature. Mostly, the electricity generation is done with coal, gas, or furnace oil, as Pakistan imports all these non-renewable energy sources

from different countries, which ultimately puts a burden on the economy and end-user in additional cost.

Therefore, a hybrid power system is essential for meeting the electrical load demand of consumers with low cost. While on the other hand, Pakistan has massive potential for solar energy with average solar insolation of 5.5 kWh/m^2/day and a potential of up to 100,000 MW using solar energy [1]. Figure 2.1 shows the electricity generation mix of Pakistan. More than 60% is generated from fossil fuels and more than 33% is generated from hydel.

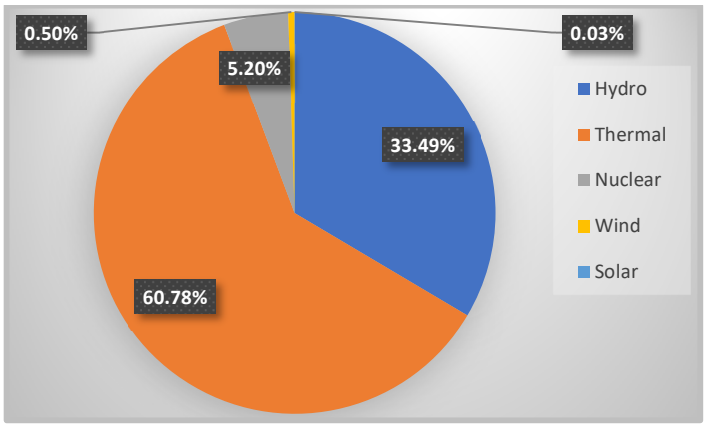

Figure 2.2: Electricity Generation Mix of Pakistan [2]

Figure 2.2 shows the solar insolation distribution in Pakistan, which clearly indicate that Pakistan has greater solar resources which could be used. These are the facts that encourage use of photovoltaic power to produce electricity and incorporate solar energy at commercial and industrial levels. In this thesis, the selected site is the premises of Shafi Texcel Limited, Lahore, Pakistan for which feasibility and cost analysis has been done using HOMER Software. The site detail and load calculation will be discussed in the second part of this paper. In the third part, the optimization of the solar system and the cost analysis has been elaborated using the HOMER software. Finally, in the end, some results, conclusion, and future work is discussed.

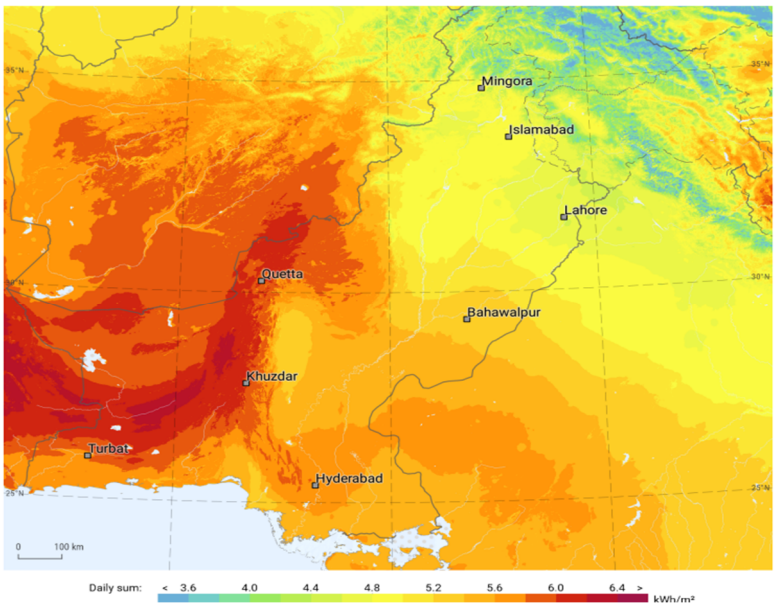

Figure 2.3: Solar Insolation levels in Pakistan [3]

2.2 Site Details and Load Calculation

2.2.1 Selected Site

First, the selected site is Shafi Texcel Limited situated on 4.5km Raiwind Manga Road, Lahore, Punjab 55150 Pakistan (31.2616, 74.1674). Figure 2.3 shows the location of site on google maps. It has more than 5 hectares of land located at the back end of factory area premises that could be used for solar installation. Figure 2.4 shows a view of selected site. Roof areas cannot be used because it has many ventilation fans, ducts, and other equipment.

Figure 2.3: Location of the Site on Google Map

Figure 2.4: Front View of the Site

2.2.2 Selected site solar insolation details

Solar irradiance is an important parameter for site feasibility. It is the light energy of sun measured at a particular site. From Figure 2.5, it can be observed that solar radiation is available throughout the year and its values vary between 3.05 to 6.90 kWh/m^2/day. The clearance index is the parameter to measure the clarity of atmosphere. Figure 2.5 also shows that for selected site.

$$\text{Clearance Index} = \frac{\text{Surface radiation}}{\text{Extraterrestrial radiation}} \qquad \text{Eq. (1)}$$

Its value is always less than one and changes between 0.556 to 0.633 throughout the year.

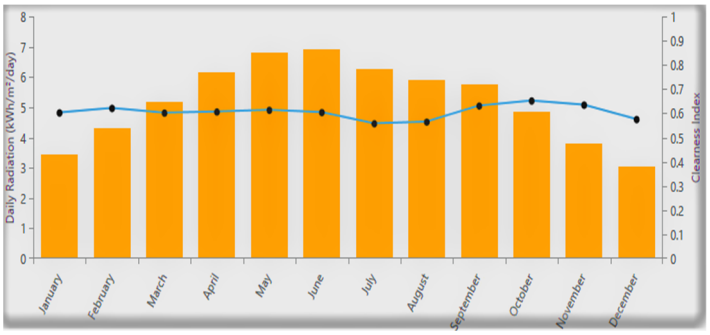

Figure 2.5: Irradiance and Clearance Index of the Site

2.2.3 Selected site electrical load detail details

The site Electrical Load is recorded and was obtained from the site. The significant load in the industry is inductive due to the use of motors for different pumps, compressors, fans, water

turbines, etc. The hourly data of load has been collected for the year 2020, and the corresponding monthly load profile is given below in Figure 2.6. The load profile in Figure 2.7 shows that the average consumed units per day are 59655, and average & peak load over the year is 2485.6 kW & 3257.7 kW. In Figure 2.6, load dips in April, June and September are due to the Covid-19 lock down imposed by the provincial government.

Load factor is the efficient utilization of electrical power network, and it can be derived from the above-given load data.

$$\text{Load Factor (LF)} = \frac{\text{Average Load}}{\text{Peak Load in given period}} \qquad \text{Eq. (2)}$$

$$\text{LF} = \frac{2485.6}{3257.7}$$

$$\text{LF} = 0.76$$

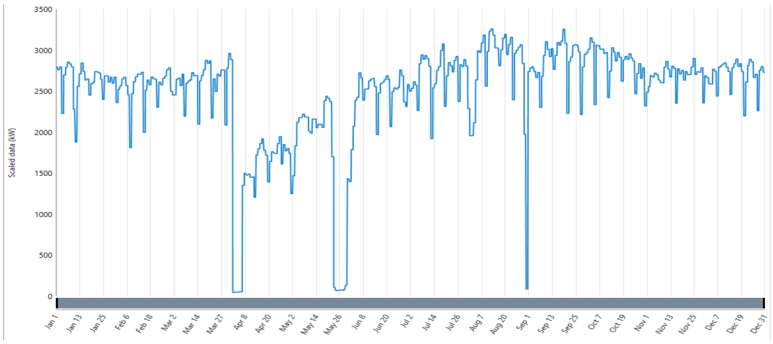

Figure 2.6: The Site Electrical Demand

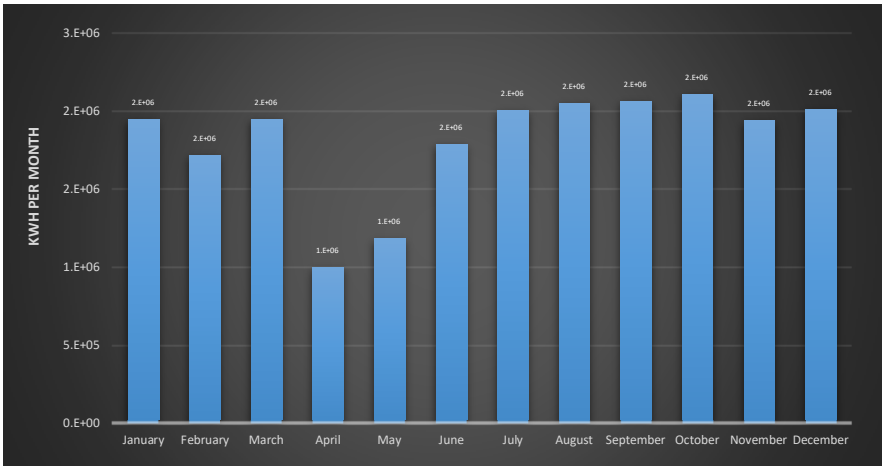

Figure 2.7: Monthly Electrical Consumption

2.3 Plant Electrical Layout

Plants are designed for flexibility in operation and maintenance without affecting the end-user. Because a continuous supply is essential for the reliable operation and customer satisfaction. Therefore, the captive power plants are designed efficiently with backup resources to supply 24/7 without any interruption. The Single Line Diagram of power flow of site is given in Figure 2.8.

In the above diagram, different sources are used for the supply of power to the load. Overall, Solar & Grid will be utilized maximum, and Gas & Diesel generators will act as backup sources. Because during the heavy storm, due to overhead transmission of grid network, the grid is highly unreliable and may cause tripping at any time. In such a scenario, Gas & Diesel GENSETS act as a backup source of power. The detailed structure, constraints, efficiency of each source is discussed below.

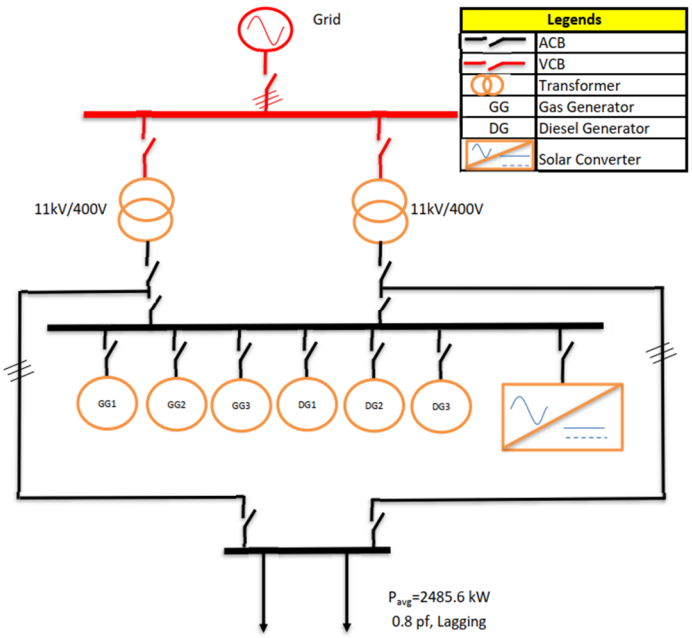

Figure 2.8: Single Line Electrical Diagram of the Site

2.3.1 Grid

Grid is an infinite bus source of power and can tackle high load variations as well. Lahore Electric Supply Company (LESCO) is a power distribution company on our selected site. It offers different tariffs as per load requirement and time of use. The contracted load as per load demand is 3500

kW, for which tariff B3 (14)T is applicable in which 20.39 PKR/kWh is charged for peak load, and 12.61 PKR/kWh charges for off Peak. The Government also offer subsidy of 1.8-1.3 Rs/kW/M [4].

Maximum demand indication (MDI) is also applied per month based on the meter reading. Peak demand is considered to be maximum if it is available for more than 15 minutes. It is charged 380 PKR/kW/M[5].

Power factor (pf) limit is also very important for taking power from grid. LESCO set pf limit to 0.9; if pf is less than 0.9, a low power factor penalty will be added to the bill because low pf disturbs the voltage level of the grid and puts extra stress on power system equipment.

2.3.2 Gas Generators

A gas generator uses natural gas to produce electricity with the help of a 4 Stoke gas engine. It has four stages to complete one power cycle i.e. intake, compression, power, and exhaust stokes. The engine's thermal efficiency is between the 35-45% and depends mainly on the intake air temperature [6]. Sui Northern Gas Pipelines Limited (SNGPL) is the distributor of gas. Caterpillar GENSET 3516 B has been selected for generation. It is 1030 ekW rating with a fuel consumption of 9776 Btu/kWh at 100 % load [7]. With the help of following equation, we can find the fuel consumption in m^3.

$$\text{mmBTU} = \frac{\text{HM}^3 \text{ x GCV}}{281.7385} \qquad \text{Eq. (3)}$$

$$9776 \text{ x } 10^{-6} = \frac{\text{M}^3}{100} x \frac{1000}{281.7385}$$

$$\text{M}^3 = 0.2754 \text{ m}^3/\text{kWh}$$

The efficiency of engine varies with load. The efficiency-load curve is given in below Figure 2.9.

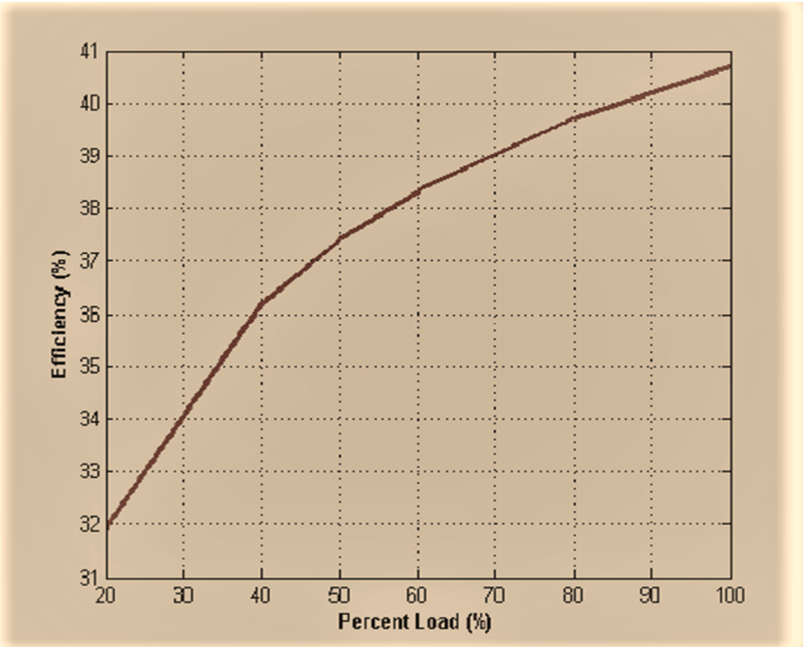

Figure 2.9: Engine Efficiency w.r.t Load for Gas Generator

Other than the operations mentioned above, some preventive maintenance schedules have to follow for the reliable and secure operation of the plant. Engine Oil and Filter should be changed entirely after 2000 hours of service. The average lube oil consumption of engine is 0.21 liters/hr @ 1030 kW [7] continuous power and oil sample testing should be done after 1000 hours to get an idea about the condition of mechanical components. RIMULA R4X 15W40 is used as lube oil [8], which prevents the deposit of impurities in the engine and improves engine and oil durability.

2.3.3 Diesel Generators

Diesel Engines also act as a backup source of power and use in a standby position. CAT 3512[9] model is used at the selected site, which has a power rating of 1056 ekW. The main difference between gas and diesel engine is the spark plug. Diesel Engines don't have spark plugs and ignition is caused by the rise in temperature due to compression. The visualization of Diesel Engine working is given Figure 2.10. The CAT 3512 Engine has a fuel consumption of 0.28 L/kWh [10]. Like the gas engine, its lube oil and filter also need to be changed every 2000 hours. Due to the

high price of High-Speed Diesel (HSD) per unit marginal cost of a diesel engine is high from all other resources. Therefore, the use of diesel is the last option in the standby power.

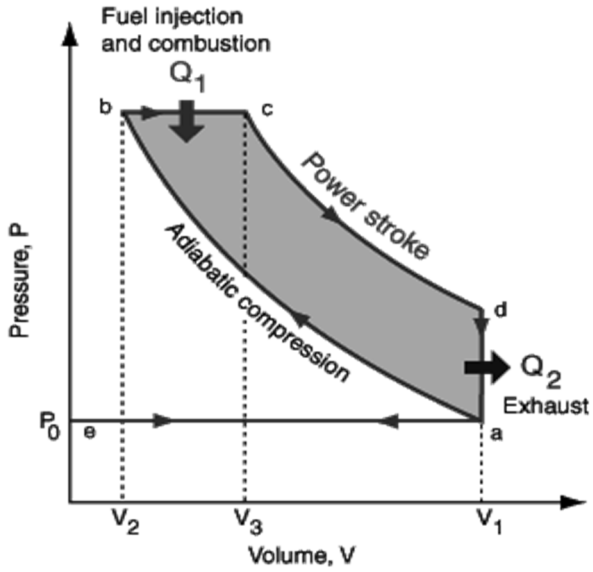

Figure 10: Four Stokes of Engine

2.4 Optimization of PV Based Captive Power Plant

For optimization of power plant, a computer tool named as HOMER (Hybrid Optimization Model for Electric Renewables) is used which was originally developed at National Renewable Energy Laboratory (NREL) [11]. In the software, the load data of one year is entered in the CSV file, on which basis HOMER has done the PV module, Solar Converter, and Storage sizing. At the end, HOMER rate the selected configuration based on Net Present Cost (NPC) and levelized cost analysis.

The configuration of the system designed in HOMER is shown in the Figure 2.11. It has two buses: Alternating Current (AC) & Direct Current (DC). DC bus voltage is 806 V_{dc} and AC bus voltage is 400V_{ac}. DC bus is connected with 480 W flat plate solar module of ENN Solar Energy480EST-480[12] with a derating factor of 85 % due to dust and high temperature.

AC bus voltage is 400 V_{rms}. Gas Genset 3516B, Diesel Generator 3512, Grid and load is connected with AC bus. Two buses are connected with the help of a solar converter. Eaton Power Xpert 2250kW[13] is used to convert the DC voltage into the AC voltage. For sizing and cost analysis different cases are considered whose detail is given below.

2.4.1 Case 01-Without Storage and Zero RE Constraint:

This case is shown in Figure 2.11. There are no constraints on the production of renewable energy from solar. In below Figure 2.12 the sizing results are shown. Figure 2.13 depicts that system takes 50.9 % of electricity from solar energy. Solar Modules having total capacity of 8382 kW along with 3119 kW Eaton inverter are required.

The analysis of land requirement has also been done in PVWatts because the availability of land is a key factor in solar installation. The landmarking and PV system capacity results are shown in the Figure 2.14.

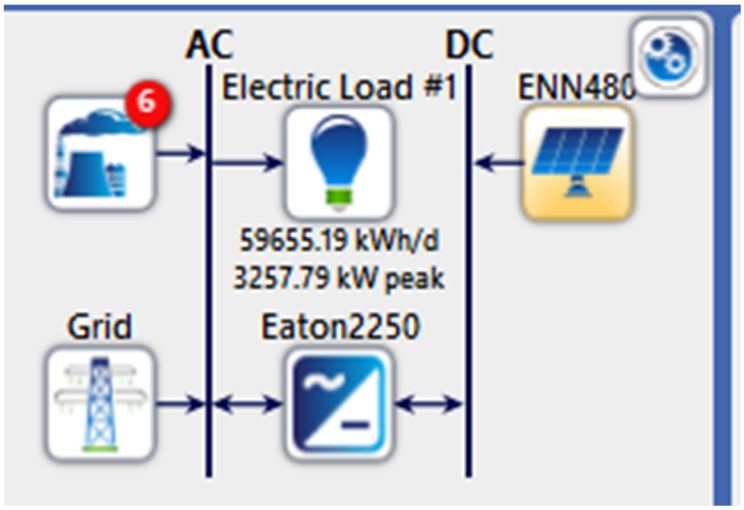

Figure 2.11: Schematic of System without Storage

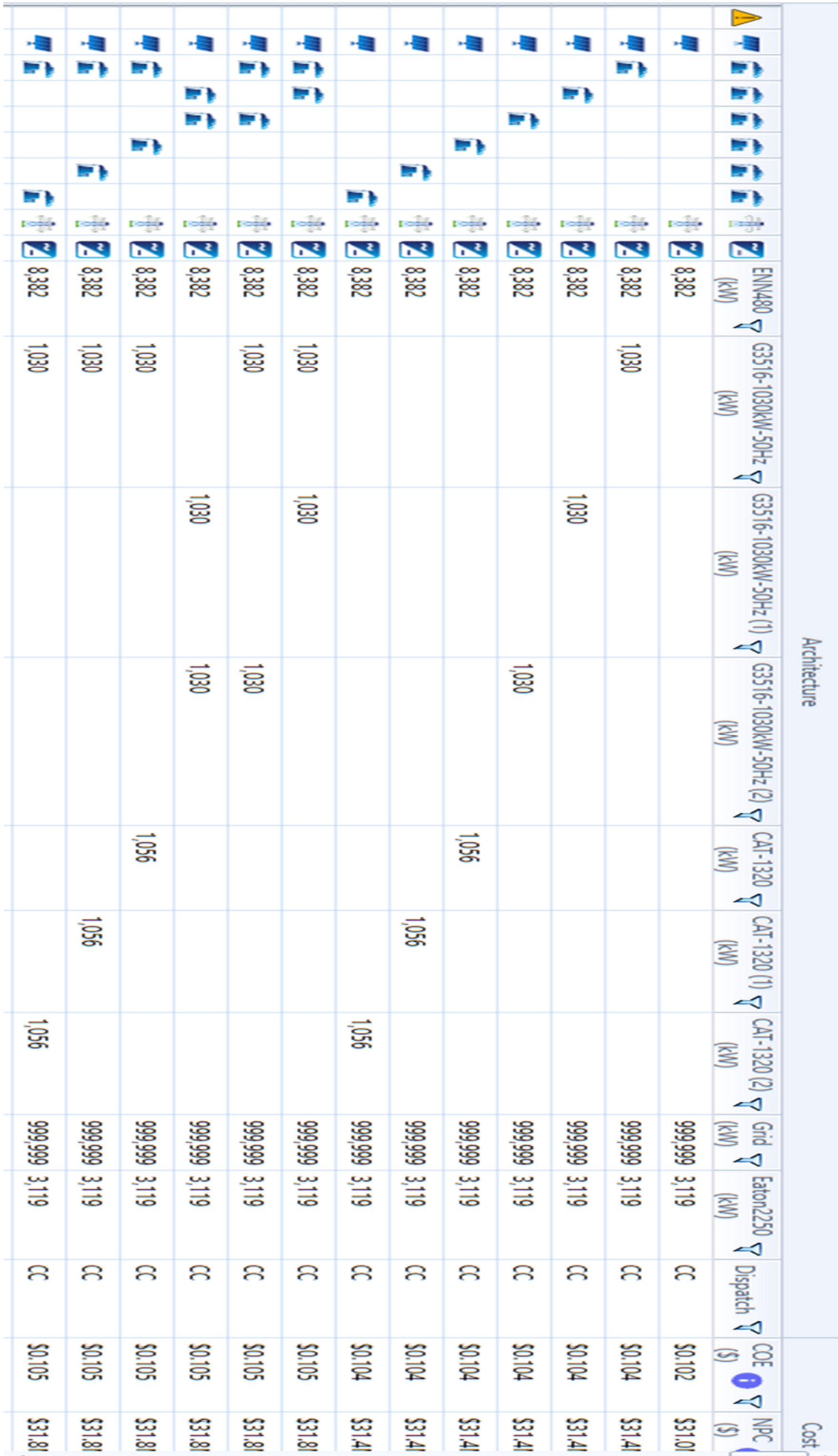

Architecture											Cost	
ENN480 (kW)	G3516-1030kW-50Hz (kW)	G3516-1030kW-50Hz (1) (kW)	G3516-1030kW-50Hz (2) (kW)	CAT-1320 (kW)	CAT-1320 (1) (kW)	CAT-1320 (2) (kW)	Grid (kW)	Eaton250 (kW)	Dispatch	COE ($)	NPC ($)
8,382							999,999	3,119	CC	$0.102	$31.0
8,382	1,030						999,999	3,119	CC	$0.104	$31.4
8,382		1,030					999,999	3,119	CC	$0.104	$31.4
8,382			1,030				999,999	3,119	CC	$0.104	$31.4
8,382				1,056			999,999	3,119	CC	$0.104	$31.4
8,382					1,056		999,999	3,119	CC	$0.104	$31.4
8,382						1,056	999,999	3,119	CC	$0.104	$31.4
8,382	1,030	1,030					999,999	3,119	CC	$0.105	$31.8
8,382	1,030		1,030				999,999	3,119	CC	$0.105	$31.8
8,382		1,030	1,030				999,999	3,119	CC	$0.105	$31.8
8,382	1,030			1,056			999,999	3,119	CC	$0.105	$31.8
8,382	1,030				1,056		999,999	3,119	CC	$0.105	$31.8
8,382	1,030					1,056	999,999	3,119	CC	$0.105	$31.8

Figure 2.12: Optimization Results without Storage

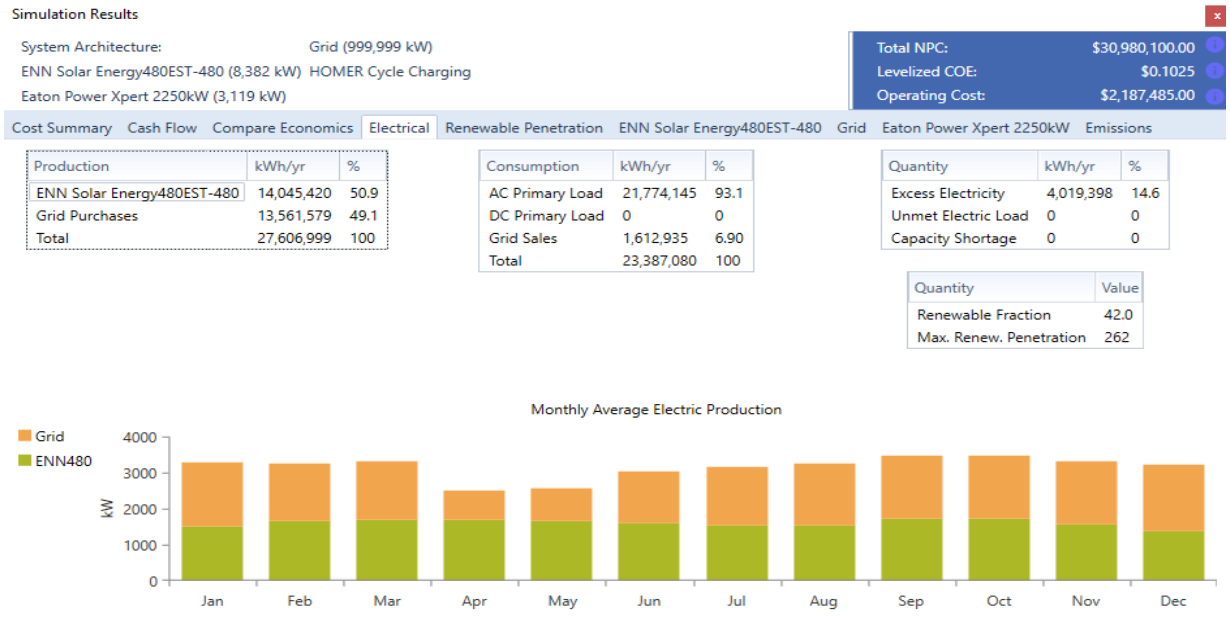

Figure 2.13: Simulation Results in HOMER (0% Constraint)

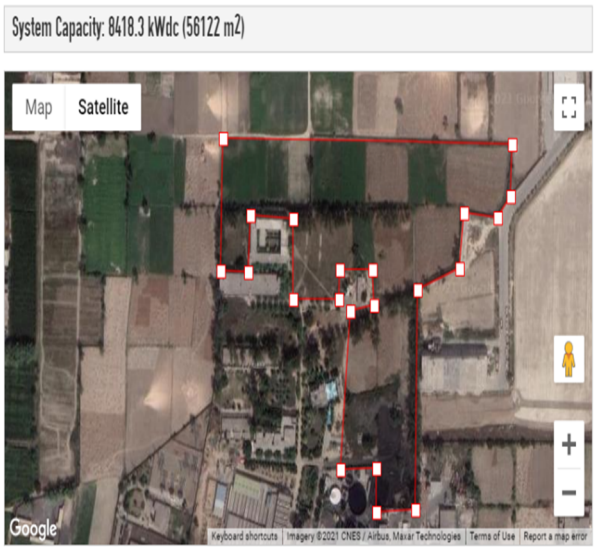

Figure 2.14: Parameters for 8382kW$_{dc}$ PV System

DC System Size	8418.3 kW
Module Type	Standard
Array Type	Fixed (open rack)
Array Tilt	20°
Array Azimuth	180°
System Losses	14.08%
Inverter Efficiency	96%
DC to AC Size Ratio	1.2
Economics	
Average Retail Electricity Rate	No utility data available
Performance Metrics	
Capacity Factor	15.8%

Figure 2.15: Land Marking for 8382 kW$_{dc}$ System

The cost analysis has also been done in the HOMER for zero storage system. For this purpose, prices of ENN Solar Energy480EST, Eaton solar inverter and CATERPILLER engines has been used.

Final cost results have been depicted in the Figure 2.16 and it can be seen that the total cost of equipment installation and operation over its whole life span named net capital cost is $

30,980,100. Levelized cost is the net present cost of electricity generation over the entire life of plant, it is $ 0.1025 for our selected site. The operating cost is $ 2187485; initial capital cost was found to be $ 2701344.87. The component level Net Present Cost (NPC) over 25 years of life is given below Table 2.1.

The cash flow analysis result has been shown in the below Figure 2.17. The upfront capital required for the entire system is $ 2701344.87. Every year operating cost of $ 2185148.24 will be consumed and at 15 years, the replacement of component $ 87721.24 will be invested. At the end of 25 years, $ 29240.41 salvage value is expected.

Table 2.1: NPC of Components in the Proposed PV System (0% Constraint)

Sr. #	Component	NPC ($)
1	Eaton Power Xpert 2250 kW	242073.53
2	ENN Solar Energy480EST	4440394.08
3	Grid	26297630.35
4	System	30980097.97

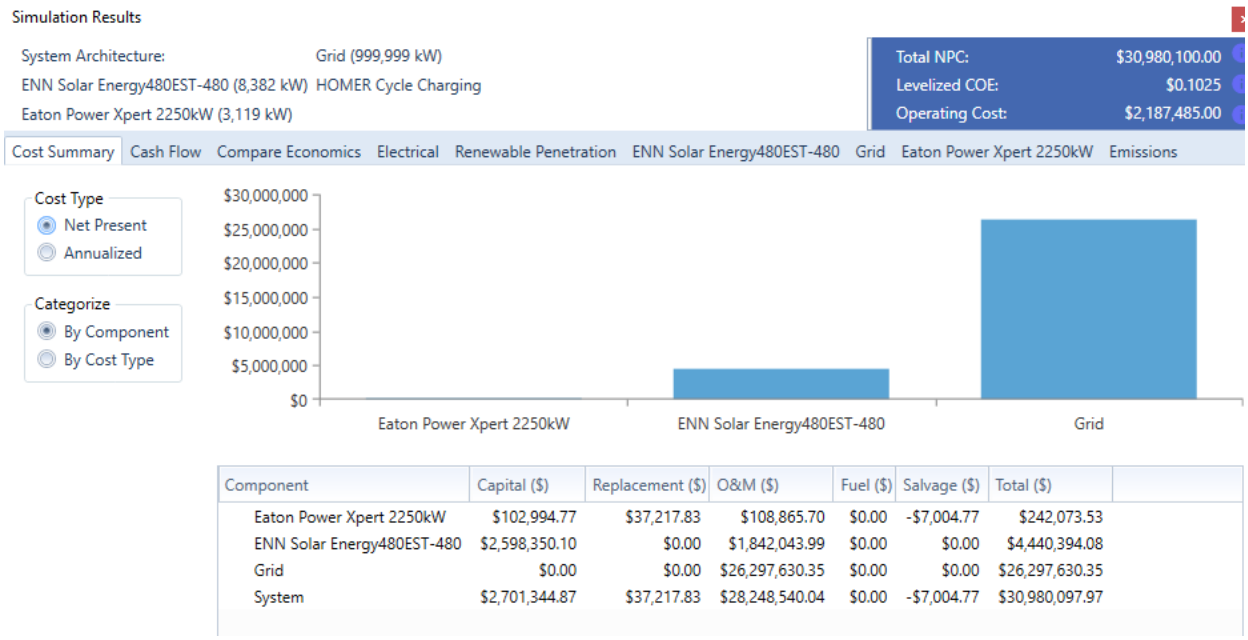

Figure 2.16: Cost Summary of 8382kW PV System

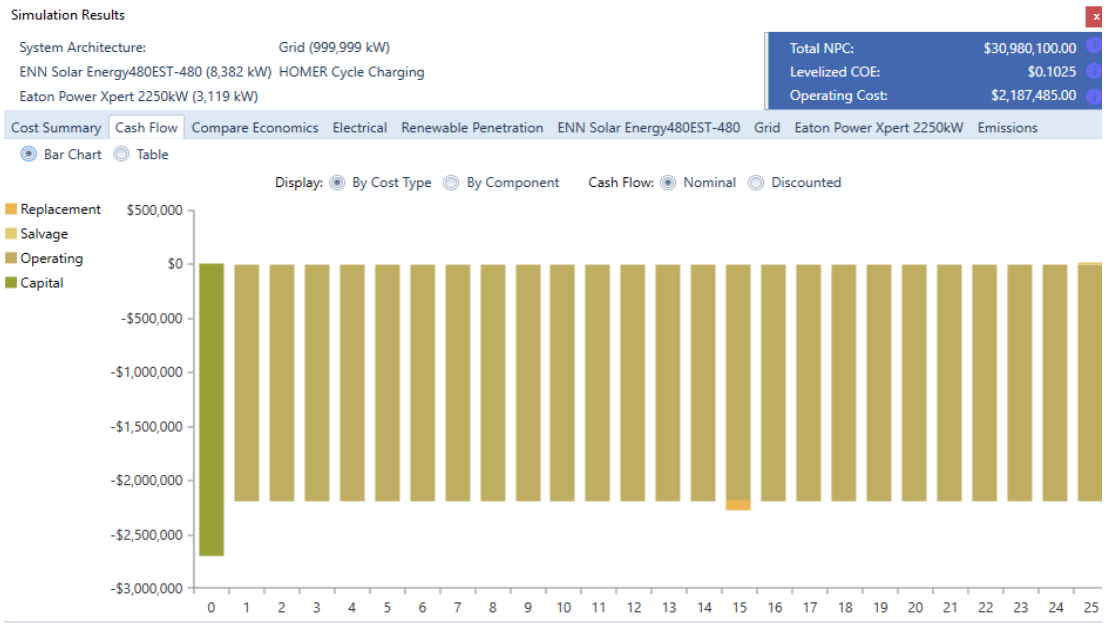

Figure 2.17: Cash Flow of 8382 kW PV System

- HOMER uses the following techniques for calculating the different costs of system.

Net present cost (NPC) represents the total operations and installation cost of the system over its entire life, which can be calculated as follow.

$$NPC = \frac{TAC}{CRF}(i, Rpr_j) \qquad \text{Eq. (4)}$$

Where TAC is total annualized cost ($), CRF is capital recovery factor, i is the interest rate and Rpr_j is project lifetime in years. Total annualized cost is the total accumulative sum of cost of each component of power system, including the capital, operation & maintenance fuel, and replacement cost.

Capital recovery factor is a ratio that is used to determine the present value of a series of equal yearly cash flows

$$CRF = \frac{i \times (1+i)^n}{(1+i)^{n-1}} \qquad \text{Eq. (5)}$$

Where n is the number of years and i is annual real interest rate.

Cost of energy (COE) is the average price of per kWh of electric energy. It can be calculated as follow.

$$COE = \frac{TAC}{L_{prim,AC}+L_{prim,\ DC}} \qquad \text{Eq. (6)}$$

Where, $L_{(prim,AC)}$ is the AC primary load and $L_{(prim,DC)}$ is primary DC load.

2.4.2 Case 01-Without Storage and Zero RE Constraint:

The extension plan is essential for every power plant. The electrical load demand is increasing day by day due to the increase in population and industrialization. Therefore, the plants should be in that area where enough land is available for future extension.

A constraint is putted to generate the 70 % electricity from PV power plant for the extension of solar power. The Figure 2.18 shows the optimum results that depicts that 18175 kW_{dc} capacity of solar ENN Solar Energy480EST modules are required along with 11990kW Eaton solar inverter. The analysis of land requisition for solar plant is done using PVWatt NREL tool. The land available for future extension is 156317 m^2, on which solar modules of 23447.5 kW with tilt angle of 20^o can be installed freely.

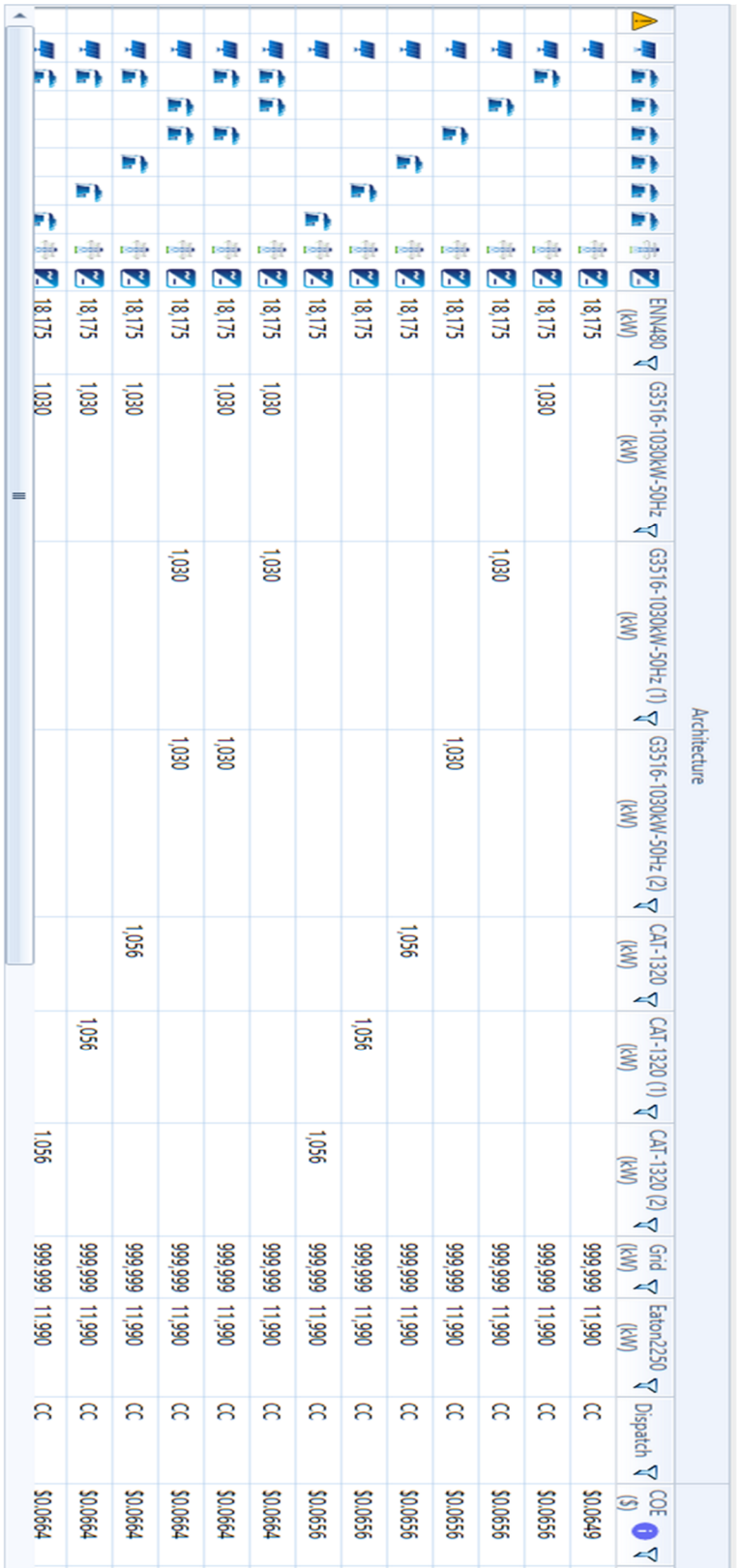

Figure 2.18: Optimization Results without Storage (70% RE Constraint)

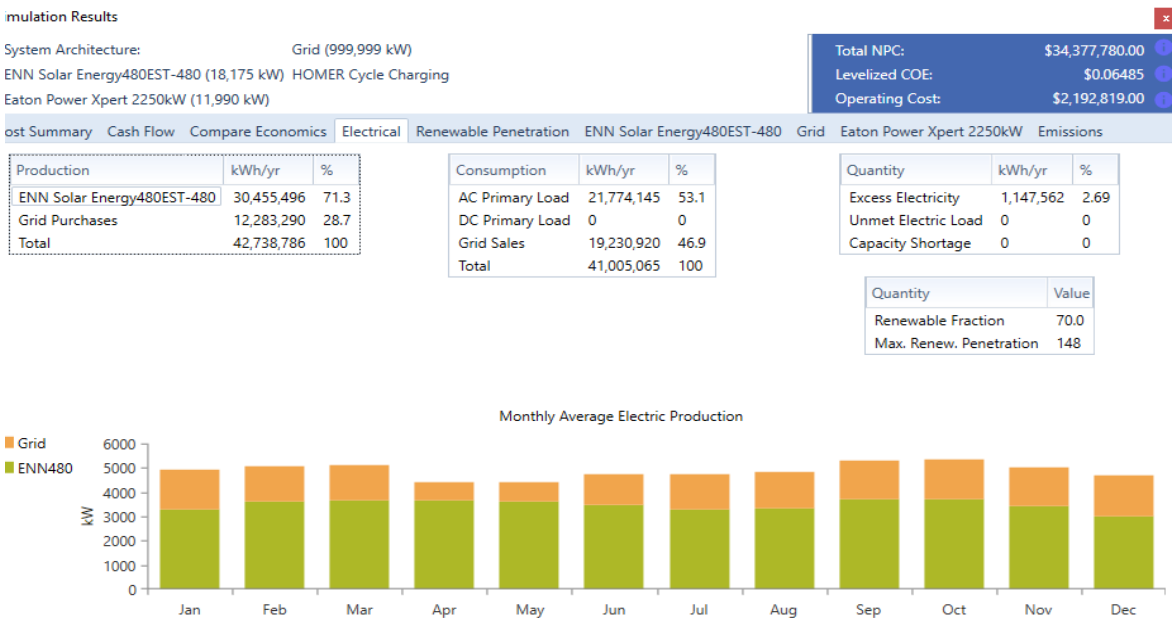

Figure 2.19: Simulation Results in HOMER (70% RE Constraint)

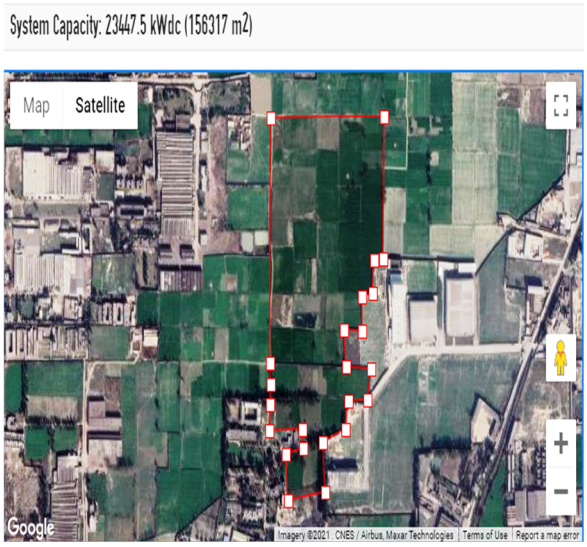

Figure 2.20: Land Marking for 18175 kW_{dc} PV System

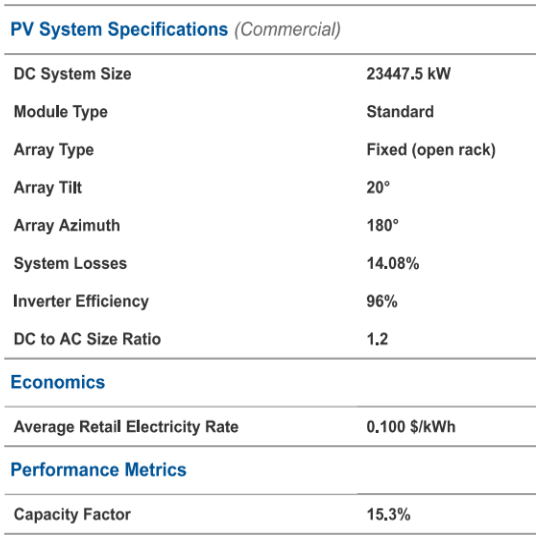

Figure 2.21: Parameters for 18175 kW PV

The cost analysis of same system has also been performed in HOMER. The final cost analysis results of the whole system have been shown in the Figure 2.22. The Net Capital Cost Required for the erection & commissioning of the system is $ 34377780. The operating cost was found to

be $ 2192819; levelized energy cost of energy is $ 0.06485. The upfront capital was found to be $ 6030074.94. On equipment level, the NPC over 25 years of life span is given below.

The cash flow analysis result has been shown in the below Figure 2.23. The upfront capital needed for the whole system with 70% generation from renewable is $ 6030074.94. Every year operating cost of $ 2183835.24 will be consumed and at 15 years for the replacement of the component, $ 337209.30 will be invested. At the end of 25 years, $ 112403.10 salvage value is expected.

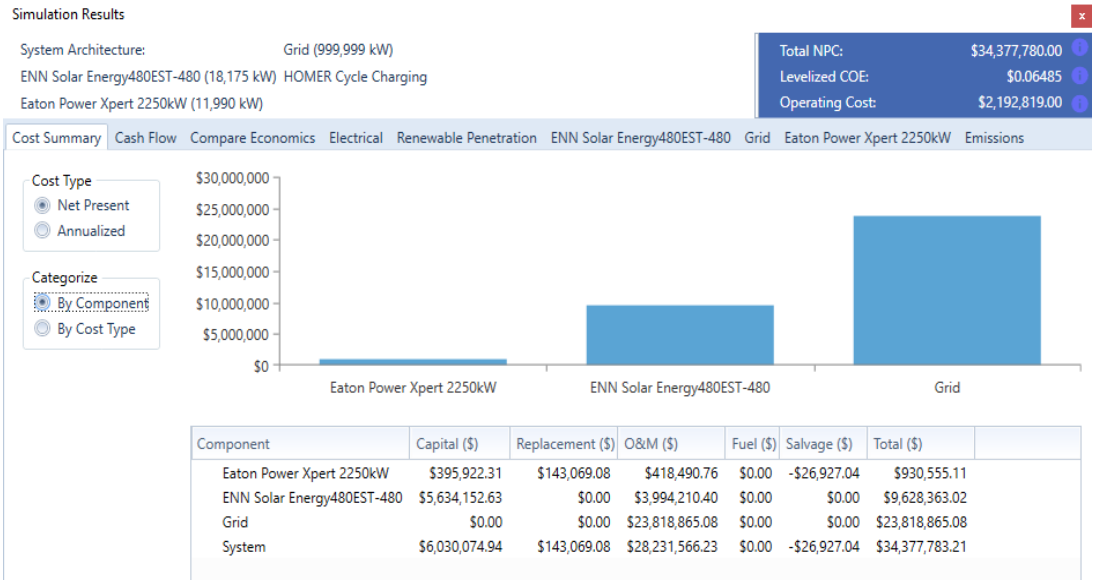

Figure 2.22: Cost Summary of 18175 kW PV System

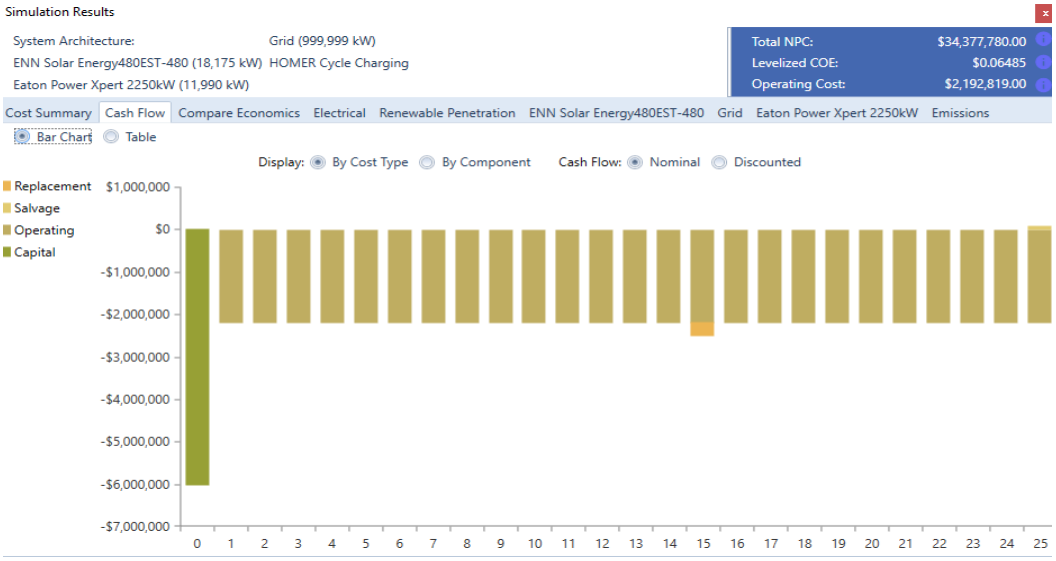

Figure 2.23: Cost Flow of 18175 kW PV System

Table 2.2: NPC of Components in System (70% RE Constraint)

Sr. #	Component	NPC ($)
1	Eaton Power Xpert 2250 kW	930555.11
2	ENN Solar Energy480EST	9628363.02
3	Grid	23818865.08
4	System	343777783.21

2.4.3 Case 03-With Storage and 0% RE Constraint

A battery is used to store the electrical energy in DC form. It also provides energy during the nighttime and zero irradiance situation. Battery is also act as a damper by absorbing or releasing the energy during the fluctuation periods. Therefore, for small systems battery play a vital role in the stabilization of output voltage and frequency. So, Trojan SSIG 12V battery having 146 Ah rating are used. 67 Strings of batteries is connected in series as per required dc range of Eaton inverter. The configuration of the stated system is shown in below Figure 2.24. As there is no constraints on the production from the renewable energy. In the first optimization, HOMER does not include the batteries in result; only take the 8382 kW_{dc} solar and grid input. In second case, HOMER take only 2412 batteries. This is because for such a large power plant, it is not fruitful to use batteries that increase system cost.

The cash flow analysis result has been shown in the below Figure 2.27. The upfront capital needed for the whole system with 0% RE constraint is $ 2701344.87. Every year operating cost of $ 2185148.24 will be consumed and at 15 years, the replacement of component $ 87721.24 will be invested. At the end of 25 years, $ 29240.41 salvage value is expected. The following deduction has been made about the cost summary of the designed system in the HOMER.

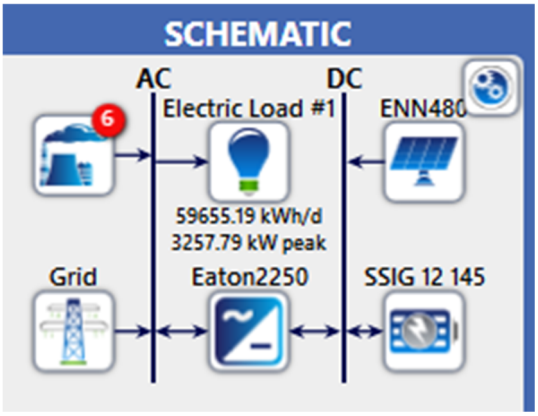

Figure 2.24: Schematic of System with Storage

Architecture

	ENN480 (kW)	G3516-1030kW-50Hz (kW)	G3516-1030kW-50Hz (1) (kW)	G3516-1030kW-50Hz (2) (kW)	CAT-1320 (kW)	CAT-1320 (1) (kW)	CAT-1320 (2) (kW)	SSIG 12 145	Grid (kW)	Eaton2250 (kW)
	8,382								999,999	3,119
	8,470							2,412	999,999	3,207
	8,382	1,030							999,999	3,119
	8,382		1,030						999,999	3,119
	8,382			1,030					999,999	3,119
	8,382				1,056				999,999	3,119
	8,382					1,056			999,999	3,119
	8,382						1,056		999,999	3,119
	8,470	1,030						2,412	999,999	3,207
	8,470		1,030					2,412	999,999	3,207
	8,470			1,030				2,412	999,999	3,207
	8,470				1,056			2,412	999,999	3,207
	8,470					1,056		2,412	999,999	3,207

Figure 2.25: Optimization Results with Storage

Table 2.3: Cost of System with Storage

Sr. #	System Cost	Cost ($)
1	Total NPC	30980100
2	Levelized cost of energy	0.1025
3	Operating Cost	2187485
4	Capital cost of System	2701344.87

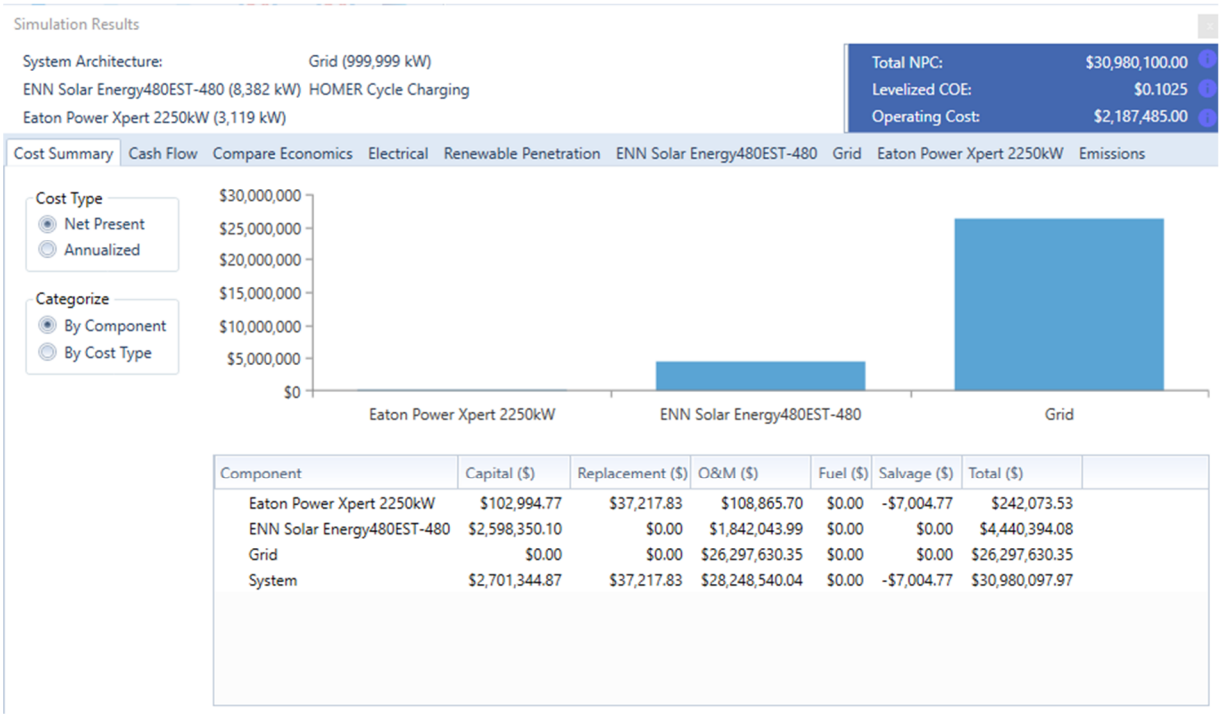

Figure 26: Cost Summary of System with Storage

2.5 Conclusion and Possible Future Work

After the detailed analysis and optimization of the system in the HOMER, it is deducted that despite the heavy capital cost of solar system, the operation and maintenance cost is very low. The per-unit cost of system with PV is the cheapest because no fuel is required for generation. For 8382 kW system, 17462 ENN-480 solar modules are required. 17 modules are connected in series for generating the desired voltage of Eaton solar inverter and 1027 such strings are connected in parallel for producing the desired output power. Such as system could be installed on the land owned by the plant.

The system with 70 % RE constraint 18175 kW_{dc} system is required for which 19 panels have been connected in series for generating little high voltage and 1993 strings of such configuration is connected in parallel for generating the desired power. Such a PV system will need purchase of nearby agriculture land. During our analysis, we did not include land purchased cost.

For the system with storage require 8382 kW_{dc} PV system same as for case-01. The same configuration as in no storage and 0 % RE constraint is required for this system because for large system it is not optimum to have a storage. Finally, there is a substantial reduction in per unit cost of electricity generation using PV system. The greater the generation from solar, a large decrease in energy cost occurs. The best system is case1 (Without Storage and Zero RE Constraint) from saving and cost point of view.

References

[1] F. Muhammad, M. Waleed Raza, S. Khan, and F. Khan, "Different Solar Potential Co-Ordinates of Pakistan," *Innov Ener Res*, vol. 06, no. 02, 2017, doi: 10.4172/2576-1463.1000173.

[2] S. Khan, H. F. Ashraf, E. Loxbo, and S. Johansson, "Analysis of Pakistan's Electric Power Sector," p. 51.

[3] F. Muhammad, M. Waleed Raza, S. Khan, and F. Khan, "Different Solar Potential Co-Ordinates of Pakistan," *Innov Ener Res*, vol. 06, no. 02, 2017, doi: 10.4172/2576-1463.1000173.

[4] LESCO Tariff - Electricity Unit Price," LESCO. https://lesco.pk/lesco-tariff/ (accessed Jul. 29, 2021).

[5] "NEPRA Electricity Bill." https://nepra.org.pk/consumer%20affairs/Electricity%20Bill.php (accessed Jul. 29, 2021).

[6] "Engine Thermal Efficiency - an overview |ScienceDirect Topics." https://www.sciencedirect.com/topics/engineering/engine-thermal-efficiency (accessed Jul. 29, 2021).

[7] "G3516B | 910kW-1300kW Natural Gas Generator | Cat | Caterpillar," https://www.cat.com/en_US/products/new/power-systems/electric-power/gas-generator-sets/18485403.html (accessed Jul. 29, 2021).

[8] ''Shell Rimula R4 X (15W-40) 4L, Heavy-duty Diesel Engine Oil, Truck Oil: Buy Online at Best Prices in Pakistan | Daraz.pk." https://www.daraz.pk/products/shell-rimula-r4-x-15w-40-4l-heavy-duty-diesel-engine-oil-truck-oil-i143464950.html (accessed Jul. 29, 2021).

[9] "2015 CAT 3512 For Sale In Edmonton, Alberta Canada," MARKETBOOK. https://www.marketbook.ca/listings/construction-equipment/for-sale/204804961/2015-cat-3512 (accessed Jul. 29, 2021).

[10] "3512 Industrial Diesel Engines | Cat | Caterpillar," https://www.cat.com/en_US/products/new/power-systems/industrial/industrial-diesel-engines/18397814.html (accessed Jul. 29, 2021).

[11] "About HOMER Energy LLC - Creators of Hybrid Renewable Microgrid System Design Software." https://www.homerenergy.com/company/index.html (accessed Jul. 29, 2021).

[12] "China Best Prices High Efficiency Monocrystalline Solar Panel." https://www.alibaba.com/product-detail/Solar-Panel-490w-480w-Panels-Solar_62350279340.html?spm=a2700.galleryofferlist.normal_offer.d_title.378e7eb6BsX9Qg&s=p (accessed Jul. 29, 2021).

[13] R. Fu, D. Feldman, and R. Margolis, "U.S. Solar Photovoltaic System Cost Benchmark: Q1 2018," *Renewable Energy*, p. 63, 2018.

Chapter 3

Dynamic Modeling of an Optimal Hybrid Power System for a Captive Power Plant in Pakistan

Preface

A version of this manuscript has been published in ***Jordan Journal of Electrical Engineering (JJEE)*** *vol 8. I am the primary author, and I carried out most of the research work, performed the literature reviews, carried out the system design, modeling, and analysis of the results. I also prepared the first draft of the manuscript and subsequently revised the final manuscript based on the feedback from the co-author and the peer review process. The Co-author, Dr. M. Tariq Iqbal, supervised the research, acquired, and made available the research funding, provided the research guide, reviewed and corrected the manuscript, and contributed research ideas in the actualization of the manuscript.*

Abstract

This paper is about the optimized design, economic feasibility, and dynamic modeling of a captive power plant in Pakistan. Renewable energy production and use is essential for power generation and provide a sustainable environment. For an efficient and reliable grid-tied photovoltaic (PV) system operation, many issues like industrial load variations and expected dynamics should be studied before implementation. To shift from conventional resources to clean energy resources, a site was selected in the Pakistan industrial area for economically optimized solar sizing design using HOMER PRO (Hybrid Optimization Model for Electric Renewables), land requirement analysis has been done using PVWatt software. After the plant's design, the system's dynamic behavior due to typical practical disturbances has been analyzed. The designed grid-tied PV system is modeled in the MATLAB/Simulink using Simscape blocksets. Results show that the optimized design system has a low per-unit energy cost and provides significant savings. The dynamic simulation results show that the system can respond to the ramp-up and ramp-down load variations in industrial settings. The system also has a fast response to step changes in irradiance, proving that the designed system is reliable and suitable for a selected site. Sizing, dynamic modeling, and simulation results are presented in this paper.

Keywords— Captive power plant; hybrid power system; HOMER PRO; PV WATT; dynamic modeling

3.1 Introduction

Electricity is one of the basic requirements for the survival of modern life. It plays a vital role in the sustainable economy of any country. According to the International Energy Agency (IEA) evaluation, 992 million people did not have electricity in 2018 and predicted that almost 674 million would remain without electricity by 2030 [1]. Different resources energy is converted into

electrical energy using specific methods depending upon the type of fuel. During this conversion process, there are some emissions which shouldn't harm the environment and ecosystem. Still, due to the electricity generation from fossil fuels, a large fraction of total CO_2 is being emitted, which is harmful to the environment and causes global warming. In 2020, the National Aeronautics and Space Administration (NASA) estimated that global temperature rose by 1.02°C since 1880 [2]. Although depletion of fossil fuels is also happening, it is inevitable to have a smooth shift to other abundant clean resources, including solar, wind, tidal, etc.

Meanwhile, a 1000 W PV system produces 150 kWh per month, which impedes 75 kg of fossil being mined, ultimately stopping 150 kg of CO_2 from being injected into the environment [3]. Renewable resources are non-consumables and give zero emission during use. Output energy from these resources depends on environmental factors such as irradiance, temperature, air, etc, which disturb the grid's stability and cause tripping. So far, most of the research has investigated the economic penetration of renewable energy into the national grid, which ultimately reduces energy cost and emissions to the environment.

The most suitable energy source for Pakistan from these renewable sources is solar energy. Due to the intermittency of solar availability, electricity is generated from the combination of different resources like solar, coal, gas, furnace oil etc., which is called a hybrid power system [4]. CAT Diesel & Gas Gensets and PV system have been used in the designed system. There are two basic types of hybrid systems one is grid-connected, and the other one is a standalone system. Standalone systems are suitable for remote locations where it is difficult to supply power, and the system operates in islanding mode. The standalone system required batteries for sustainable operation during night time and stormy weather. Therefore, these systems have a low Load Factor (LF) which increases the capital and maintenance cost [5].

While on the other hand, grid-connected system locations should be near the main grid where they can be synchronized with the national grid. The grid also acts as batteries and can deliver or absorb the extra power generated by the PV system. Therefore, site selection plays a vital role in the efficiency of the hybrid power system because the site should be in that area where a prominent solar irradiance is available along with the main grid for generating and transmitting sufficient electricity. The chosen site is Shafi Texcel Limited (31.2616, 74.1674), and the solar will be installed on the land owned by the industry. Lahore Electric Supply Company (LESCO) is an electricity provider company and offers Net metering.

The average load of the industry is 2185 kW and the peak load is 3100 kW which has LF of 76 %. The load data of the 2020 year is being used for PV system sizing purposes is depicted in figure 3.1. The load fluctuations in figure 3.1 during April & May are due to the Covid-19 lockdown placed by the government.

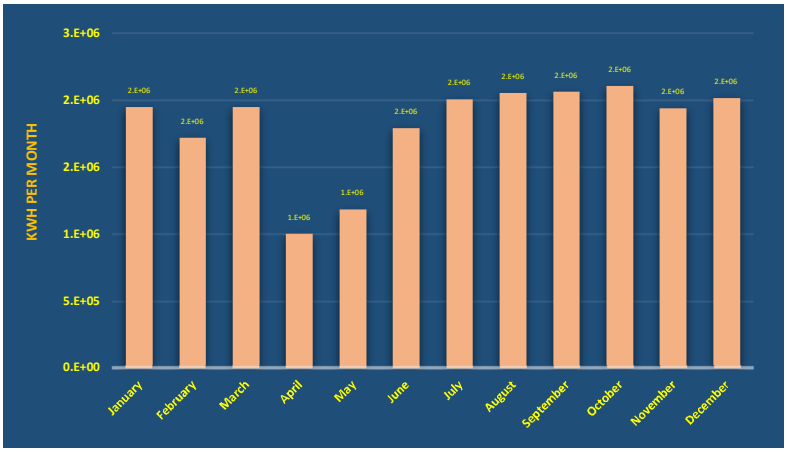

Figure. 3.1. Monthly electrical consumption.

After doing the sizing of PV system in HOMER, it is most important to have a deeper look into the system's dynamic response. PV system and grid modeling have been done in Simulink using the Simscape block set. A detailed literature review has been done in the II part of this paper. A

detailed sizing and mathematical design of whole plant is discussed in the third part. In IV part, the detailed simulation of system in Simulink and results has been discussed.

3.2 LITERATURE REVIEW

Many studies have been done on hybrid renewable energy systems (HRES) to achieve a lower cost in developing countries because the system design varies from site to site. In literature, various methods have been used to optimize PV systems and dynamic analysis. For sizing of a PV system, there are two techniques used. One is a Computer-based Method, and the other is Manual Formulation Methods[6]. Over time, many manual methods are eliminated due to the modern development in computer-aided tools. In the old methods, mathematical formulas mainly consider the tilt angle, irradiance, storage, etc., for sizing purposes. Four coefficients are required in the manual sizing method called loss of load probability to design the standalone PV system [7].

Computer-aided tools are used for accurate and perfect sizing because a computer can perform tedious calculations in a very short time and give more accurate results. In software, load profile and site selection are required, and they obtained the weather data from the assigned directory. There are many software for sizing and optimization of PV systems. For example, PV Planner, SAM (System Advisor Model), PVsyst, HOMER etc.

The authors of [8] developed a linear programming-based model for finding the eco-logical and economic optimized system for an off-grid system. The model was tested on two different continent countries: one in India (Narendra Nagar) and the other in Columbia (Titutmate). It was found that sizing of the optimized system mainly depends upon the load demand curve of site and renewable provides significant fuel saving. In [9], the authors did the economic feasibility of hybrid renewable energy systems (HRES) for rural electrification in Iran. The selected site is a remote rural village named Sheikh Abolhassan. The study comprises of economic viability of a diesel-renewable energy system. In the second stage, further additional penetration of renewable to fed

current to the grid is discussed using the HOMER. N. Tahir et al [10] designed a grid-tied hybrid power system in which a diesel generator is used along with PV system. A 03-kW solar power system is modeled, and optimization analysis is carried out using the HOMER PRO.

M. Nurunnabi et al. [11] designed a PV system for a rural area in Bangladesh. The maximum load demand of that area is very low i.e. 60 kW, and there is very small load fluctuation in the residential load. Chaichan et al. [12] studied the various design cases for the solar water pumping system of rural site in Oman. The cost of energy was found to be US$ 0.4743/kWh which is cheapest and have 0 % carbon emissions. A system [13] is de-signed for Bani Walid, Libya, which has average load demand 35.98 MW and peak load demand is 85 MW. The financial optimization was done in the HOMER and results show that 76.8 MW PV system along with 26 Hoppecke batteries are required. A detail scenario of renewable energy policies in Indian state of Gujarat is discussed. Some social barriers in the way of renewable and their solution are also revealed [14]. Benalcazar, P et al [15] done the optimized sizing and scheduling of hybrid energy system for Morona Santiago and the Galapagos Islands. A mathematical programming models is used for technical and economic feasibility of two islanding PV systems. It shows that the hybrid system is suitable for eliminating the subservience of rural areas on fossil fuels and providing power to remote areas. In [16], the author designed and simulated the PV system for a boat carrying 20 passengers in Bangladesh. From HOMER sizing results, 10.6 kW PV system is required. DC motors are used; therefore, no inverter is required for this system.

In some [17] literature, rural electrification has been done, and rural areas operate in the islanding mode of operation. Expanding the electrical network for low power density areas is very expensive. Therefore, a hybrid power system is the best solution. PV systems mainly provide power during sunny days, and diesel/gas gensets are used as a backup source for providing power during emergency conditions.

After sizing the PV system, it is compulsory to look deeper at the steady-state and transient behavior of grid-tied systems because the power system is always under disruptions due to continuous load and irradiance changing. Therefore, the system should be stable enough to bear such changes. Different software's are used for studying the dynamic modeling few of such are Power factory Dig SILENT, LabVIEW, Matlab/Simulink, etc. But Simulink is one of the famous and provides a broader view of the system response.

Literature review indicates that many have done the sizing, optimization, and scheduling of systems for economic feasibility, but no significant study is available on the dynamics of a hybrid power system. The power system security, resilience, and stability are crucial for the consumer's reliable and uninterruptable power supply.

Many have discussed small PV systems for houses, water pumps, Reverse Osmosis plants, etc. But no pertinent research has been available on hybrid systems for industrial units on a Utility scale with extensive load variations. To cover this gap, a site (Shafi Texcel Limited) is selected which has large load variations like Atlas Copco compressor 630 kW & Stenter Bruckner 220 kW, which just put high stress on the system when turning on. The designed system covers the following objectives of the hybrid renewable system in Pakistan.

- Design an HRES that can provide lowest Levelized cost of energy (LCOE).
- The system should respond to rapid changes in irradiance.
- Implementation of Integral Regulating technique in Incremental Conductance (IC) method to reduce the steady state error.
- The designed system should have capability to handle the abrupt change in consumer load because there are significant variations in industrial load.

Results show that designed PV system can handle up to 1.5 MW ramp up or ramp down and causes no tripping. To handle the irradiance variations, incremental conductance technique is used by

which system can handle up to 300 W/m^2 step-change in irradiance. Complete modeling and simulation results are presented below.

3.3 MATHEMATICAL MODELING OF HYBRID RENEWABLE POWER SYSTEM

The mathematical modeling of different parts of components are discussed in the following sections.

3.3.1 PV System Sizing

A detailed sizing of the PV system in HOMER has been depicted in figure 3.2. The optimization results indicated that a 8382 kW_{dc} capacity PV system is required for the selected site. A detailed design has also been published in IEEE IEMCON conference [18]. Some site sizing details in HOMER PRO are shown in the figure 3.2 and land detail in PVWatt is shown in figure 3.3. To generate the desired input voltage, 13 modules of 480 W are connected in series and 670 such series modules are connected in parallel. There are two such strings to generate the required power.

Table 3.1. 480 W HELIENE solar module specifications.

Sr. #	Parameter	Symbol	Rating
1	Peak Rated Power	P_{mpp} (W)	480
2	Cell per Module	N_{cell}	96
3	Maximum Power Voltage	V_{mpp} (V)	52.26
4	Maximum Power Current	I_{mpp} (A)	9.24
5	Temperature Coefficient of V_{oc}	%/C^o	-0.31
6	Temperature Coefficient of I_{oc}	%/C^o	0.045

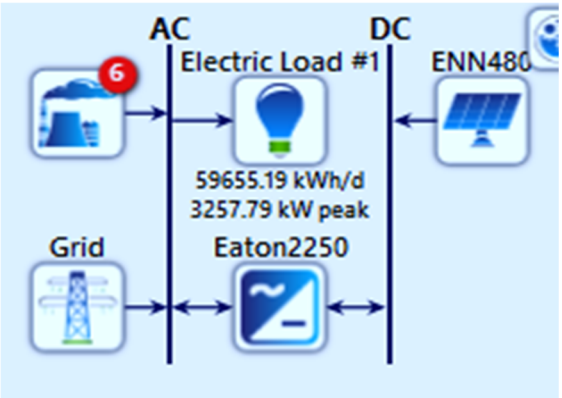

Figure 3.2. PV sizing system schematic in HOMER PRO

Figure 3.3. PV sizing site land analysis in PV Watt.

A 480 W panel specifications are given in the table 3.1. Figure 3.4 shows that the maximum power point voltage of one string is 679 V at 25 °C and maximum power point current is 6190.8 A.

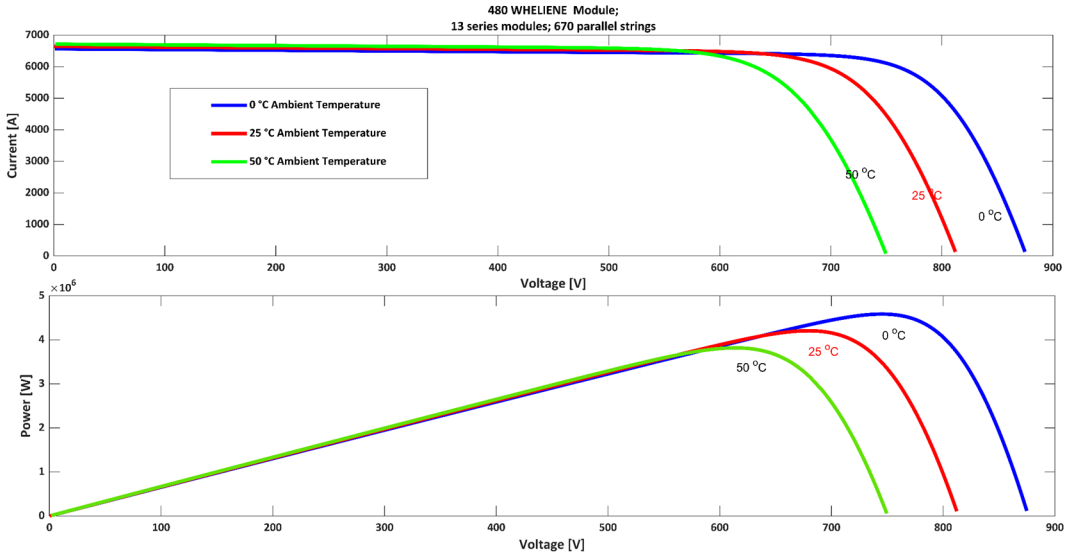

Figure. 3.4. PV module P-V & I-V characteristics.

The equivalent circuit model defines the I-V curves of a PV cell for given operating conditions. Different models have been used depending upon the accuracy and computation. The simplest model is the single diode model of PV cell shown in figure 3.5 having five parameters. The Eqs. (1) and (2) for this model can be formulated using Kirchhoff's law.

$$I = I_L - I_D - I_{sh} \quad (1)$$

$$I = I_L - I_o\left(e^{\frac{V+IR_s}{nV_T}} - 1\right) - \frac{V+IR_s}{R_{sh}} \quad (2)$$

Where I_L is light generated current and I_o is the saturation current of diode. V_T is the thermal voltage and R_s & R_{sh} represent the series and shunt resistance respectively. Diode ideality factor is denoted by n.

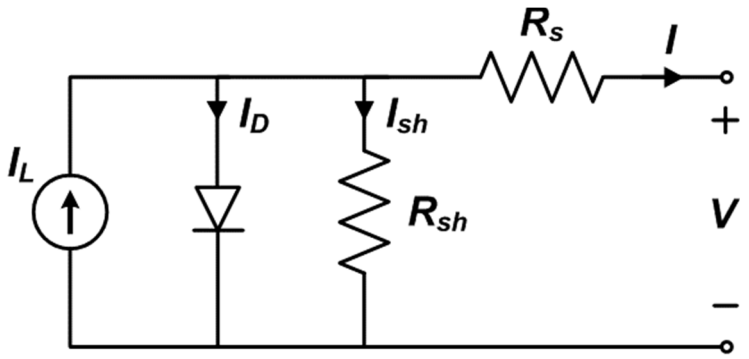

Figure. 3.5. Single diode model of PV cell.

3.3.2 Maximum Power Point Tracking

As the solar energy is dependent on irradiance, the shape of I-V characteristics curve changes and it can also be observed from figure 3.6 that the I-V curve is non-linear. The power taken from PV module depends upon the operating point on the curve. The maximum power output of a PV system is only available at one point which is called maximum power point (MPP). If the load resistance gets changed, this MPP will change, and PV output power/efficiency will decrease. Therefore, we use a maximum power point tracker (MPPT) which keeps the impedance seen by the PV module a constant at MPP.

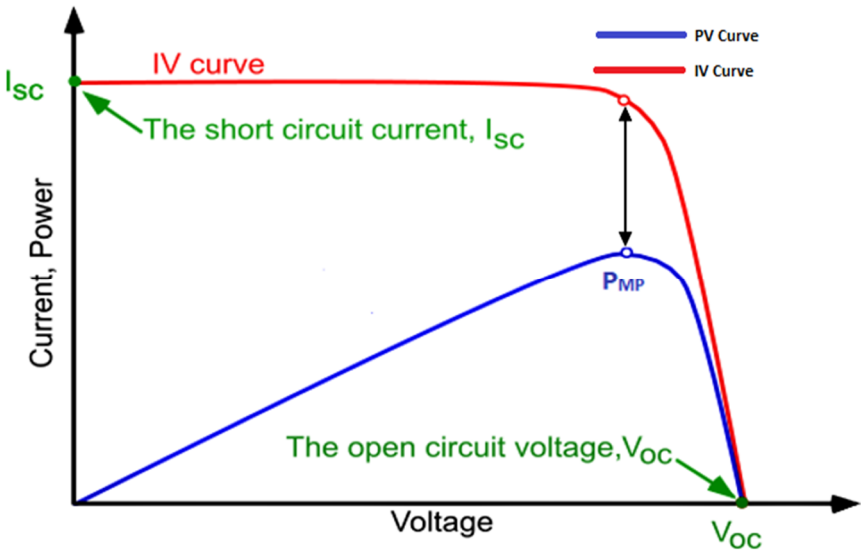

Figure. 3.6. P-V curve maximum power point.

Different techniques have been used for tracking MPP. The most efficient technique for abrupt irradiance changes is the Incremental Conductance method. It can be seen from the PV characteristics curve in figure 3.6 that the slope of the curve is zero at maximum power point. IC method follows Eq. (3) principle and at MPP dI/dV become equal to -I/V.

$$\frac{dP}{dV}=I\frac{dV}{dV}+V\frac{dI}{dV} \tag{3}$$

As "dP" /"dV" "=0" at MPP so the final expression is

$$\frac{dI}{dV}=-\frac{I}{V} \tag{4}$$

Maximum power point conditions are shown in the table 3.2.

Table 3.2. MPP tracking conditions.

Condition	Constraint	Explanation
$\frac{\Delta I}{\Delta V}=-\frac{I}{V}$	If P=MPP	Achieved MPP
$\frac{\Delta I}{\Delta V}>-\frac{I}{V}$	If P<MPP	Left to MPP
$\frac{\Delta I}{\Delta V}<-\frac{I}{V}$	If P>MPP	Right to MPP

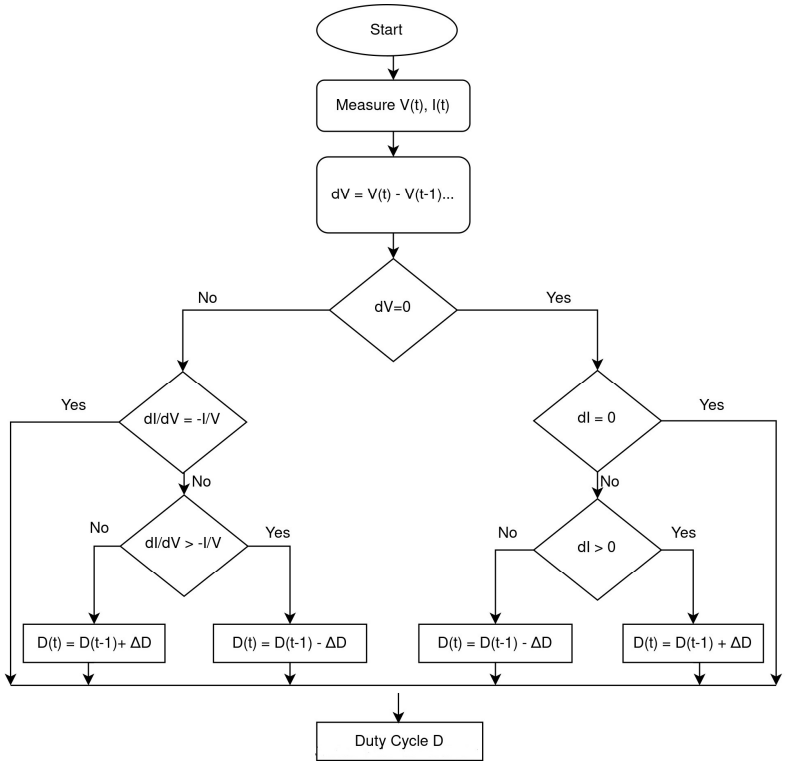

Figure. 3.7. Flow chart of incremental conductance.

Figure 3.7 shows the IC algorithm, in which firstly ΔI & ΔV is determined then depending upon the values if else conditions are used for the final duty cycle. If ΔV & ΔI both are zero, then there is no change in the duty cycle. In all other cases, an increment/decrement will happen depending upon the conditions described in Table 3.2. If ΔI/ΔV>-I/V, an increment will occur; otherwise, decrement will take place in duty cycle.

During the calculation, the sum of I & V dI/dV will never be exactly zero, but there will be some error. Integral Regulator technique is used to eliminate this error, which minimizes the residual steady-state error. Integral calculates the instantaneous error and adds it to controller output after multiplying it with gain of controller.

3.3.3 Design of Boost Converter

A boost converter is a dc step-up transformer with high output voltage and low current compared to input voltage & current respectively. Ideally, the total power on both sides of the converter

remains constant. The output voltage is controlled with the help of switch S shown in figure 3.8, which may be MOSFET, IGBT or transistor. By controlling the duty cycle (D) of this switch, output voltage (V_o) can be controlled.

$$V_o = \frac{-1}{1-D} \times V_i \quad (5)$$

$$I_L = (1-D) \times I_s \quad (6)$$

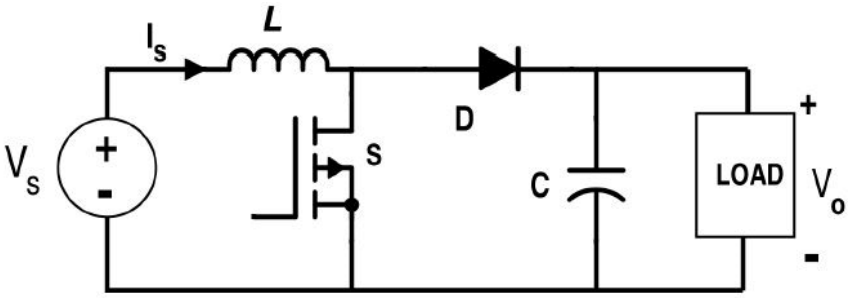

Figure. 3.8. Boost converter circuit.

The Eqs. (5) and (6) are used to design the converter whose duty cycle is constant along with input & output voltages but in PV system converter due to change in irradiance input voltage will change, which will cause change to the duty cycle of switch for operating the system on MPP. Therefore, the conventional equations for design of input inductor and capacitor remain no more valid.

Input inductor and output capacitor should always operate in continuous conduction mode; both should not discharge completely during the off cycle. Therefore, the ripple in input current ("Δ" "I" _"L") is usually taken as 13% of total input maximum current in Eq. (8) [19].

$$L_{boost} = \frac{V_s \times (V_o - V_s)}{\Delta I_L \times f_s \times V_o} \quad (7)$$

Here,

$$\Delta I_L = 0.13 \times I_o \times \frac{V_o}{V_s} \quad (8)$$

$$L_{boost} = 5.0811\ \mu H \quad (9)$$

The capacitor on the output side regulates the voltage and delivers the power during the half cycle of pulse. It can be calculated using Eq. (10) [20].

$$C_{boost} = \frac{P}{2 \times \omega \times u \times U_c} \quad (10)$$

Here, U_c is the mean voltage across the capacitor, and u & "ω" are the amplitude and angular frequency of output ripple voltage respectively.

$$C_{boost} = 0.84215\ F \quad (11)$$

The switching frequency f_s of converter is 5 kHz because at higher frequency switching losses increases.

3.3.4 DC-AC Inverter

The boost converter's output is fed to the input of inverter for converting the DC power into AC power. As grid is AC network and inverter is being synchronized with it. There are different topologies for designing of inverter depending upon the voltage level, harmonics, etc requirement. Neutral Point Clamping (NPC) topology is selected with 3 level bridge.

NPC is a multilevel inverter as shown in figure 3.9 that provides the clamping diodes for sharing proper voltage across the switches. Due to its multilevel nature, it offers good quality wave with fewer harmonics.

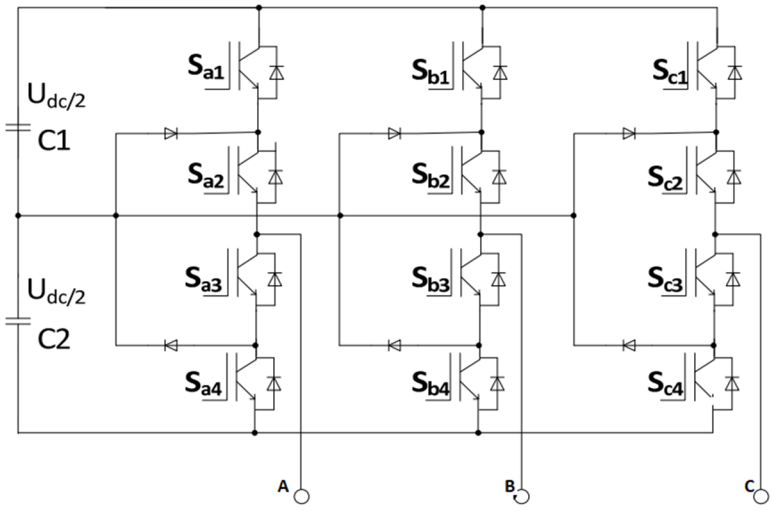

Figure 3.9. Inverter NPC topology.

To control the switching frequency of the inverter, the Sinusoidal pulse width modulation (SPWM) technique is used. A sine reference signal is compared with two triangular carrier signals for generating the desired pulses as shown in figure 3.10. In NPC topology, switches S1 & S3 operate in complementary mode, and S2 & S4 also operate in complementary mode; otherwise, it may short circuit the source through any leg of inverter switches. The switching frequency of inverter is 1650 Hz when a 50 Hz sine wave is compared with 1650 Hz triangular wave.

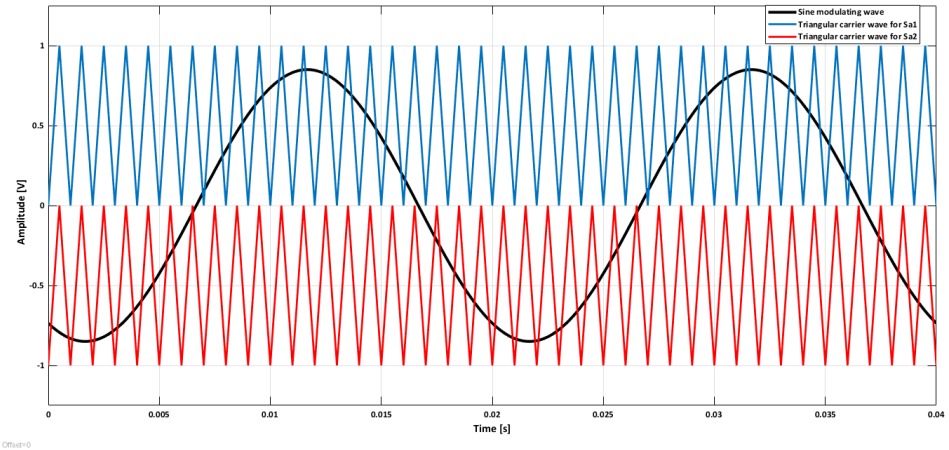

Figure. 3.10. NPC switching modulating wave vs carrier wave

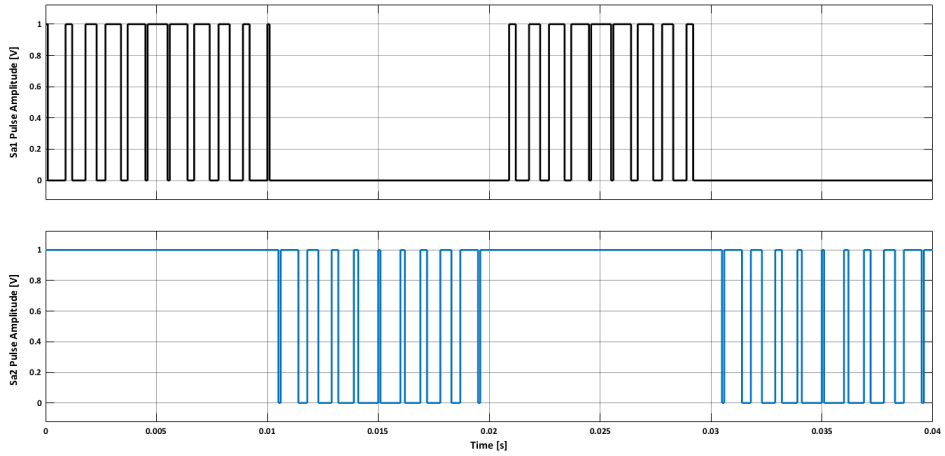

Figure. 3.11. NPC switching pulses pattern

3.3.5 Grid Synchronization & Inverter Power Control

Grid is a source of power and can deliver or absorbed any amount of power. For a grid-tied PV system, the grid also acts like a battery. For the grid-tied operation, proper synchronization and

power control of the inverter are vital in stable operations. For synchronization, voltages angle, magnitude and phase should also be same; otherwise, it may disturb the stability of the power system.

To control the voltage parameters of the inverter, it is compulsory to have an idea about the grid voltage magnitude, phase, and frequency. As grid quantities are AC and inverter input is dc; therefore, it is necessary to transform the grid quantities into d-q frame of reference, a 2-D synchronous frame rotating at a constant speed so that quantities in that frame appear as constant quantities. Below Eqs. (12) and (13) are used for dq transformation [21].

$$\begin{bmatrix} V_d \\ V_q \end{bmatrix} = \sqrt{\frac{2}{3}} \begin{bmatrix} \sin\omega t & \sin(\omega t - \frac{2\pi}{3}) & \sin(\omega t + \frac{2\pi}{3}) \\ \cos\omega t & \cos(\omega t - \frac{2\pi}{3}) & \cos(\omega t + \frac{2\pi}{3}) \end{bmatrix} \times \begin{bmatrix} V_a \\ V_b \\ V_c \end{bmatrix} \quad (12)$$

$$\begin{bmatrix} I_d \\ I_q \end{bmatrix} = \sqrt{\frac{2}{3}} \begin{bmatrix} \sin\omega t & \sin(\omega t - \frac{2\pi}{3}) & \sin(\omega t + \frac{2\pi}{3}) \\ \cos\omega t & \cos(\omega t - \frac{2\pi}{3}) & \cos(\omega t + \frac{2\pi}{3}) \end{bmatrix} \times \begin{bmatrix} I_a \\ I_b \\ I_c \end{bmatrix} \quad (13)$$

Two control loops have been used to control the active & reactive power. These two loops keep the power balance on both AC and DC sides of the inverter. The outer loop is the voltage loop and inner loop is current loop. The voltage loop keeps the voltage at the input of dc bus of inverter constant. As the irradiance changes which ultimately causes a change in dc voltage of inverter input. The objective of this loop is to change the active power reference, so the power delivered to grid changes as per irradiance variation.

The inner current loop takes the active and reactive power reference and regulates the current fed into the grid. In our designed model shown in figure 3.12, the reactive power reference i.e. quadrature axis is set to zero. Therefore, the inverter will deliver only active power to the grid and zero reactive power.

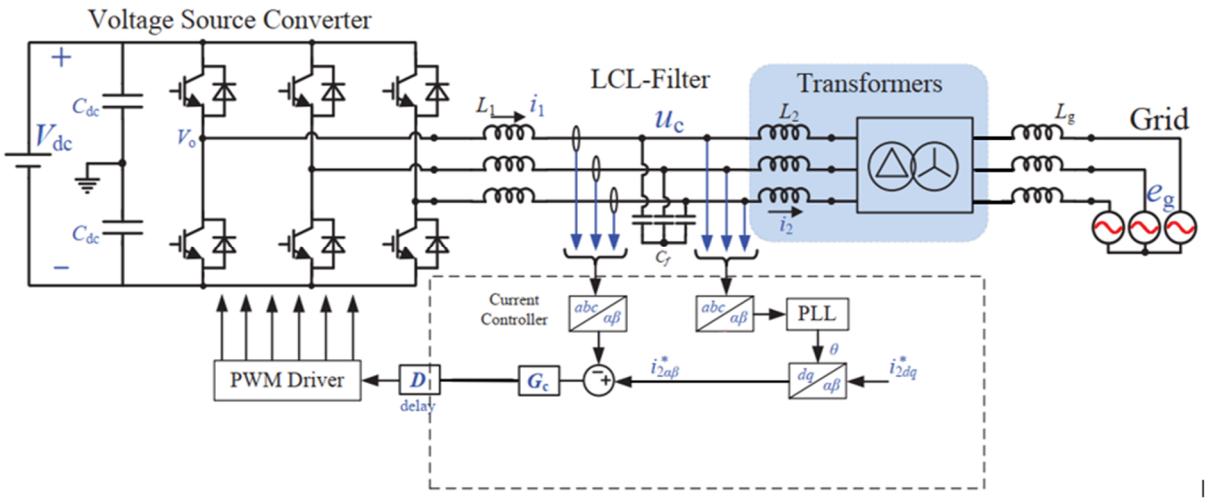

Figure. 3.12. Schematic configuration of PV grid synchronization.

3.3.6 LCL Filter Design

A filter is a combination of resistor, capacitor, and inductor that passes a certain amount of frequency and attenuates the undesirable frequency signal. The inverter output waveform is not a pure sinusoidal signal. It is compulsory to reduce the harmonic content in that waveform for which different filters can be used. But LCL filter shown in figure 3.13 is the most suitable because it provides high attenuation for unwanted signals and the inductor & capacitor of less rating are required for this one.

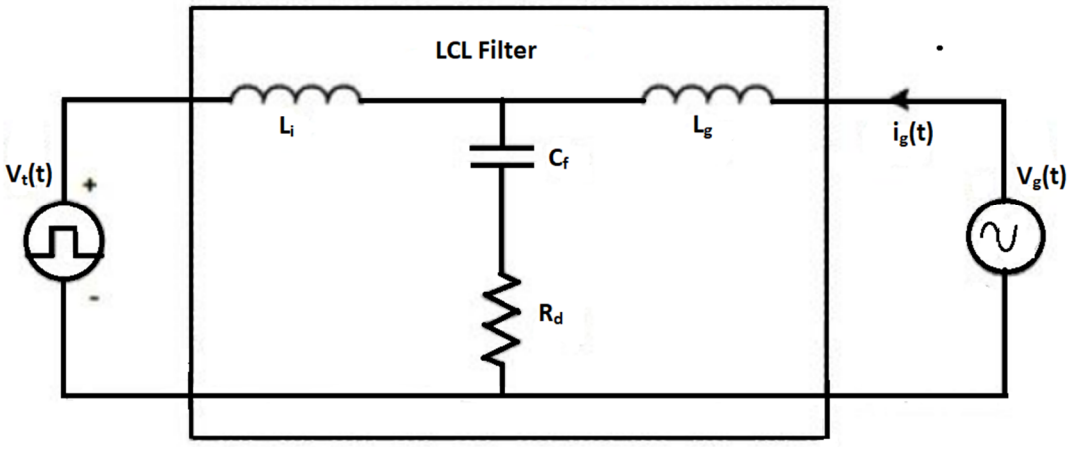

Figure 3.13. LCL filter configuration.

The first step in designing LCL is to calculate the inverter side inductor (L_i), which can be calculated using the below Eq. (14) [22].

$$Li = \frac{U_{dc}}{16 \times f_s \times \Delta I_L} \tag{14}$$

Here, U_{dc} is the dc link voltage and f_s is the system frequency. ΔI_L is the current ripple taken as 10% of maximum current and can be calculated as following equation.

$$\Delta I_L = 0.1 \times \frac{P_{nominal} \times \sqrt{2}}{V} \tag{15}$$

After putting all parameters in Eq. (14), the final value of inverter side inductor is given below

$$Li = 20.94\ \mu H \tag{16}$$

The grid side inductor L_g can be calculated using the below Eq. (17).

$$Lg = 0.6 \times Li \tag{17}$$

$$Lg = 16.766\ \mu H \tag{18}$$

Finally, the filter capacitor (C_f) design is such that there should be a maximum 5% oscillation in the inverter output voltage for the stable operation of grid-tied PV system. The capacitance can be calculated by using the below formula in Eq. (19).

$$C_f = \frac{P_{nominal}}{\omega_{grid} \times V_{ph\text{-}grid}} \tag{19}$$

$$C_f = 4.01146\ mF \tag{20}$$

The final step is to have a look at the resonance frequency of the filter. At resonance frequency, impedance and admittance cancel each other and the circuit behaves as a resistor. The resonance frequency must be far from power frequency and minimum should be half of switching frequency. Resonance frequency can be determined using Eq. (21).

$$f_{res} = \frac{1}{2\pi} \times \sqrt{\frac{Li+Lg}{Li \times Lg \times C_f}} \tag{21}$$

The resonance frequency came to be 778 Hz, and the value of damping resistor is calculated with the help of this one. Damping resistor (R_d) reduces oscillation and prevent short circuit at a resonance frequency. It can be calculated as below Eq. (22).

$$R_d = \frac{1}{3 \times \omega_{res} \times C_f} \tag{22}$$

$$R_d = 0.01763\ \Omega \tag{23}$$

3.4 MODELING OF THE DESIGNED HRES IN SIMULINK

MATLAB provides a numeric computation environment developed by MathWorks and Simulink is a MATLAB blocks-based programming interface that provides the modeling, analysis, and simulation of dynamical systems. For modeling of hybrid power system, Simscape blocksets are used. All modeling has been done using the calculated parameters and the effect of real time conditions is also included in the block's parameters like transformer saturation, excitation current, inductor resistance, etc.

Firstly, in the PV system, the desired level of irradiance and temperature is achieved using the signal builder block and the output of this block act as input of PV array block. Further, the boost converter circuit is built under real conditions and switching pulses are given to the MOSFET of converter by MPPT to extract the maximum power solar modules. To convert the DC voltage to AC voltage, Sine PWM techniques are used on the NPC converter and LCL is constructed for filtering purpose.

Figure 3.14 shows the complete schematic modeling of the designed captive power plant. The calculation about the sub blocks parameters is discussed in section 3. In modeling, transformer saturation, controller limits, IGBT internal resistances, and damping resistor effects have also been considered. A PV array block is used for implementing the one string of PV module; other is the replica of it. The parameters given in table 3.1 are inserted into this module. The output of PV

array is connected to boost converter with the help of coupling capacitor which stabilizes the dc voltage with the help of MPPT. NPC 3-level bridge inverter is used for dc-ac conversion which is further connected to grid with the help of LCL filter. As grid is an infinite source of power because it has a slack/swing bus which can handle any amount of power. In Pakistani distribution companies, regional grid input voltage is 132 kV which is step down to 11 kV for distribution purpose and then 11 kV is further reduced to 400 V. The length of 11 kV feeder for our selected consumer is 2 km whose inductance and resistance effect is also taken into account. Finally, for the synchronization of both sources, the phase lock loop is used to track the angle of grid voltage used in d-q frame for generating the desired pulses and grid phase angle voltage. For observing the behavior of system, three phase power measurement block is being used which only consider the positive sequence component for measurement.

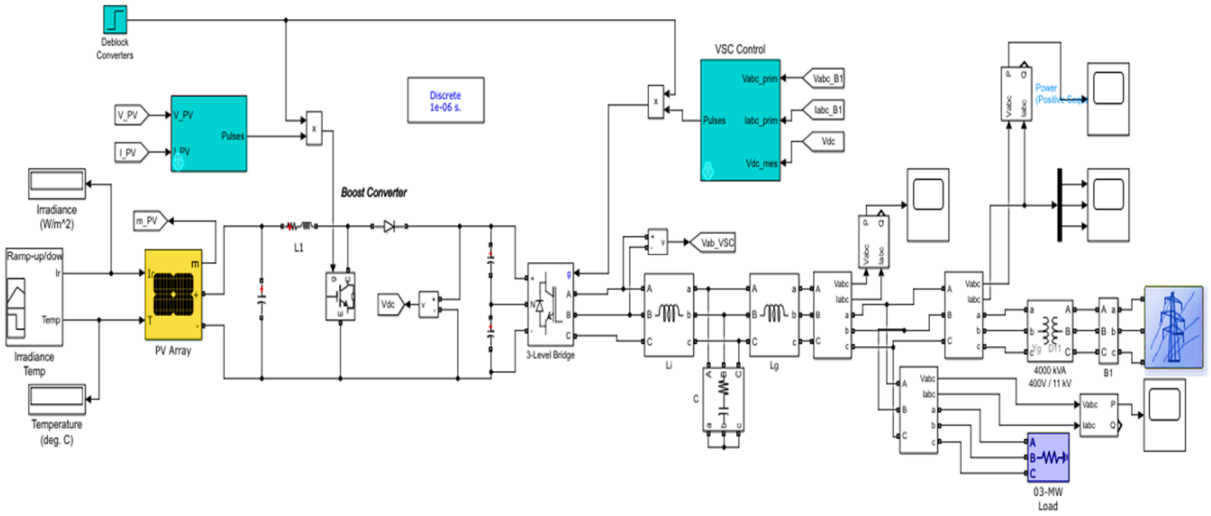

Figure. 3.14. Modeling of the system in Simulink.

3.4.1 Power Generation

As solar PV system is a base load power plant and responsible for providing the maximum power to the system. Therefore, the frequency of the incoming PV system should be slightly more than the grid; then, it will be able to deliver the power to the grid and load. The above figure 3.14 shows

that the point of common coupling is the node between the LCL filter and 400V/11 kV distribution transformer. At this point, the power distribution happens and due to variance in the industrial load, extra power is fed to the grid with the help of net metering. The three-phase peak voltage at PCC during the grid-tied operation is shown below in figure 3.15. In which, during the transient period when t<1s, the voltage error is more than 5 % but after this the voltage steady state error reduces to 2% and finally voltage become stable after 0.4 s.

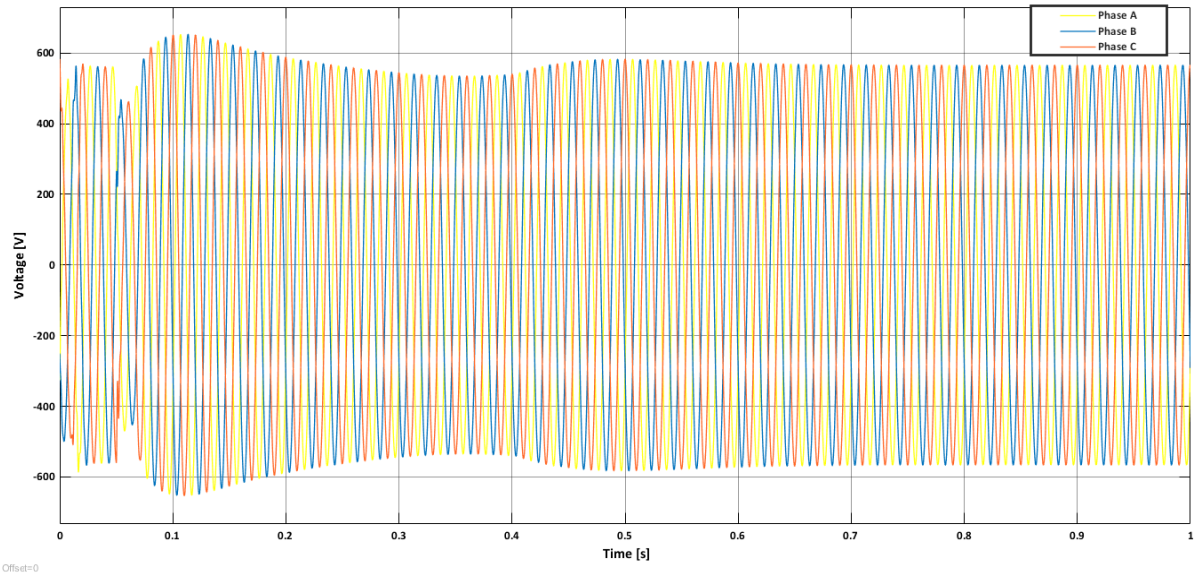

Figure. 3.15. Peak Voltage at 400 V bus.

3.4.2 Power Distribution on 400 V Bus

The power at the common bus varies with irradiance, and during the low irradiance and night time, the power will also be delivered by the grid as per load demand but during the high irradiance PV system will transfer surplus power to grid. So, an exchange of power occurs as per weather conditions and load demand. It is depicted in figure 3.16.

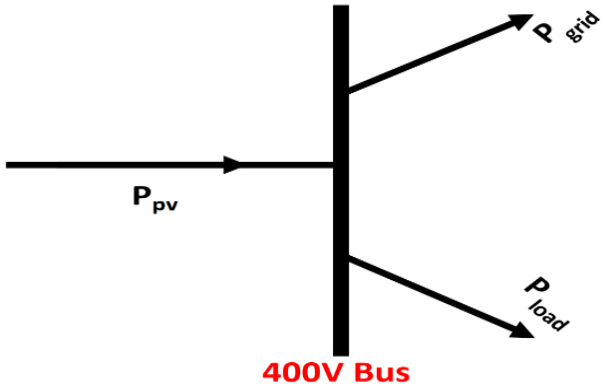

Figure. 3.16. Power distribution at 400 V bus.

$$P_{pv} = P_{load} + P_{grid} \quad (24)$$

P_{grid} may be the source or load of power depending upon the solar irradiance level. When delivering power to load and act as a source, it will be negative. A complete dynamic response of system is shown in the below figure 3.17 which shows that after 0.4 s, the steady state error is zero. The power delivered by the PV system is equal to the sum of power absorbed by the grid and load. The system transient response time can be reduced but it increases the initial percentage overshoot. Figure 3.17 shows, PV system supply 3000 kW to the local load and additional power 805 kW to the grid.

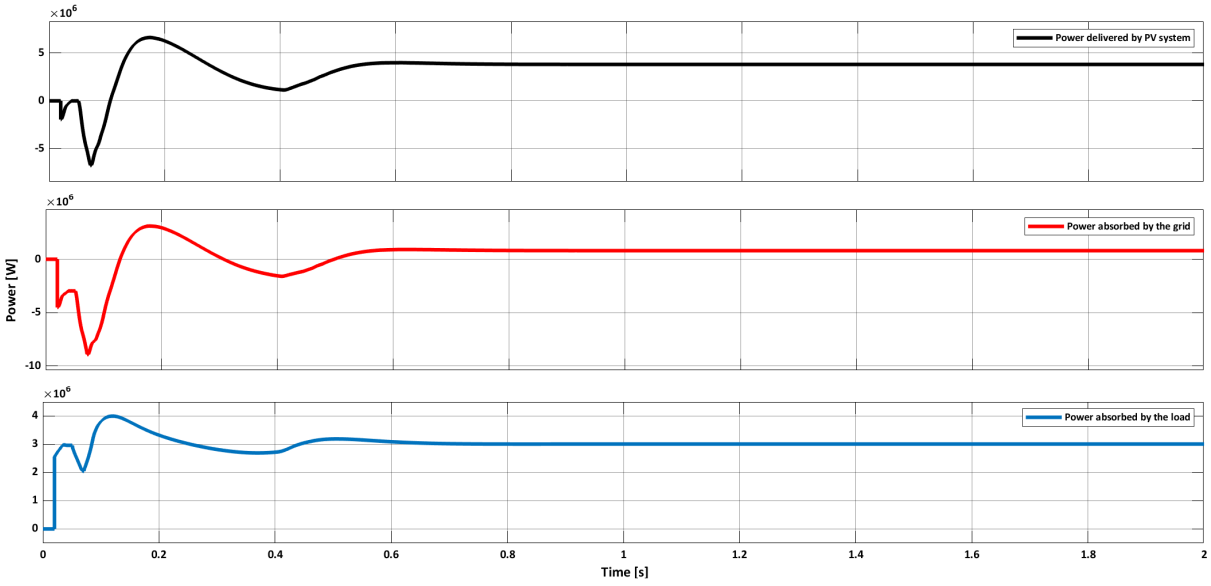

Figure. 3.17. Power distribution of PV system in Simulink.

3.4.3 Effect of abrupt change in irradiance

The Intensity of irradiance on any site depends on various factors like time, weather, season, and atmospheric conditions. The dust, clouds, rain, fog etc. affect the amount of irradiance reaching on earth.

As the output of PV panel is directly dependent upon irradiance which ultimately change the power output of PV system. Therefore, the system should be fast enough to overcome the response of transients. For this purpose, a step-change in irradiance is given to the PV array to study the STEP response which ultimately changes the output power while maintaining the grid's stability. The simulation results for step change are shown in the figure 3.18. A step change of 300 W/m^2 happened at 0.9 s, which shift the irradiance at 600 W/m^2 and eventually causes a change in the output power of PV. As our load remained constant, therefore the extra power is being supplied to the grid.

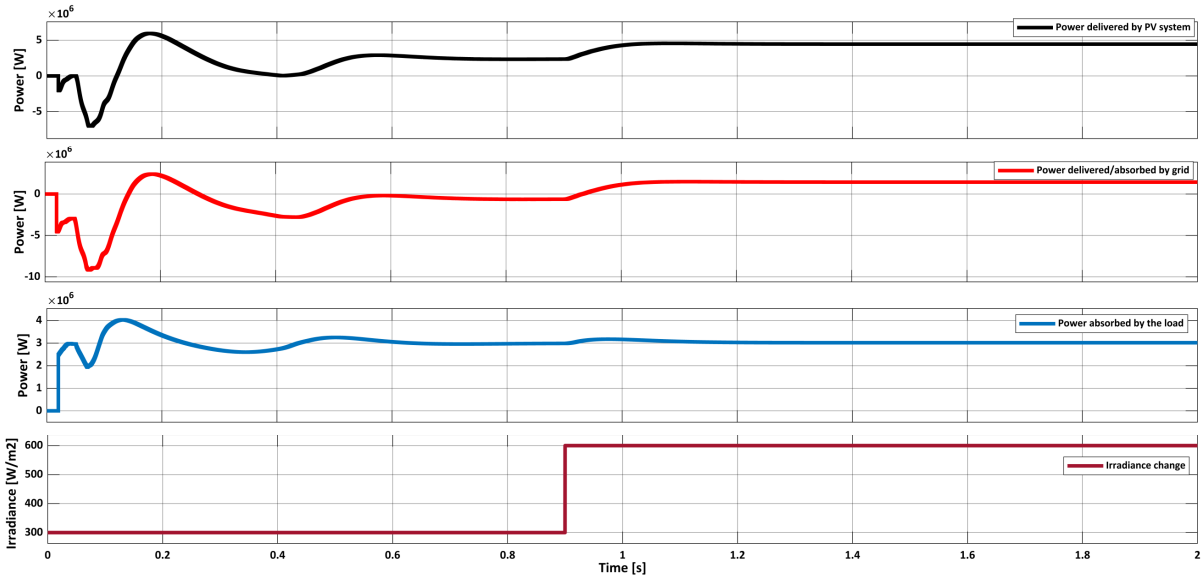

Figure 3.18. HRES behavior to step change in irradiance.

3.4.4 Effect of load variations

As the load on the power system keeps on changing continuously and the small load variations do not matter, most of the load in the industry is inductive load, which runs large conveyers, compressors, fans, and pumps that take a large amount of current.

Therefore, the system should be stable enough to bear such a large disturbance and maintain the synchronization of the voltage and frequency. Therefore, a 1.5 MW abrupt change in the load has been applied at 0.9s to 1.5s for observing the system's response. It can be seen from figure 3.19 the load increases and power delivered to the grid decreases, and the system remains stable.

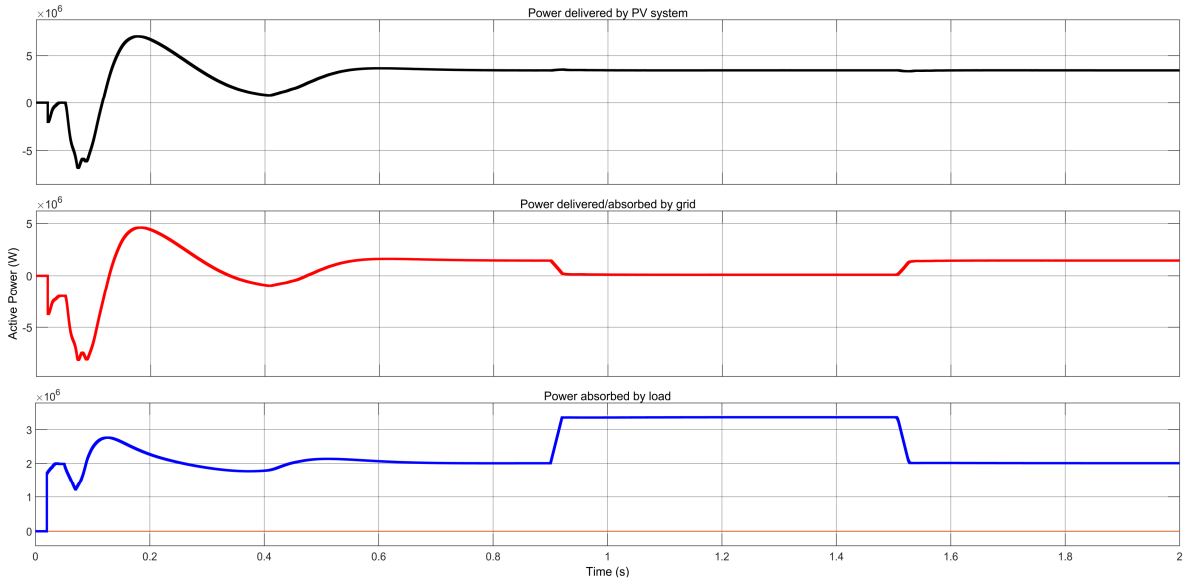

Figure 3.19. Effect of load variations on the system.

3.5 Conclusion

A detailed sizing, modeling and dynamic analysis of a hybrid power system have been presented in this paper. Firstly, the HOMER pro sizing results are depicted, which shows that 8382 kW dc solar modules are required for the optimum operation of a captive power plant. The solar's levelized cost of energy is cheapest because modules prices have dropped significantly in recent years. The dynamic analysis of the designed system has been done in Matlab/Simulink, which shows the transient and steady-state behavior of the grid-tied PV system under Pakistani conditions.

For tracking the maximum power point, a modified Incremental Conductance method is used which improved the residual steady state error. After designing the boost converter, DC-AC NPC inverter is synchronized with the grid with the help of a PLL. An LCL filter is being used between grid and inverter because for synchronization both sources should have same waveform. Grid is

designed by 132 kV slack bus for extra power handling. The voltage, frequency and power factor are the main parameters of designed system for smooth operation. The voltage on the 400 V bus remains under 400±5% and frequency remain 50±2% designed limit which improves the system's stability. The current quadrature component is set to zero which stabilize the PV system power factor at unity. The system behavior under disturbance, irradiance step response are presented, which show the PV system power fed to the grid while maintaining the voltage & frequency within the limit. The following primary result and conclusion have been deducted during testing of designed HRES.

- The system provides lowest per unit cost of energy i.e 0.1025 $/kWh.
- Designed HRES can handle load fluctuations of 1.5 MW.
- The system has fast enough response to tackle 300 W/m^2 step change in irradiance by increasing the power delivered to grid.
- Designed system voltage remain stable at 400 V during any interruption in the system.

The paper finds the limitation and hurdles in easing the renewable energy integration and suggested the system design to the industrial units in Pakistan. Finally, simulation results show that the designed system can handle interrupts and disturbances. The Incremental conductance control, inverter active & reactive power control, used, has fast response which improves the stability of whole system. This system sizing and modeling show that the deigned system if implemented can greatly reduce site energy cost while maintaining the same power quality.

In future, the designed system can be improved by reducing the settling time and per centage overshoot of the system.

REFERENCES

[1] International Energy Agency. Energy Access Outlook 2017: From Poverty to Prosperity; *International Energy Agency*: Paris, France, 2017.

[2] A. S. Khan and S. A. Chowdhury, "GHG emission reduction and global warming adaptation initiatives by UNFCCC," *2nd International Conference on the Developments in Renewable Energy Technology (ICDRET 2012)*, 2012, pp. 1-6.

[3] Omer, A.M. Energy, environment and sustainable development. Renew. Sustain. *Energy Rev. 2008*, 12, 2265–2300.

[4] I. Nassar, I. Elsayed and M. Abdella, "Optimization And Stability Analysis Of Offshore Hybrid Renewable Energy Systems," *2019 21st International Middle East Power Systems Conference (MEPCON)*, 2019, pp. 583-588, doi: 10.1109/MEPCON47431.2019.9007963.

[5] M. Jayakumar and V. Rajini, "Investigation of photovoltaic water pumping system," *2013 International Conference on Circuits, Power and Computing Technologies (ICCPCT)*, 2013, pp. 275-282, doi: 10.1109/ICCPCT.2013.6528841.

[6] V. Raviprasad and R. K. Singh, "Optimal sizing of PV power plant using sizing ratio for powering critical load with parallel redundant architecture," *IET Chennai Fourth International Conference on Sustainable Energy and Intelligent Systems (SEISCON 2013)*, 2013, pp. 101-107, doi: 10.1049/ic.2013.0300.

[7] S. Das and T. Malakar, "A Probabilistic Load Flow with Uncertain Load Using Point Estimate Method," *2018 15th IEEE India Council International Conference (INDICON)*, 2018, pp. 1-5, doi: 10.1109/INDICON45594.2018.8987005.

[8] Huneke, F.; Henkel, J.; González, J.A.B.; Erdmann, G. Optimisation of hybrid off-grid energy systems by linear programming. *Energy. Sustain. Soc*. 2012, 2, 7.

[9] Asrari, A.; Ghasemi, A.; Javidi, M.H. Economic evaluation of hybrid renewable energy systems for rural electrification in Iran—A case study. Renew. *Sustain. Energy Rev. 2012*, 16, 3123–3130

[10] N. Tahir and H. Jatala, "Design optimization and analysis of hybrid power system," *2014 International Conference on Energy Systems and Policies (ICESP)*, 2014, pp. 1-5, doi: 10.1109/ICESP.2014.7346994.

[11] M. Nurunnabi and N. K. Roy, "Grid connected hybrid power system design using HOMER," *2015 International Conference on Advances in Electrical Engineering (ICAEE)*, 2015, pp. 18-21, doi: 10.1109/ICAEE.2015.7506786.

[12] Chaichan, M.T., Kazem, A.H.A., El-Din, M.M.K., Al-Kabi, A.H.K., Al-Mamari, A.M. and Kazem, H.A. (2017) Optimum Design and Evaluation of Solar Water Pumping System for Rural Areas. *International Journal of Renewable Energy Research*, 7, Art. No. 1.

[13] Fathi Mosbah and Tariq Iqbal, "Sizing of A Large Isolated Solar Energy System for Bani Walid, Libya," *Journal of Clean Energy Technologies* vol. 6, no. 6, pp. 385-393, 2018.

[14] Elavarasan, R.; Shafiullah, G.; Kumar, N.M.; Padmanaban, S. "A State-of-the-Art Review on the Drive of Renewables in Gujarat, State of India: Present Situation, Barriers and Future Initiatives". *Energies 2019*, 13, 40

[15] Benalcazar, P.; Suski, A.; Kamiński, J. Optimal Sizing and Scheduling of Hybrid Energy Systems: The Cases of Morona Santiago and the Galapagos Islands. *Energies 2020*, 13, 3933.

[16] Al Mehedi, M.A.A. and Iqbal, M.T. 2021. Optimal Design, Dynamic Modeling and Analysis of a Hybrid Power System for a Catamarans Boat in Bangladesh. *European Journal of Electrical Engineering and Computer Science*. 5, 1 (Feb. 2021), 48-61. DOI:https://doi.org/10.24018/ejece.2021.5.1.294.

[17] Y. Abid, M. A. Khan and T. Muhammad, "Design and Analysis of hybrid power generation system for Rural Electrification. A case study," *2019 3rd International Conference on Energy Conservation and Efficiency (ICECE)*, 2019, pp. 1-6, doi: 10.1109/ECE.2019.8921160.

[18] L. Ahsan and M. T. Iqbal, "Design of an Optimal Hybrid Energy System for a Captive Power Plant in Pakistan," *2021 IEEE 12th Annual Information Technology, Electronics and Mobile Communication Conference (IEMCON)*, 2021, pp. 0820-0826, doi: 10.1109/IEMCON53756.2021.9623260.

[19] H. B. Massawe, "Grid Con`nected Photovoltaic Systems with SmartGrid functionality," M.S. Thesis, Dept. ElKraft, NTNU, Trondheim, Norway, 2013.

[20] Feng Gao, Ding Li, P. C. Loh, Yi Tang and Peng Wang, "Indirect dc-link voltage control of two-stage single-phase PV inverter," *2009 IEEE Energy Conversion Congress and Exposition, 2009*, pp. 1166-1172, doi: 10.1109/ECCE.2009.5316399.

[21] D. Hameed, S. Hamayoon, A. A. Malik and O. A. Ansari, "Solar grid-tied inverter, with battery back-up, for efficient solar energy harvesting," *2016 IEEE Smart Energy Grid Engineering (SEGE)*, 2016, pp. 95-99, doi: 10.1109/SEGE.2016.7589507.

[22] H. Li, W. Wu, M. Huang, H. Shu-hung Chung, M. Liserre and F. Blaabjerg, "Design of PWM-SMC Controller Using Linearized Model for Grid-Connected Inverter With LCL Filter," *in IEEE Transactions on Power Electronics*, vol. 35, no. 12, pp. 12773-12786, Dec. 2020, doi: 10.1109/TPEL.2020.2990496.

Chapter 4

Low-Cost, Open Source Emoncms Based SCADA System for a Large Grid Connected PV System

Preface

*A version of this manuscript has been published in **MDPI Sensors Journal**. I am the primary author, and I carried out most of the research work, performed the literature reviews, carried out the system design, modeling, and analysis of the results. I also prepared the first draft of the manuscript except introduction & literature review (which is carried by Jabbar) and subsequently revised the final manuscript based on the feedback from the supervisor. The Co-author, Dr. M. Tariq Iqbal, supervised the research, acquired, and made available the research funding, provided the research guide, reviewed and corrected the manuscript, and contributed research ideas in the actualization of the manuscript.*

Abstract

This article describes a low-cost Supervisory Control and Data Acquisition (SCADA) system for a PV plant with local data logging. Typically, SCADA systems that are available on the market are proprietary (commercial), which are expensive and individually configured for a particular site. The main objective of this paper is to design a low-cost and open-source monitoring solution (hardware and software) to meet the requirements. The hardware used for this SCADA consisted of Arduino, Raspberry Pi, sensors, serial communication cables, and an open-source web view platform. This open-source platform manipulates, logs, and visualizes PV and environmental data. Emoncms runs on the Debian operating system. Field instruments were connected to two remote terminal units (RTUs). A PV array provided data to the RTU1, while an inverter output provided data to the RTU2, and the Raspberry Pi received the collected data in JSON format. As these data arrived, Emoncms used Emonhub as its main module, which refines data and then displays it on Emoncms's WebView. The Raspberry Pi also stores data locally. Data logging was tested for 6 h, but the final results showed that data logging can last much longer. From an hour to a year, the data trend can be viewed on a user-friendly dashboard.

Keywords: SCADA; Emoncms; Internet of Things; Raspberry PI; EmonHub, Solar Energy

4.1 Introduction

Monitoring, control, and data acquisition are all referred to as SCADA. All these functions are comprised of both hardware and software components. In addition to collecting, monitoring, and processing real-time data, it also allows industrial organizations to control processes in real-time from either local or remote locations. In SCADA system, a human-machine interface (HMI) is used to interact with sensors and devices, and log files are generated. Industrial organizations depend on SCADA systems to eliminate down-time and increase efficiency while processing data

and making smarter decisions. As depicted in figure 4.1, a programmable logic controller (PLC) or remote terminal unit (RTU) is among the essential components of SCADA systems. A PLC or RTU is a microcomputer that communicates with objects of various types, a factory machine, a human-machine interface, a sensor, or an end device are some examples, and routes the information to a computer running SCADA software. As a result of SCADA software, data is processed, distributed, and analyzed, enabling operators to make important decisions as a result [1-2].

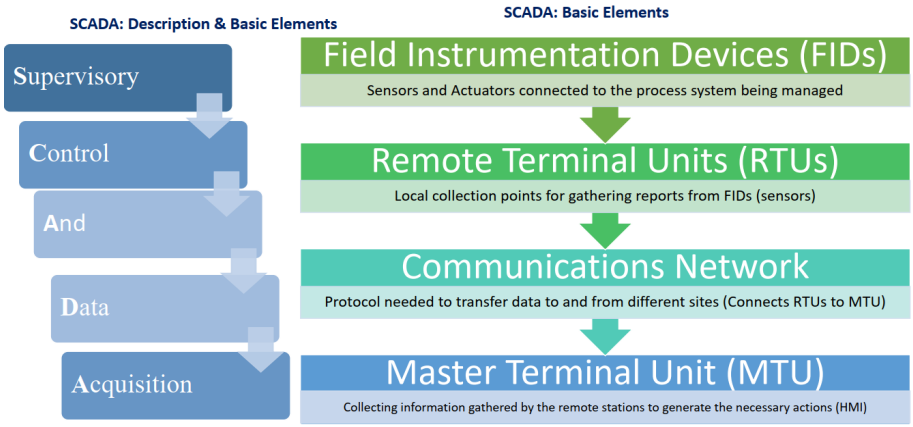

Figure. 4.1. System components.

Finally, the SCADA system is used in some process and utility applications to enhance the performance of system. Currently, global warming is dictating the world to reduce carbon emissions and use renewable energy as an alternative. In this dilemma, solar energy is playing a vital role in the electricity industry to fulfill the customer demand at cheap and carbon-free sources. Therefore, after doing the sizing [2] and dynamic modeling of a system [3], the SCADA of a system has been designed for the real-time monitoring of system which provides user-friendly monitoring along with the local data logging that ultimately provides a secure and reliable system. In Part 2 of the paper, a detailed literature review has been revealed. Parts 3 and 4 provide a complete system description and each component description respectively. In part 4 implementation methodology of the de-signed SCADA system has been expounded. Part 5 presents the results.

4.2 Literature Review

During this research, a comprehensive literature review was conducted, and some of the useful sources have been outlined here. In [4], vulnerability of SCADA systems to cyberattacks is discussed by the authors. The authors emphasize that SCADA systems' cybersecurity is becoming increasingly important as industrial digitization increases. They explored methods for distinguishing genuine cyberattacks from equipment faults. In particular, the authors examined "replay attacks" (RA), which are a relatively complex cyberattacks. Mathematical formalisms, comprehensive analysis, and experiments on a rotating machinery are the tools used in this study to differentiate between the equipment faults and the RA cyber-attacks. In another study the authors say, real-time information has become imperative for managing renewable energy assets with the rapid growth of renewable energy generation worldwide. The authors claim that as of now, the renewable energy sources have not been monitored in real time using cost-effective condition monitoring techniques to ascertain the optimal utilization of these invaluable. The authors presented an application of Supervisory Control and Data Acquisition (SCADA) using the Internet of Things for monitoring a hybrid system combining wind, photovoltaics, and energy storage systems. The authors utilized ThingSpeak for real-time monitoring of electrical parameters and the system is integrated with Matlab/Simulink using KEPServerEX client. The authors considered the cost effectiveness of the system by implementing low-cost electronic components. The proposed system enables system operators to access the system remotely. The claim through simulations and experiments that proposed system has been proven to be feasible, reliable, and cost-effective [5]. In [6], a SCADA system is used to remotely control and monitor inverters with grid connectivity. To maintain stable energy prices and maintaining network stability require utility providers proper monitoring and control of grid connected inverters. The number of grid connected inverters increases with the number of batteries tied with the power system, the authors considered these

crucial aspects as a part of this research. Testing results have led to significant improvements to the SCADA system, and its main components is an Internet of Things (IoT) server. In response to changes in energy prices, renewable energy generation fluctuates, the proposed SCADA system in this study can automatically manage the inverter to get economic benefits. The authors also used an algorithm to enhance economic benefits.

The authors [7] presented a low-cost and open-source SCADA system by using the internet of things (IoT) and advanced SCADA system design. The proposed system applies, ESP32 micro controller, Voltage sensors, current sensors, ThingsBoard IoT server and HMIs. For data transfer the authors configured Message Queuing Telemetry Transport (MQTT). The proposed system by the authors is successfully tested and is claimed to be feasible as a low-cost and open-source SCADA system for remote monitoring and control. As a part of [8], the authors used ESP32 and Arduino IoT Cloud are used to implement an open source, low-cost, IoT-based SCADA system for a rural Base Transceiver Station (BTS). A Wi-Fi network is used as a communication channel to transmit data from a current, voltage, temperature, and humidity sensor to the Arduino IoT Cloud. To monitor and control the system, widget-based dashboards on Arduino IoT Cloud is used in the course of this study. The authors also developed a mobile application for control and monitoring purpose. The control logic for high temperatures and low voltages is implemented using LEDs. An illustration of the proposed system was shown using a prototype created by the authors.

In [9], a SCADA system is implemented to manage energy in intelligent buildings. Modern buildings are equipped with several technologies that come together in this SCADA system such as illumination, temperature, ventilation etc. In this study a hierarchical cascade controller is implemented which involves centralized SCADA controlling the inner loops and local PLCs controlling the outer loops. The SCADA platform is layered with a predictive controller. Based on

several distributed user interfaces and energy waste minimization constraints, optimizing user preferences is achieved through the development of a predictive controller. It is demonstrated that temperature and luminosity can be controlled in large areas by using a variety of test methods. The authors also implemented a communication channel for communication between SCADA system and MATAB ap-plication. SCADA is suggested as a best solution for distribution network problems such as low productivity and complexity by the authors of [10-11]. Power electronic interfaces are critical to the development and success of emerging microgrids (MGs). The authors emphasize that the SCADA systems can improve the efficiency and productivity of active distribution networks and MGs. They used LAMBDA MG (a real microgrid used) test bed as a case study in this research and obtained real-time results from the SCADA system to demonstrate the ability of a central energy management system (CEMS) to create a proper energy balance, and thus minimize the exchange of power between LAMBDA MG and the main grid[12]. Microgrid operations could benefit from an effective SCADA system in terms of safety, reliability, and economics. Prominent use of information and communication technologies was started to enhance the operational efficiency of conventional power plants. This attracted more investment in the power sector and minimized the per unit cost of electricity [13]. In [14], the author suggested a frequency control solution by using adaptive control techniques and modeling predictive control. The findings revealed that the control algorithm converges to an optimal point, which makes the system robust.

Microgrid operations could benefit from an effective SCADA system in terms of safety, reliability, and economics. A microgrid intelligent monitoring platform was based on the SCADA systems that connect the lower central controller and upper WEB (World Wide Web) monitoring system. As a result of the SCADA system, the microgrid can be maintained in a stable and secure manner by acquiring, storing, and processing real-time data, performing load balancing and resource

recovery, and establishing security at the same time [15]. According to the authors of [16], automating in a smart way can reduce costs while meeting energy demands. In residential, commercial, and industrial settings, the Internet of Things (IoT) can be used to improve energy management. They presented an open-source, low-cost, and reliable home monitoring and control system [17]. They claimed that by using analog sensors, Message Queuing Telemetry Transport (MQTT), an ESP32, and Node-RED, the proposed SCADA system was capable of allowing remote access to appliances and controlling them over local Wi-Fi. Many researchers have investigated the architecture and different techniques of the SCADA system for commercial SCADA systems, which are expensive and far beyond the budgets of small- and medium-sized organizations. Others have designed the lowcost SCADA using an open-source WebView platform, but the security of a system is compromised because data are stored in a remote server. Therefore, a comprehensive SCADA system is designed to overcome the following issues:

- Provide a low-cost SCADA system that is within the range of the customer's budget as compared to the available commercial systems
- The designed SCADA system itself should consume minimum power.
- Data should be stored locally so that only the right person with the right authorization can access it.
- HMI should provide a user-friendly interface.

4.3 System Description

The designed SCADA system for a PV plant is depicted in Figure 2, which has 15 rows and 313 columns of PV modules. For demonstration purposes, only one row is being used. Two Arduino Mega 2560s (Arduino, Somerville, MA, USA), which acted as remote terminal units (RTUs), were used for taking the data from PV field sensors. In the design configuration, a low-cost Dell

computer was used with Raspberry Pi software (Raspberry Pi foundation, Cambridge, UK). For this purpose, 32-bit Debian with a kernel version of 5.10 was installed on the x86 processor. The specifications of the proposed system HMI/RPI are given below:

- Architecture: x86
- Threads per core: 02
- Core per socket: 02
- Sockets: 1
- CPU GHz: 1.9

After that, emoncms which is an open-source SCADA used for data visualization and logging is installed on the above-stated system. The built-in scripts are used for the installation purpose on Debian operating system. The following scripts have been installed in chronological order.

- PHP
- MQTT
- REDIS
- MYSQL

It is strongly encouraged that emoncms should be on a dedicated machine because using it with the other programs can cause malfunctioning. Hereafter, emoncms is configured for the local setup for which "settings.ini" has been setup which is available in "/var/www/emoncms/" directory. After doing the registration and login creation, the following files given in table 4.1 need to be set up as per user requirements.

Table 4.1. Setup filepaths.

Function	Directory
Data	/var/opt/emoncms
Location of main code	/var/www/emoncms
Install location for modules symlinked to www	/opt/emoncms

Log file Directory	/var/log/emoncms
Installation location of Emonscripts codes	/opt/openenergymonitor

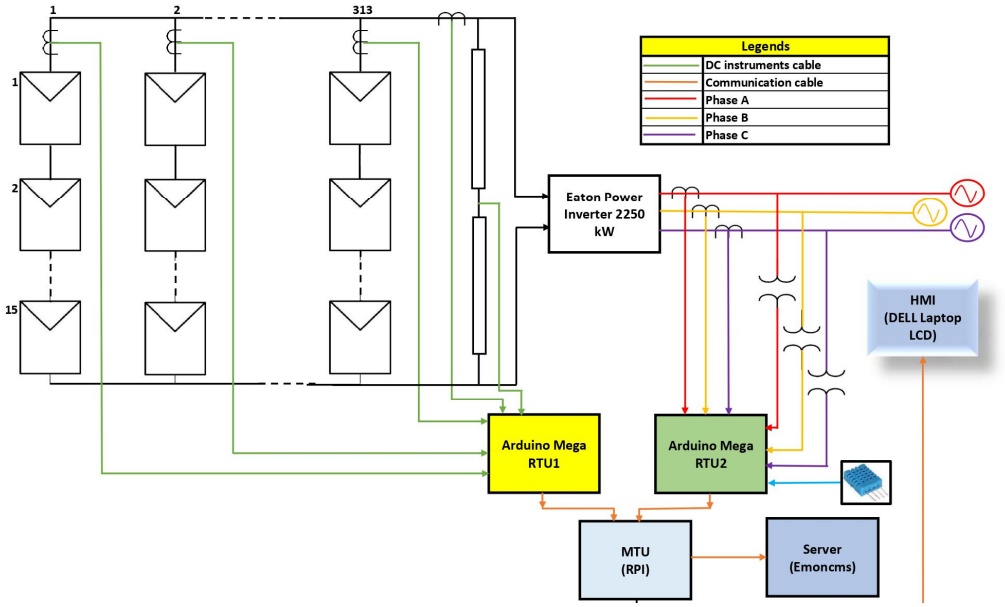

Figure. 4.2. Schematic of PV monitoring system.

4.4 Components of the designed system

As part of the SCADA system presented in this article, AC current, DC current, voltage, temperature, and humidity sensors collct data from the field devices. The Arduino Mega 2560 microcontroller was used, which takes data from all of the field instruments and then processes and parses the data to a Raspberry Pi-based server. After this, Emoncms takes the data from the port of the RPI and saves the logs along with the display on the computer screen (HMI). The comprehensive detail of each component is described below.

4.4.1 Sensors

The presented Sensors are the eyes and field instruments devices (FIDs) that take the data of a physical quantity and convert it to a readable analog voltage shape for measurement purposes. Based on the physical stimulus, measurements are divided into three sections in the designed system, which are stated below.

- DC/PV side parameters (V_{dc}, I_{sc}, I_{scl})

- AC side measurements (V_{ac}, I_{ac})
- Environmental factors (°C, %)

All the sensors used in the system are compatible with the industrial requirement. All selected sensors in table 4.2 can easily be mounted on DIN rail which is industrial standard used widely all over the world. Table 4.3 shows the price and power consumption of all the components. The dimensions of the DIN rail are given in figure 4.3. Its top hat width is 35 mm.

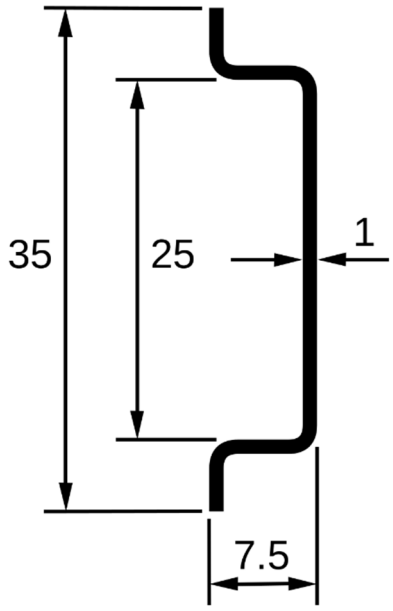

Figure. 4.3. Dimensions of DIN rail.

Table 4.2. Sensor models.

Sr.#	Manufacturer	Model	Function
1	CR Magnetics	CR5210	DC Current Transducer
2	CR Magnetics	CR5310	DC Voltage Transducer
3	CR Magnetics	CR4510	AC Voltage Transducer
4	CR Magnetics	CR4310	AC Current Transducer
5	Aosong Electronics	DHT11	Temperature & Humidity

Table 4.3. Sensor power consumption and price.

Sr.#	Manufacturer	Model	Price ($)	Power Consumption (W)
1	CR Magnetics	CR5210	116.26	0.84
2	CR Magnetics	CR5310	190.07	0.84
3	CR Magnetics	CR4510	210.40	0.36

4	CR Magnetics	CR4310	99.99	0
5	Aosong Electronics	DHT11	5.00	0.0015
6	Arduino	Mega 2560	70.00	0.27
7	RaspberryPi	Dell	70.00 $	30 W

4.4.2 DC current and voltage sensor

CR5210 was used as a DC current sensor, and CR5310 was used as a DC voltage sensor. Both provided the output DC signal in the range of 0–5 V_{dc} which is directly proportional to the input signal. It also provides the built-in isolation between the input and output sides which will save our remote terminal unit from overvoltage on the input pins. The input voltage range of CR5310 is 0–600 V_{dc} and the input current range of CR5210 is 200 A_{dc}. The connection and wiring of the sensors are shown in Figure 4, and both needed a 24 V DC supply for input power because it was an industrial practice to use bit high voltage; otherwise, AC may interfere with it and cause malfunctioning.

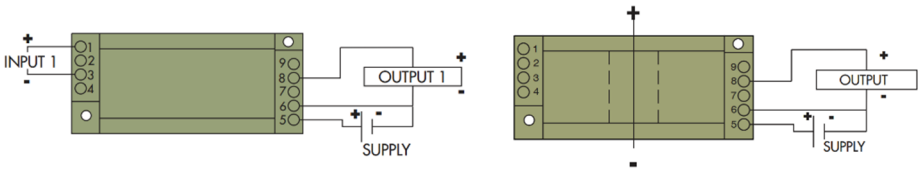

Figure. 4. Wring of DC transducer: (a) Voltage sensor CR5310; (b) Current sensor CR5210.

The technical specifications of the CR5210 current sensor are given in table 4.4.

Table 4.4. CR5210 Specifications.

Sr.#	Specifications	Value	Units
1	Basic Accuracy	1	%
2	Linearity	10-100 FS	%
3	Thermal Drift	500	PPM/ °C
4	Operating Temperature	0-50	°C
5	Max Response time	250	ms

4.4.3 AC current and voltage sensor

CR4500 was used as an AC current sensor, and CR4310 was used as an AC voltage sensor. Like the DC sensors, these also provided an output DC signal, ranging from 0–5 Vdc which has a direct linear relationship with the input parameter along with the 24 V power supply. CR4500 is a low-

cost, fully integrated, rugged, hall effect-based linear current sensor with a current range of 0–200 A, along with isolation on both sides of the CT. Table 5 shows the voltage measuring range of CR4310 is 0–500 VAC. Figure 5 shows that the wiring of the sensor and CR4500 does not need any input supply. Only the wire-carrying current will act as a primary winding. It can be demonstrated from Table 4.6 that it has an accuracy of 0.75% and can measure a signal of only 50/60 Hz frequency. The detailed wiring of the sensors is given in Figure 5.

Table 4.5. CR4310 Specifications.

Sr.#	Specifications	Value	Units
1	Basic Accuracy	0.5	%
2	Calibration	True RMS sensing	--
3	Frequency Range	20-5000	Hz
4	Operating Temperature	0-60	°C
5	Supply Voltage	24 ±10 %	Vdc

Table 4.6. CR4500 Specifications.

Sr.#	Specifications	Value	Units
1	Basic Accuracy	0.75	%
2	Calibration Signal out	0-5	Vdc
3	Frequency Range	50/60	Hz
4	Operating Temperature	-30 to 60	°C
5	Insulation class	600	V

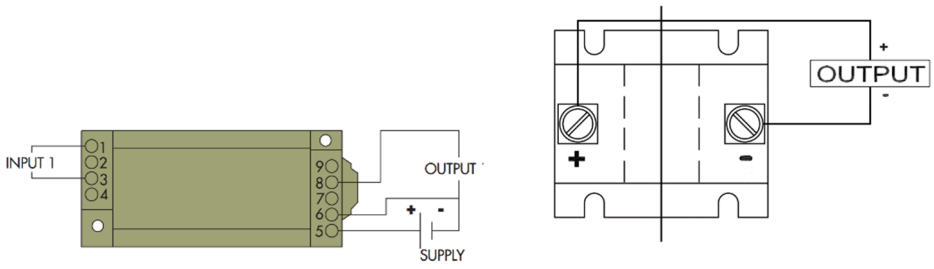

Figure 4.5. Wiring connection of AC transducers: (a) AC voltage sensor CR4310; (b) AC current sensor 4500

4.4.4 Environmental sensor

The temperature has a direct impact on the performance and efficiency of PV systems. Solar modules are tested under STC conditions i.e. 25 °C but they might be installed on a much higher

temperature. The higher temperature has a direct impact on the open circuit voltage and short circuit current, which is depicted in figure 4.6.

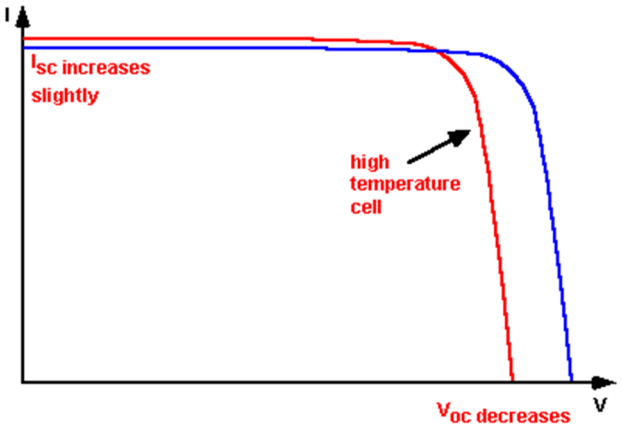

Figure. 4.6. Effect of temperature on PV module characteristics.

Humidity has also a direct effect on the Direct Normal Irradiance (DNI) and Global Horizontal Irradiance (GHI) which ultimately affect the output of PV system. So, DHT11 sensor has been used for measuring both parameters. Table 4.7 shows that DHT has a calibrated signal output and guarantees long-term stability and excellent reliability. It has a resistive type of humidity measurement component for humidity and NTC thermistor for temperature which are connected to build an 08-bit microcontroller that provides fast response, good quality, and cost saving. The configuration of DHT with the microcontroller unit is shown in figure 4.7.

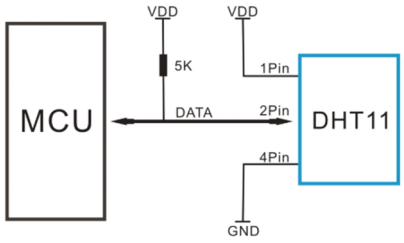

Figure 4.7. DHT11 interfacing with Arduino.

Table 4.7. DHT11 Specifications.

Sr.#	Specifications	Temperature	Humidity
1	Resolution	1 ℃	1 %RH
2	Accuracy	±4 ℃	±4 %RH
3	Range	0-50 ℃	20-90 % RH
4	Response Time	06 s	10

4.4.5 Remote Terminal Units (Arduino Mega 2560)

Arduino mega is a Atmega2560-based microcontroller and is widely used due to its low cost and low power consumption. It has 54 digital input/output pins out of which 15 can be utilized as a PWM generator. In addition, it has 4 UARTS, 16 input analog pins, 16 MHz crystal oscillator, in Circuit Serial Programming (ICSP) header, and a reset button. Its input voltage limit is 7-20 V which makes it feasible to power up using a USB cable, Lithium Cell, or any battery. It has a flash memory of 250KB, static RAM has a size 8KB, and EEPROM is 4KB. The detailed pin configuration and layout of RTU are shown in figure 4.8.

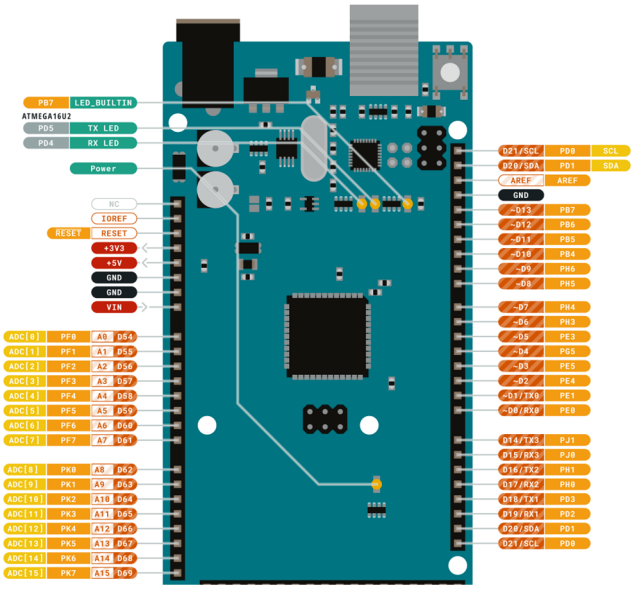

Figure 4.8. Arduino Mega 2586 pin layout [12].

Arduino mega is programmed using the Arduino compiler Integrated Development Environment (IDE). The program is written in Arduino IDE using its language and libraries which are almost

similar to the C/C++ language. Arduino is connected with serial port of the PC using type A/B cable for programming and communication. Firstly, the Arduino program called “sketches” are written in IDE for measuring the field instruments parameters. Then the values of these parameters are observed using the specific baud rate which is 38400 bits per second in our case.

4.4.6 Master Terminal Unit (RPI)

As a part of future Raspberry is a small single-board computer that has been modified through several versions and features. It has a lot of applications ranging from small toys to industrial control. It requires an operating system (OS) usually called as Raspbian to carry out the operations. The main flexibility of the MTU is that any computer can also be transformed into the RPI as per need. In the designed case, an old core i3 computer is used as a RPI and Debian is the OS for this PC. It has 15.6’’ screen and processor has flowing specifications.

- A 1.90GHz quad-core x86 Intel CPU
- 500GB ROM
- 4GB RAM
- One hundred Base Ethernet
- Three USB ports (2 USB 3.2 & 1 USB 2.0)
- Full HDMI port
- Micro SD card slot
- VideoCore IV 3D graphics core

4.4.7 Emoncms

As it has already been discussed, Emoncms is an open-source platform and provide versatile packages as per user demand. The main objective is to display the data on HMI for visualization and observing the behavior of system. It also offers an easy package where an account can be

created on Emoncms website and data is stored on the remote server which limits the data storing capabilities along with exposing that data the hacker which compromises the security and reliability of system. So, Emonpi is used for storing the data locally and acts as a local server whose specifications are shown in the figure 4.9.

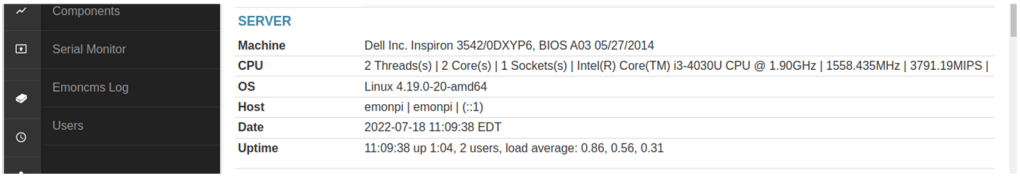

Figure. 4.9. Dell laptop as local server.

Emoncms is itself a WebView platform it needs many other modules and data in a specific format called JSON to display on the HMI. Below figure 4.10 explains emoncms interconnectivity of different modules, in which the main module is EMONHUB. Emonhub takes data from RTU in raw form and refines it using the MQTT module. Mosquito can also be used instead of MQTT for data formatting. Emoncms webview needs PHP, MYSQL, and REDIS for data visualization and logging. If any one of them is not working, there will be an error.

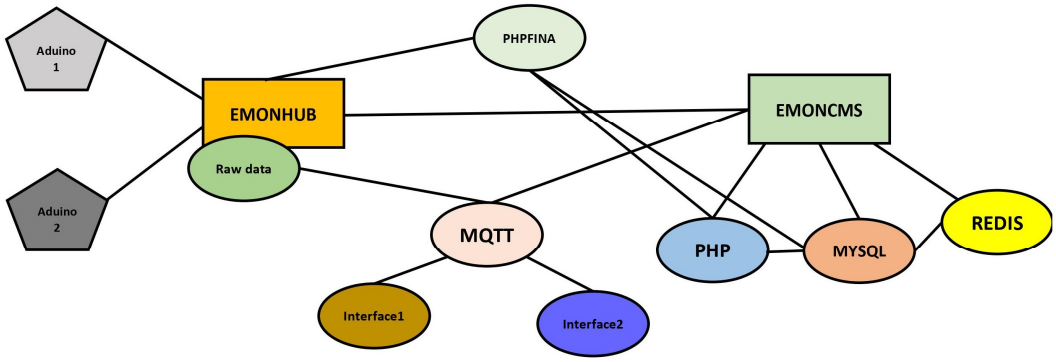

Figure. 4.10. Emoncms connectivity modules.

4.5 Implementation Methodology

In the implementation of the designed system, voltage sensors are connected in parallel and current sensors are connected in series. DC transducers are connected on the analog pin A0, A2, A4 of RTU1 (Arduino mega 1), and AC transducers are connected on the analog pin A0, A4 of RTU2 (Arduino mega 2). In addition, DHT11 is also connected to Tx, Rx pin of RTU2. Below Algorithm 1 will represent the pseudocode of Arduino which is compiled and built in the Arduino chip.

Algorithm 1: Arduino Sensor Data Reading Algorithm

```
Initialization;
1. Set the baud rate of 38400 bps;
2. Define the DHT libraries;
3. While read and store the AC current Sensor CR43100;
    4. Read and store the AC Voltage Sensor CR4510;
    5. Take and store the temperature and humidity value from DHT11;
    if sample are equal to 10
        7. Take average store all data in final variables;
    else
        9. Parse the data in JSON format;
        10. Push parsed data to the MTU;
        11. Go to step 3;
    end
End
```

Algorithm 2 along with the below figure 4.11 flow chart represents the complete SCADA system from RTU to HMI.

Algorithm 2: Data Logging Algorithm

Initialization;

1. Read Field devices values on Arduino Mega 1 (RTU1) analog PIN 0,2,4;
2. Read Field devices values on Arduino Mega 2 (RTU2) analog PIN 0,2,4;
3. Connect the Both RTU to the MTU with Serial Cable;
4. Login into the Emoncms;
5. Detect the Read Only or Read & Write API keys;
6. Format the data in JSON format;
7. Push data to serial port;
8. While Start Emonhub
    9. Receive data into the Emonhub;
    10. Check the status of Emonhub data transmission;
    If no data receipt
        11. Display message in status screen;
    Else
        12. Go step 1;
    End
End

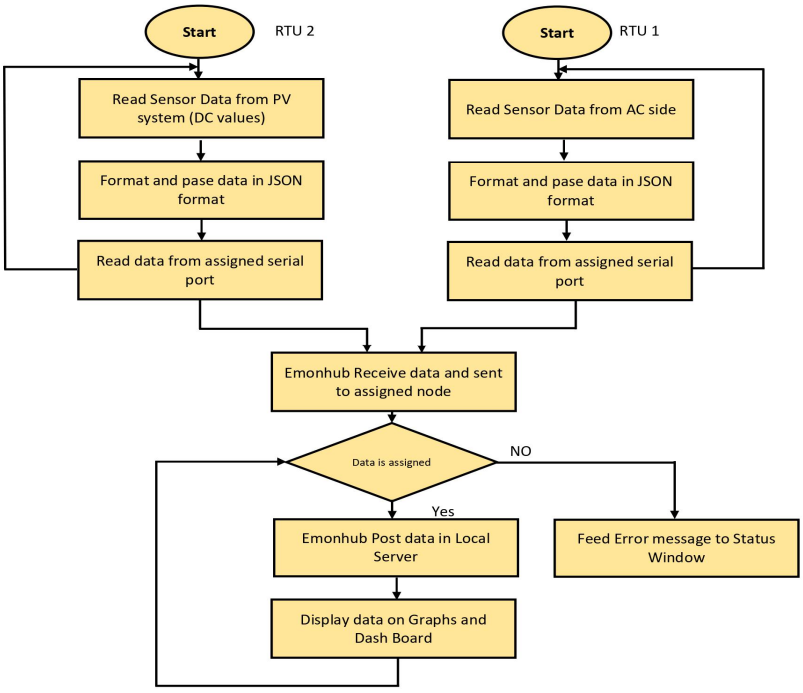

Figure. 4.11. Flowchart of complete data processing.

4.6 Prototype design and Results

The proposed SCADA system setup is shown in Figure 4.12 using the above-stated hardware and operating principles. Figure 4.12 shows that the current and voltage transducers are connected to the corresponding Arduino, and both are connected with the MTU, which is a Dell laptop. Different power supplies were used to generate the desired voltage. A 24 V supply was used for proving the Vcc and ground to all sensors. To provide the DC voltage, a variable supply was used with an output voltage that varied between 0–60 Vdc. A 12 V DC incandescent bulb and rheostat were used as a DC load to generate the load current. On the AC side, an autotransformer was used which provided isolation and protection from the grid along with the variable voltage. A 100 W incandescent bulb was used on the AC side as a load. The physical fluke voltmeters and current meters were installed on point of interest to cross-check the measurements of field parameters. After connecting all of the field devices to the RTU, both Arduinos were connected to the RPI, using a USB 2.0 Cable Type A/B, which provided the communication.

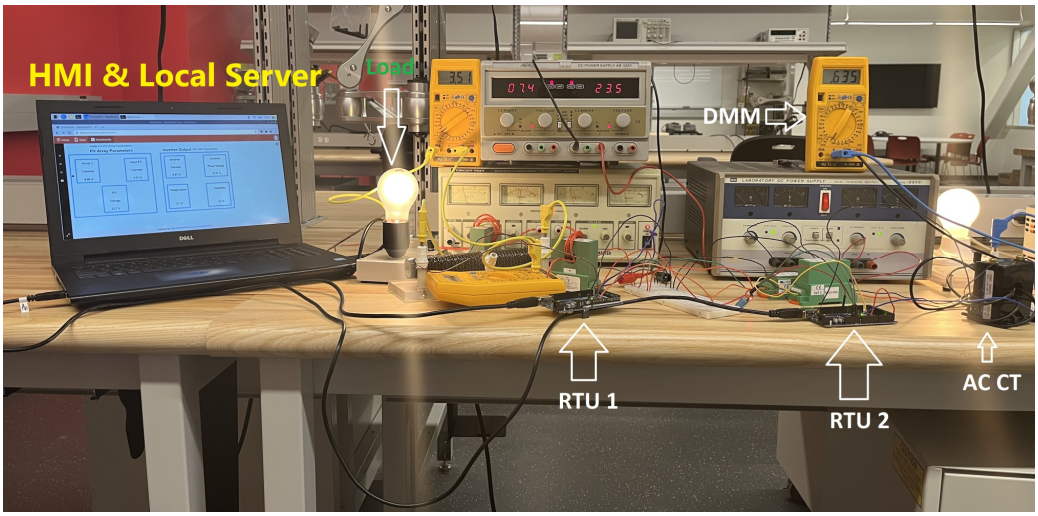

Figure. 4.12. Hardware setup.

The system was turned on for 6 h and data logging was performed. During the testing of the system, different digital multimeters were connected to points of interest to observe the value of the

parameters. The values calculated with the designed setup were very close to the actual multimeter value and had an accuracy error of less than 5% over the entire measurement range. The designed system is capable of storing and logging PV system data for months or years. Various dashboards were created to observe the trend of different values and also to create a user-friendly environment for observations. Figure 13 shows the dashboard for observing the instantaneous values of PV arrays, the inverter output, and environmental factors.

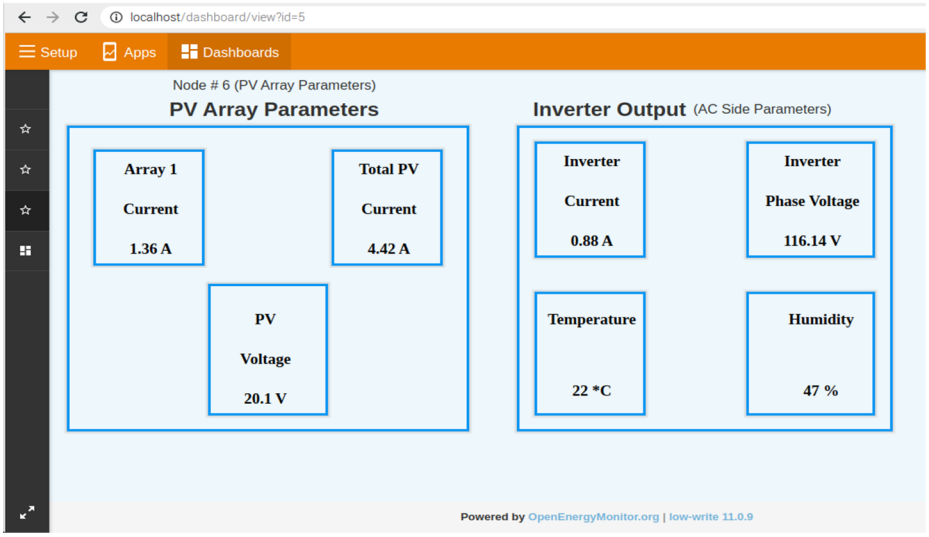

Figure. 4.13. Instantaneous values of field instruments.

In figure 4.14 below, the data has been logged and the graph has been plotted from that data. The below figure shows the Inverter output current, Phase voltage, Temperature, humidity, and display of all parameters on one graph for a period of 6 hours. The recording period can be adjusted using the tab just above the graph

Figure 4.14. AC side parameters trend.

Figure 4.15 demonstrates the PV array parameters. It depicts the behavior of the total PV current, PV voltage, and Array 1 current. This data was logged for 6 h for basic testing, but the system is capable of logging data as long as needed without any modification or addition. The emonPi provided both local and remote data logging using the Emoncms web application display, which maintains the data with the privacy of your home. A total of 10 GB storage was enough for a node with six feeds to store the data. The designed system also provides the least possible wear out of memory, which ultimately increases the lifetime of the hard disk. More sensors could be added, such as logging the PV current for each PV string.

Figure. 4.15. DC side parameters behavior.

4.7 Discussion

The following are a few key features of the designed system, which was verified through successful testing:

- Emoncms-based SCADA system: Using the Emoncms platform, the system offers all of the features common to most recent SCADA systems, such as data acquisition, data transmission, remote terminal units (RTU), and master terminal units (MTUs).
- Data monitoring: Monitoring data remotely is possible through the WebView feature of the system.
- Low-cost and open-source components: Low-cost and open-source components contribute to the overall low cost of the proposed SCADA system with all the features of modern, expensive commercial systems.
- Data storage: It is also possible to view the data trends for any time period, from one hour to one year.
- User friendly dashboard: Data monitoring is made easier with the dashboard's userfriendly interface.
- No license fee: The designed system has no license fee or yearly fee to cover software.
- Private and secure system: Due to local data storage, the design system is not sending data to any remote server. It is 100% private and secure.

4.8 Conclusion

Most of the industries in the world are located in remote areas, due to the large land requirements and each country's industrial legislation. Therefore, it is compulsory to have a local source of data logging to calculate the monthly and annual costs and return on investment, along with the cost effectiveness and reliability. Indeed, the SCADA was modified through many tiers from the

distributed control system to the IoTs, but mostly, it remained proprietary and costly. As in power system applications, batteries, inverters, PV system, etc. are purchased from different manufacturers, which give interfacing and compatibility issues during the monitoring and control. Thus, an open-source SCADA is an inevitable solution that permits "mix and match" components from different manufacturers. In addition, proprietary SCADA is very costly, and only major companies with big revenues can afford this. In such a situation, an open-source Emoncms SCADA system is the best, most reliable, cost-effective solution, and a 100% private and protected system. In the designed system, the low-cost, open-source SCADA system was designed with IoTs architecture, which is the latest one. The initial capital cost of the whole SCADA system was CAD $761.72, and the running cost of the system was zero because it is open source and storing the data in the local server. The designed system's overall cost was less than any system studied in the above literature or mentioned on the supplier's website. For example, the system "NOVUS 8845000080 SuperView SCADA Software (ITM Instruments Inc., Sainte-Anne-de-Bellevue, QC, Canada)" costs CAD $911, but including the hardware, the cost will be much higher.

The hardware design of the system was also performed and had four major modules: field instrumentation devices (current, voltage, and temperature sensors), remote terminal units (Arduino Mega microcontroller), master terminal units (RPI and Emoncms), and the SCADA communication channel (local communication through serial port). To test the system, it was set up in the lab and different voltage and current sources were used to observe the behavior of the system. The system voltage and current were changed and a corresponding change in the output was also observed. Additionally, conventional digital multimeters were used to cross-check the parameters of the system. The system also stored the data locally and created dat and meta files in the "/var/opt/emoncms/phpfina" directory. From testing, it was deduced that the designed system could work in a robust environment and log the data in a real-time environment with great accuracy

and precision. Furthermore, the power consumption of the whole designed SCADA system was less than 35 W, including the HMI display which consumed significant power, i.e., a 30 W consumption. The design system's total cost was only CAD $761.72, which is the least cost of an open-source SCADA system with industrial sensors, while commercial SCADA has a proprietary software license fee; an annual fee running into thousands of dollars per year.

Funding: This research was funded by Natural Sciences and Engineering Research Council of Canada (NSERC) and School of Graduate Studies (SGS) Memorial University.

Conflicts of Interest: The authors declare no conflict of interest.

References

[1] Inductive Automation. Available online: https://inductiveautomation.com/resources/article/what-is-scada. (Accessed on 25 July 2022).

[2] L. Ahsan and M. T. Iqbal, "Design of an Optimal Hybrid Energy System for a Captive Power Plant in Pakistan," *2021 IEEE 12th Annual Information Technology, Electronics and Mobile Communication Conference (IEMCON),* 2021, pp. 0820-0826, doi: 10.1109/IEMCON53756.2021.9623260.

[3] Ahsan, L., & Iqbal, M. (2022). Dynamic Modeling of an Optimal Hybrid Power System for a Captive Power Plant in Pakistan. In *Jordan Journal of Electrical Engineering (Vol. 8, Issue 2, p. 195).* ScopeMed. https://doi.org/10.5455/jjee.204-1644676329

[4] D. Li, N. Gebraeel and K. Paynabar, "Detection and Differentiation of Replay Attack and Equipment Faults in SCADA Systems," *in IEEE Transactions on Automation Science and Engineering, vol. 18*, no. 4, pp. 1626-1639, Oct. 2021, doi: 10.1109/TASE.2020.3013760.

[5] Qays, MO, Ahmed, MM, Parvez Mahmud, MA, et al. Monitoring of renewable energy systems by IoT-aided SCADA. *Energy Sci Eng. 2022*; 10: 1874- 1885. doi:10.1002/ese3.1130

[6] A. B. Abdulsalam, H. A. J. Alsaadi and Z. Hamodat, "Control And Management of Solar PV Grid Using Scada System," *2022 International Congress on Human-Computer Interaction, Optimization and Robotic Applications (HORA),* 2022, pp. 1-5, doi: 10.1109/HORA55278.2022.9799994.

[7] Lawrence O. Aghenta, M. Tariq Iqbal. Design and implementation of a low-cost, open source IoT-based SCADA system using ESP32 with OLED, ThingsBoard and MQTT protocol[J]. *AIMS Electronics and Electrical Engineering, 2020, 4(1): 57-86.* doi: 10.3934/ElectrEng.2020.1.57

[8] C. N. Oton and M. T. Iqbal, "Low-Cost Open Source IoT-Based SCADA System for a BTS Site Using ESP32 and Arduino IoT Cloud," *2021 IEEE 12th Annual Ubiquitous Computing, Electronics & Mobile Communication Conference (UEMCON),* 2021, pp. 0681-0685, doi: 10.1109/UEMCON53757.2021.9666691.

[9] J. Figueiredo and J. Sá da Costa, "A SCADA system for energy management in intelligent buildings*," Energy Build.,* vol. 49, pp. 85–98, 2012, doi: https://doi.org/10.1016/j.enbuild.2012.01.041.

[10] M. Kermani, D. L. Carnì, S. Rotondo, A. Paolillo, F. Manzo, and L. Martirano, "A Nearly Zero-Energy Microgrid Testbed Laboratory: Centralized Control Strategy Based on SCADA System," *Energies, vol.* 13, no. 8, 2020, doi: 10.3390/en13082106.5.

[11] S. Li, B. Jiang, X. Wang, and L. Dong, "Research and Application of a SCADA System for a Microgrid," *Technologies, vol. 5,* no. 2, 2017, doi: 10.3390/technologies5020012.

[12] A. Zare and M. T. Iqbal, "Low-Cost ESP32, Raspberry Pi, Node-Red, and MQTT Protocol Based SCADA System*," 2020 IEEE International IOT, Electronics and Mechatronics Conference (IEMTRONICS)*, 2020, pp. 1-5, doi: 10.1109/IEMTRONICS51293.2020.9216412.

[13] E. Lázár, R. Etz, D. Petreuș, T. Pătărău and I. Ciocan, "SCADA development for an islanded microgrid," *2015 IEEE 21st Inter-national Symposium for Design and Technology in Electronic Packaging (SIITME)*, 2015, pp. 147-150, doi: 10.1109/SIITME.2015.7342314.

[14] A. Kelati and H. Gaber, "IoT for Home Energy Management (HEM) Using FPGA*," 2021 IEEE 9th International Conference on Smart Energy Grid Engineering (SEGE),* 2021, pp. 54-57, doi: 10.1109/SEGE52446.2021.9534986.

[15] M. U. Saleem, M. R. Usman, M. A. Usman and C. Politis, "Design, Deployment and Performance Evaluation of an IoT Based Smart Energy Management System for Demand Side Management in Smart Grid*," in IEEE Access,* vol. 10, pp. 15261-15278, 2022, doi: 10.1109/ACCESS.2022.3147484.

Chapter 5

Conclusion and Future Work

5.1 Conclusion

In this thesis the feasibility of design, analysis and monitoring of renewable power plant has been discussed. The penetration of PV system is increasing day by day due to roaring prices of fuel which increase the per unit cost of energy. The global temperature is rising and weather is going to be severe day by day which forces the world to invest to carry on the research and development on PV and wind system. At recent time, due to the new manufacturing strategies in PV system, there is a steep decline in the prices of PV module which make it feasible over the conventional power plant. Therefore, it is need of time to take the advantage of this to save the environment as well as power generation cost.

Firstly, the sizing of PV system has been done in HOMER Pro. There are three cases discussed here. In case 1 (without storage), 8382 kW_{dc} system is required to fullfill the load demand without any battery. This case has a $ 0.102 per unit cost without any constraint on renewable power generation. In 2nd case, 70 % fixed generation constraint is putted on the renewable system which need a PV system of 18175 kW with per unit cost of $ 0.0649. In 3rd case, battery storage is also implemented to take the power during off irradiance hours, but the results are same as case 1 because grid also act like a battery and provide power during night time. The capital and operating cost of batteries is very high. Eventually, in the first phase, it is concluded that case 1 with 8382 kW PV system is the most economical and reliable system for the selected site.

In the 2nd phase, the dynamic of the most economical system designed in the 1st phase has been discussed. The system was modeled in the MATLAB/Simulink using the Simscape blockset. During the modeling, the incremrntal conductance with integral control has been used along with the NPC inverter and LCL filter. The control of the grid tied inverter has been design with reference to SPWM technique. In the control of synchronization, feedforward compensation techniques has been used which increase the stability of whole system. During the testing, system was observed under different loading conditions and power swings. The designed system can handle 1.5 MW step load and 300 W/m^2 step irradiance change which make it reliable. From these testing, it was concluded that designed system is reliable, secure and has capability to bear interrupts without any power outage or shut down.

In the 3rd and final phase of thesis, a low cost and open-source monitoring system has been designed. The Emoncms SCADA is used for the monitoring of field devices parameters. Two Arduino mega units has been used as RTUs for taking the data from field devices. The Arduino mega take the data from current, voltage, and environmental sensors and are connected to the Master terminal unit RPI. The RPI take the data from the serial port and push it to the main module of EMONCMS called as EMONHUB. EMONHUB receive this raw data and parse it into the JSON format with the help of MQTT. This data is then sent to the EMONCMS web view platform which has a user-friendly HMI display. This data is also stored in the RPI (DELL Laptop) for the future planning and event recording purposes. The hardware of this designed system implemented in the lab and system was let go to record the data for 6 hours. The data was record and stored successfully with any interruption and the right person with authorization can access this data which makes the system reliable, rugged and secure.

Finally, the design, analysis, modeling, and monitoring of a hybrid renewable power systems for a plant in Pakistan has been carried out successfully. It is deduced the if designed reliable system is

implemented it will provide a cost savings along with the carbon emissions. Despite this, this will also help the govt to solve the economic crisis due to the electrical short fall and also generate opportunities for each person to invest in distributed system for earning money through net metering.

5.2 Research Contribution/Problem Solutions

The contribution of this research work is to find the best solution to the problem enumerated in section 1.6 summarised below.

1. A textile unit " Shafi Texcel Limited" has been chosen for conducting the feasibility study of PV plant. PV plant sizing has been done in HOMER PRO developed by the NREL. Different cases have been discussed and the most feasible and reliable is the 8382 kW grid-tied PV system is needed to generate the lowest cost energy.
2. The control and dynamic of the above-made feasible system are modeled in MATLAB/Simulink using the Simscape block set which shows that the design system can handle 1.5 MW load and 300 W/m^2 irradiance step change.
3. For the monitoring and control of a designed system, EMOMCMS open source SCADA system is used which was configured on a Debian Linux which is installed on a local PC. Industrial Field instruments from different manufacturers have been used for taking the field data, which increased the interoperability of SCADA system. The Emoncms log the data locally and the person with the right authorization can access it, which makes the design system secure and reliable.

5.3 Future Work

As a part of future work, the modeling of the system should be done along with the reduced order dynamic model of system. The reduced order model is the most resent and latest hot topic in the field of PV system research. This model will have less computation complexity and can run from months to years on any computer machine. Reduced order dynamic model will help in improving the transient response of system during the large interruptions.

From SCADA point of view, The open source SCADA system based on Emoncms can be upgraded to a wireless system so that the data could be controlled and monitored wirelessly. An email alert system can be incorporated into the SCADA system already developed using Swift-mailer. A control button can be Added to control motor start/stop from SCADA system.

Articles in Refereed Publications

- L. Ahsan and M. Iqbal, "Dynamic Modeling of an Optimal Hybrid Power System for a Captive Power Plant in Pakistan," *Jordan Journal of Electrical Engineering, vol. 8, no. 2.* ScopeMed, p. 195, 2022. doi: 10.5455/jjee.204-1644676329.
- Ahsan, L.; Baig, M.J.A.; Iqbal, M.T. Low-Cost, Open-Source, Emoncms-Based SCADA System for a Large Grid-Connected PV System. *Sensors* 2022, 22, 6733. https://doi.org/10.3390/s22186733

Refereed Conference Publications

- L. Ahsan and Mssss. T. Iqbal, "Design of an Optimal Hybrid Energy System for a Captive Power Plant in Pakistan," *2021 IEEE 12th Annual Information Technology, Electronics and Mobile Communication Conference (IEMCON)*, 2021, pp. 0820-0826, doi: 10.1109/IEMCON53756.2021.9623260.

Regional Conference Publications

- Luqman Ahsan and M. Tariq Iqbal, Design of Hybrid Electrical Power System for an Industrial Unit in Pakistan, presented at the *31st Annual IEEE NECEC conference St. John's*, November 19th, 2021.